l'institut Agro
agriculture • alimentation • environnement
AGRO CAMPUS OUEST

☐CFR Angers   ■CFR Rennes

UNIVERSITÉ DE LORRAINE

Aix✶Marseille université
Initiative d'excellence

ENSAIA
École de l'Innovation et de la Transition
NANCY

mio
Mediterranean Institute of Oceanography

|	
Année universitaire : 2019 - 2020 Spécialité : Ingénieur agronome Spécialisation (et option éventuelle) : Sciences halieutiques et aquacoles, préparée à Agrocampus Ouest (option Ressources et écosystèmes aquatiques)	**Mémoire de fin d'études** ■ d'ingénieur de l'École nationale supérieure d'agronomie et des industries alimentaires (ENSAIA), école interne de l'institut national d'enseignement supérieur pour l'agriculture, l'alimentation et l'environnement ☐de master de l'École nationale supérieure des sciences agronomiques, agroalimentaires, horticoles et du paysage (AGROCAMPUS OUEST), école interne de l'institut national d'enseignement supérieur pour l'agriculture, l'alimentation et l'environnement ☐d'un autre établissement (étudiant arrivée en M2)

Spatial and temporal variability of spawning in Mediterranean coastal fishes

Par : Marine DI STEFANO
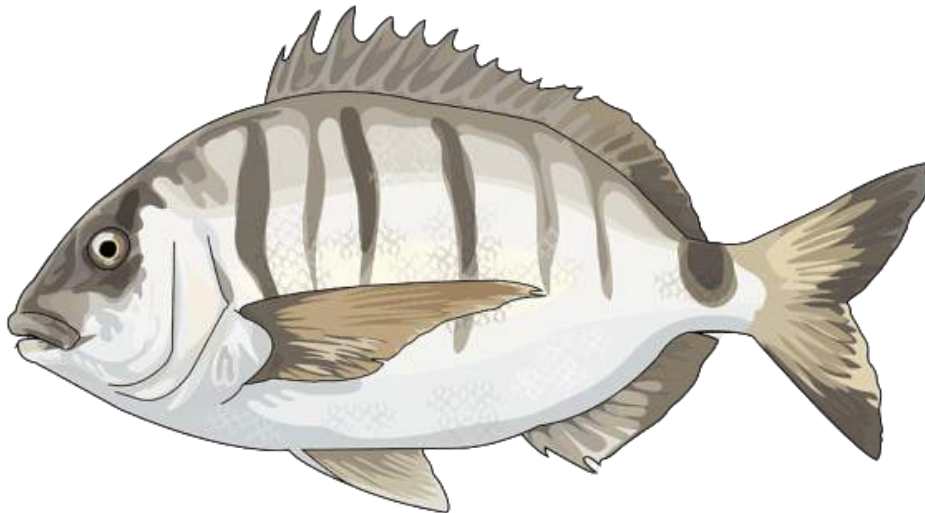
Soutenu à Rennes, le mercredi 16 septembre 2020

Devant le jury composé de :
Président : Etienne RIVOT, enseignant-chercheur à Agro Campus Ouest

Maître de stage : Vincent ROSSI, chercheur CNRS

Enseignant référent : Olivier LE PAPE, enseignant-chercheur à Agro Campus Ouest

Autres membres du jury : Martin HURET, chercheur Ifremer

Les analyses et les conclusions de ce travail d'étudiant n'engagent que la responsabilité de son auteur et non celle d'AGROCAMPUS OUEST

Contents

List of Figures

List of Tables

Acknowledgements

1 Introduction

Most marine organisms have a bipartite life cycle (D'Aloia *et al*, 2015 ; Figure 1) which starts with a dispersive larval phase (in red) where individuals are dispersed by currents across the seascape, followed by a relatively sedentary phase (in green) where the individuals are generally associated to a specific habitat (Thresher *et al*, 1989). The early-life stages are composed of several main events: the actual spawning when the gametes (eggs and sperms) are released in the water column by the adults (fertilization is generally external) ; the hatching that is when larvae are released from the eggs after a short period of incubation ; and, finally, the settlement which corresponds to the metamorphosis of the larvae into juveniles with significant swimming abilities, allowing them to settle in nurseries (Thresher *et al*, 1989 ; Figure 1). While the settlement of juveniles will not be studied here (essentially because the spatial movements associated with this event are thought to be relatively small, e.g. a few hundred of meters to a few kilometers), both recently fertilized eggs and larvae have the potential to be dispersed by ocean currents over large distances, spawning tens to hundreds of kilometers (Cowen *et al*, 2006). Dispersal, defined as the movement of individuals away from their "natal source" (Nathan *et al*, 2003 ; Burgess *et al*, 2016), determines the spatial scale at which local population are ecologically connected to each other. For the organisms characterized by bipartite life-cycles, such as most coastal fishes, the spatial scales of ecological connectivity are mainly determined by the dispersal of early-life stages (Gaines *et al*, 2007). Connectivity refers, in fact, to the exchange of biological material between geographically separated populations of a same species (Cowen & Sponaugle, 2009). All populations exchanging individuals are called sub-populations and are part of a meta-population. An open population receives and/or sends individuals from and to the other sub-populations, contrary to a closed population which not or to a limited extent (Cowen & Sponaugle, 2009 ; Pineda *et al*, 2007). Thus, with a sufficient level of exchange, connectivity can have impacts on the population demography, sustainability and structure. For instance, gene flows can affect evolutionary processes - genetic connectivity - and dispersal processes can impact growth and mortality rates - demographic connectivity (Cowen & Sponaugle, 2009 ; Dubois *et al*, 2016).
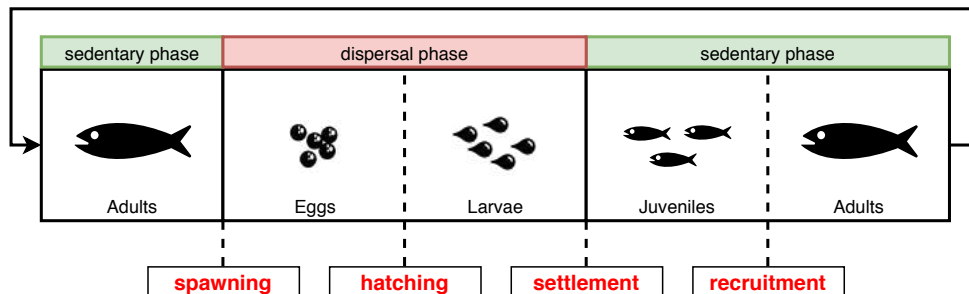
Figure 1: Schematic representation of a bipartite life cycle of any fish species (D'Aloia *et al*, 2015). Two parts can be distinguished: a sedentary phase (in green) where individuals are closely associated with their habitat and a dispersive larval phase (in red) where early-life stages are dispersed by ocean currents, connecting distant populations (Thresher *et al*, 1989).

Demographic connectivity is a fundamental process influencing the dynamics and persistence of spatially structured populations (Burgess *et al*, 2014), so assessing connectivity patterns is key to predict the putative impact of potential perturbations on the populations, and design effective management strategies (Dubois *et al*, 2016). In this context, determining the location and onset of spawning represent a key element to appraise the dispersal of propagules (eggs and larvae) and hence to understand connectivity patterns (Legrand *et al*, 2019). If one knows the periods and locations which are particularly favourable for the spawning of a given species, they could be good candidates for protection since they send regularly and plenty of larvae to other places, contributing to the replenishment of both local and distant sub-populations. Actually, the conservation and the protection of coastal species are major challenges of fishery science, as these species are often over-exploited, especially in the Mediterranean sea (FAO, 2018). Anthropogenic stressors such

as pollution, habitat destruction and climate change also threaten the stability of marine ecosystems and rearrange fish stocks, notably by modifying ocean temperature and biogeochemistry (Bianchi & Morri, 2000 ; Claudet & Fraschetti, 2010 ; Coll *et al*, 2010). Thus, the protection of certain spawning areas could allow a better management of the ecosystems to limit these negative impacts because it could permit a regular export of larvae (named recruitment subsidy) to other sites, protected or not (Pelc *et al*, 2010), and could allow a more sustainable exploitation of marine living resources.

Management of critical areas for exploited fish can be made thanks to tools like Fisheries Restricted Areas (FAO, http://www.fao.org/gfcm/data/maps/fras/en/) or Marine Protected Areas (MPAs) which are mainly employed for coastal species conservation (Fogarty *et al*, 2007). Their design and implementation could be based on many parameters, such as connectivity (Fogarty *et al*, 2007) or the definition and presence of "Essential Fish Habitats" (Druon *et al*, 2015). Actually, few management tools have been considering population connectivity, thus limiting their efficiency (Fogarty *et al*, 2007) and pointing out the necessity of a change in the management approach. Studying nurseries, Druon *et al* (2015) found variability in the settlement location and period. Hence, early-life stages tends to vary a lot over space and time. Assuming that spawning could vary as much as nurseries, a dynamic management is needed in order to adapt to the oceanic variability. Otherwise, where stable areas are identified and to follow the current trend of fixed protection measures, defining new protected areas could be a common way of protecting resources, as highlighted in Di Franco and Guidetti (2011).

Environmental factors that can control the onset and the duration of fish spawning, particularly in Sparids which have an economical importance in the Mediterranean Sea, were already investigated. In the following, we review information concerning Teleost fishes in general, therefore potentially including patterns arising from species with a very large set of biological traits. We then focus particularly on Sparids, especially the Mediterranean ones, and on *Diplodus sargus sargus*, which is the target species of this project. Many factors like photoperiod, sun or moon cycles have been invoked and studied to understand the variability of spawning in many marine organisms.

Numerous studies have pointed out temperature as a cue of fish spawning, both in freshwater (King *et al*, 2016) and in marine species – such as the estuarine benthic goby *Pseudogobius olorum*, the pelagic herring *Clupea harengus* or the temperate demersal dusky grouper *Epinephelus marginatus* (Gill *et al*, 1996; Winters & Wheelers, 1996; Hereu *et al*, 2006). Coastal upwelling events could also play a role in the initiation of the spawning period, especially by providing nutrients from the wind-driven uplift of cold and enriched deep waters to the surface, to pelagic fish like anchovies or sardines or to demersal species (Lluch-Belda *et al*, 1991; Coulson *et al*, 2019). Increasing concerns about climate change lead authors to look for possible shifts – temporal and/or spatial – in spawning caused by the warming trend of coastal and oceanic water masses, shifts that have already been observed for cod *Gadus morhua* or sole *Solea solea* (Fincham *et al*, 2013; McQueen & Marshall, 2016; Auth, 2017). Ocean warming due to the climate change has also been linked to modifications of the hydrodynamics, hence affecting the connectivity of early-life stages (Cowen & Sponaugle, 2009 ; Van Gennip *et al*, 2017). In conjunction with temperature, several authors have described the influence of photoperiod on the spawning onset of several fishes (Mischke & Morris, 1997; Vinagre *et al*, 2009). If spawning onset would be only determine by photoperiod, it would occur each year at the same period since it is the day length, which depends only on the location and the day of the year considered (often described as a ratio of the day length on the night length). Actually, De Vlaming (1972) challenged the role of photoperiod on controlling spawning at the benefit of temperature by arguing that changes of photoperiod are indeed well-correlated with the evolution of sea water temperatures, both variables being strongly dependent on latitude.

Temperature as a spawning cue for Sparids has been investigated by multiple studies in various places. Mouine *et al* (2011) studied the reproductive biology of four *Diplodus* species in the Gulf of Tunis. They showed that the spawning period of *D. sargus* and *D. annularis* was associated with a rise in Sea Surface Temperature (SST) from the onset to the end of the spawning (14.8°C to 15.6°C and 17.4°C to 20.8°C respectively), unlike those of *D. vulgaris* and *D. puntazzo*, associated with a decrease (16.4°C to 15.8°C and 24°C to 22°C respectively) knowing that the first two *Diplodus* spawn in spring or early summer and the other two in fall-winter. Thus, this changes in the temperature regime probably triggers the spawning. In the

Canarian archipelago, Pajuelo *et al* (2003) determined that the spawning of *D. cervinus cervinus* occurs for SST between 21°C and 24°C; Pajuelo *et al* (2006) showed that *D. vulgaris* spawning season occurred in winter when water temperatures were the lowest, with a peak of the spawning activity in January; Pajuelo *et al* (2008) observed that the peak of reproduction of *D. puntazzo* coincided with the start of seawater cooling (i.e. decreasing temperature) around September. Sheaves (2006) realized a meta-analysis on Sparids to assess the influence of temperature on the spawning onset and highlighted that spawning is triggered by temperature, but in diverse ways depending on latitude. Indeed, the lower the latitude, the closer the spawning dates are to the lowest SST months but also to the minimal photoperiod months. It also appears that temperature is the preponderant factor because the relationship at monthly time-scales between temperature and spawning is stronger than the one with photoperiod. Sheaves (2006) also highlighted that Sparids have different timing of spawning, depending on the area they are living in, but nearly the same general range of water temperature at the end, which can probably be linked with gamete, egg or larvae development and survival needs. Concerning *D. vulgaris* in Southwestern Portugal, Gonçalves (2003) invests the spawning period via the study of the gonadosomatic index which is the ratio of the weight of the gonad reported on the fish weight (GSI = gonad weight / total live weight). He thus found an inverse correlation between the gonadosomatic index and both photoperiod and SST, thus highlighting the potential influence of those environmental drivers on both the starting and duration of spawning. He also showed that the reproduction occurred between October and January at low temperatures (14.1°C to 15.5°C) and at irradiance of 6 hours maximum. Though, there seems to be confusion between irradiance and photoperiod – both words are used as the number of sunny uncovered-sky hours, despite having theoretically different meanings. Indeed, irradiance is the energy received per unit time on a unit horizontal area for a given wavelength and can largely vary over time due to the day of the year and the weather, clouds, leaf cover, etc. Morato *et al* (2003) and Mouine *et al* (2007), for *D. sargus* in the Azores and *D. sargus sargus* in the Gulf of Tunis respectively, analysed the gonadosomatic index and the monthly variations in gonad maturity to determine the spawning period. When associating these two latter indicators with seawater temperatures, they found that spawning individuals first appeared in March when sea surface temperature increased from its minimum, around 15°C. The reproduction period lasted until June and stopped when temperature rises above 17°C. Thus, the optimal spawning temperatures seem to range between 15°C and 17°C. They speculated that this range of seawater temperatures occurs in spring when high densities of plankton are available for larvae when developing during their dispersive larval stage. This is typical of temperate areas where plankton productivity is seasonal, explaining why predator highly develops due to the synchrony between predator and prey populations – the so-called match-mismatch hypothesis (Cushing, 1990). A comparison between results from multiple regions of the world determined that the spawning period increased in duration and started earlier when the latitude decreased (Morato *et al*, 2003). Potts *et al* (2014) conducted a meta-analysis on the *D. sargus* sub-species and discovered that the spawning started for seawater temperatures ranging from 15°C to 20°C, while they also concluded that photoperiod was not a major determinant of spawning initiation. So in conjunction with De Vlaming arguments, photoperiod and irradiance will not be studied in this report. These results suggest an influence of temperature on the onset and duration of spawning for *D. sargus*. Furthermore, Di Lorenzo *et al* (2014) detected exceptional and unusual movements of *D. sargus sargus* outside of their home range between the 31st March and the 17th May in Torre Guaceto MPA, South-East Italy. They concluded that these movements were indicative of spawning behaviour, so that April-May would be the spawning season. They also found that SST had increased from 13°C to 18°C during this period. Aspillaga *et al* (2016) described the same kind of exceptionally far-reaching movements correlated with the increase of in-situ temperature in early spring, shortly after the winter minimum. A part of these articles is summarized in the Table 3.

Nevertheless, temperature will be the central studied factor here because, on the one hand, the bibliographic review suggests that it triggers spawning for very diverse species of fishes (see Table 1) and, on the other hand, numerous factors are themselves depending on temperature variability (see Figure 18). Moreover, authors studying temperature along with other factors influencing spawning often concluded with the preponderant role of temperature (De Vlaming, 1972 ; Sheaves, 2006 ; Potts *et al*, 2014).

Table 1: Factors influencing spawning according to literature. Blue: Sparids ; black: other Teleosts.

Factor	Species	Area	Articles
Temperature	Teleosts	Victoria, Australia	King *et al*, 2016
	Clupea harengus	Newfoundland, Canada	Winters & Wheelers, 1996
	Pseudogobius olorum	Western Australia, Australia	Gill *et al*, 1996
	Teleosts	Oregon, USA	Auth, 2017
	Solea solea	Irish sea, North Sea, Channel	Fincham *et al*, 2013
	Gadus morhua	North Sea, Scotland	McQueen & Marshall, 2016
	Epinephelus marginatus	Medes Islands MPA, Catalonia, Spain	Hereu *et al*, 2006
	Thunnus thynnus, *Auxis rochei*, *T. alalunga*	Balearic archipelago, Spain	Reglero *et al*, 2012
	Sparidae	Meta-analysis	Sheaves, 2006
	D. sargus subspecies	Meta-analysis	Potts *et al*, 2014
	D. sargus, *D. annularis*, *D. puntazzo*, *D. vulgaris*	Gulf of Tunis, Tunisia	Mouine *et al*, 2011
	D. cervinus cervinus	Canarian archipelago, Spain	Pajuelo *et al*, 2003
	D. vulgaris	Canarian archipelago, Spain	Pajuelo *et al*, 2006
	D. puntazzo	Canarian archipelago, Spain	Pajuelo *et al*, 2008
	D. vulgaris	South Western Portugal	Gonçalves, 2003
	D. sargus	Azores archipelago, Portugal	Morato *et al*, 2003
	D. sargus sargus	Gulf of Tunis, Tunisia	Mouine *et al*, 2007
	D. sargus sargus	Torre Guaceto MPA, Puglia, Italia	Di Lorenzo *et al*, 2014
	D. sargus	Medes Islands MPA, Catalonia, Spain	Aspillaga *et al*, 2016
Photoperiod	Teleosts	Meta-analysis	De Vlaming, 1972
	Lepomis macrochirus	Story County, Iowa, USA	Mischke & Morris, 1997
	Dicentrarcus labrax	West Coast of Portugal	Vinagre *et al*, 2009
	D. vulgaris	South West Coast of Portugal	Gonçalves, 2003
	Sparids	Meta-analysis	Sheaves, 2006
Irradiance	*D. vulgaris*	South West Coast of Portugal	Gonçalves, 2003
Moon / Tides	*Cheilinus undulatus*	Republic of Palau	Colin, 2010
	Paracirrhites forsteri	Kuchierabu-jima Island, Japan	Kadota *et al*, 2010
	Takifugu niphobles	Kyushu Island, Japan	Yamahira, 1997
	Epinephelus marginatus	Medes Islands MPA, Catalonia, Spain	Hereu *et al*, 2006
	Thalassoma bifasciatum	Puerto Rico	Appeldoorne *et al*, 1994
	Acanthopagrus pacificus	Queensland, Australia	Sheaves & Molony, 2013
	Acanthopagrus berda	Kosi estuary, South Africa	Garratt, 1993
Dark / Night	*Osmerus mordax*	Newfoundland, Canada	Bradbury *et al*, 2004
	Acanthopagrus berda	Kosi estuary, South Africa	Garratt, 1993
Upwelling	*Centroberyx gerrardi*	South-Western Australia	Coulson *et al*, 2019
	Sardinops, Engraulis	California, USA	Lluch-Belda *et al*, 1991
Demography	Teleosts	Meta-analysis	Wright & Trippel, 2009
Lipid storage	*Gambusia affinis*	Illinois, North Carolina, New Jersey, USA	Reznick & Braun, 1987
Settlement (competition and food availability)	*D. annularis*, *D. sargus*, *D. puntazzo*, *D. vulgaris*, *Oblada melanura*, *Sarpa salpa*	Marseille, France	Harmelin-Vivien *et al*, 1995
	D. puntazzo, *D. sargus*, *D. vulgaris*	North-West Mediterranean Sea	Planes *et al*, 1999

The focus of this study is the white seabream *Diplodus sargus* (Linnaeus, 1758). Considering the previous literature review, this Sparid is a good model species to study the role of temperature in controlling spawning. *D. sargus* is a demersal fish of the Sparid family economically relevant in the Mediterranean fisheries, targeted both by recreational and professional fisheries (Sala *et al*, 1998). Relatively sedentary at adult stage with an home range of approximately 1 or 2 km² (Di Lorenzo *et al*, 2014 ; Aspillaga *et al*, 2016), it inhabits rocky coasts and *Posidonia oceanica* meadows (Guidetti, 2000). It is a keystone species as it feeds on the sea urchins *Paracentrotus lividus*, that graze macroalgue such as *Posidonia oceanica* and can cause regime shift in ecosystems if not regulated (Hereu *et al*, 2005). The sexual maturity happens at about 4 years old (Mouine *et al*, 2007 ; Mouine, 2009). The spawning period fluctuates from February to the end of June (Table 3), accordingly to the Mediterranean region, and happens once a year. The eggs - that hatch after about 2 or 3 days (Ranzi, 1933; Divanach *et al*, 1982 ; Jug-Dujakovic & Glamuzina, 1988) - and larvae disperse offshore during circa 13 to 19 days (Di Franco & Guidetti, 2011 ; Di Franco *et al*, 2012b) likely within the shallow layers of the water column, between 0 to 10 meters depth (Olivar & Sabatés, 1997) until the competence phase appears - which is the capability of swimming, appearing at the end of the dispersion, just before settlement (Clark *et al*, 2005). The juveniles (approximately 1 cm of total length) can then be found in nurseries from 0 to 2 m depth in sandy-rocky bays (Harmelin-Vivien *et al*, 1995 ; Lenfant & Planes, 1996) and, after about 6 months at about 6 to 8 cm long, they can join the adult fraction of the population in a phase named recruitment (Cuadros *et al*, 2018 ; Figure 1). *D. sargus* can be 30 cm long (even 40 cm very rarely), but large adults are limited in the Mediterranean Sea due to over-exploitation (Mouine *et al*, 2007).

This study aims at determining how abiotic factors influence the variability of fish spawning, using the Sparid *Diplodus sargus* as a model species. Our investigations focus on the impacts of the inter-annual variability of ocean temperature and currents in controlling the onset, duration and termination of spawning. We first exploit juveniles observations (acting as proofs of effective spawning) with a backward-in-time Lagrangian model (a particle tracking model, parameterized with observed data) to locate the place and period of spawning and to assess its respective contribution in providing larvae to the surrounding nurseries. Such spawning areas then help to determine a range of modelled temperature, concordant with the bibliography, that would trigger spawning. Based on this range of temperature and the multi-year outputs of a regional ocean model, we model and analyse the inter-annual variability of dispersal and spawning locations and duration over ten years, from 2005 to 2014, in some ecoregions of the Mediterranean Sea. We finally perform factorial model experiments to help determining which factors, between currents and temperatures, prevail on the inter-annual variability of spawning. These results are then discussed against the literature and are interpreted in a management context.

2   Material and Methods

2.1   Geographical context

The Mediterranean Sea is the largest and deepest marginal sea on Earth (Coll *et al*, 2010). It is situated between Europe, Africa and Asia continents and connects to the Atlantic Sea through the Gibraltar Strait, leading to specific and variable intra-annual circulation patterns, with two subregions (western and eastern sub-basins) divided by the Siculo-Tunisian Strait (Pinardi & Masetti, 2000 ; Figure 2). The Mediterranean Sea is a biodiversity hot spot, containing 6.3 percent of the macroscopic marine organisms over the oceans of the world (Bianchi & Morri, 2000 ; Coll *et al*, 2010). Endemism is also important, representing one quarter of the Mediterranean biota (Bianchi & Morri, 2000). For instance, the Adriatic Sea contains 37 to 45 endemic species (Coll *et al*, 2010), apparently due to its particular topography constraining the oceanic circulation (semi-closed sea, exchanging water masses via the Strait of Otranto ; Millot & Taupier-Letage, 2005 ; Poulain *et al*, 2013) and due to its diversity of macro-habitats, spanning fine sandy sediments, rocky outcrops and seagrass meadows. One of this endemic species is the submarine plant *Posidonia oceanica*, regrouping in meadows, thus representing a crucial habitat for many Mediterranean fishes, including *Diplodus sargus*. More generally, scientists view the Mediterranean sea as a model ocean because its overall functioning as well as the pressure it faces (strong demographic pressure, major political differences, over-fishing, pollution,

climate change and loss of biodiversity) are similar to those of the world's ocean.

Professional Mediterranean fisheries are represented by a large part of artisanal and coastal fisheries with boats of around 12 meters (80 percent of the Mediterranean fishing fleet, see European Commission website, https://ec.europa.eu/fisheries/cfp/mediterranean_en). The multiplication of countries around the Mediterranean Sea lead to a difficulty of applying fisheries rules as a basin scale, thus making this sea as one of the more over-exploited in the world, with 75 percent of the stocks being over-fished (Tsikliras *et al*, 2015 ; FAO, 2018). There is a urgent need to develop research and management for a more sustainable exploitation of fish stocks and a more efficient protection of threatened species in this sea.
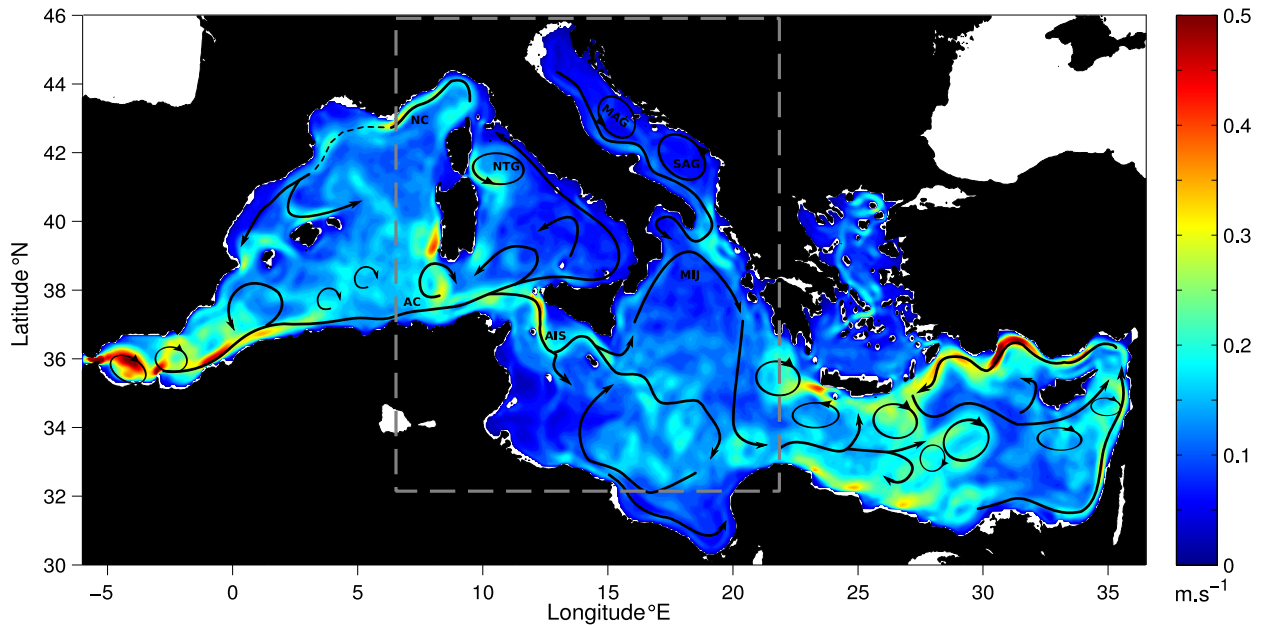
Figure 2: Schematic representation of surface currents adapted from Poulain *et al* (2012) and mean modulus (m.s^{-1}) of the surface velocity field adapted from Dubois *et al* (2016). The domain studied is indicated by the grey lines. AC = Algerian Current, AIS = Atlantic-Ionian Stream, MIJ = Mid-Ionian Jet, NC = Northern Current, NTG = North Tyrrhenian Gyre, SAG = Southern Adriatic Gyre, MAG = Middle Adriatic Gyre.

The oceanic regions studied in this report are the Ligurian Sea, the Ionian Sea, the Tyrrhenian Sea and the Adriatic Sea, which are all located in the Mediterranean Sea (Ayata *et al*, 2018). Two other ecoregions were also studied: the coast of Algeria and the "Gabes" eco-region, encompassing the Siculo-Tunisian Strait, Malta to the East and the Gulf of Gabes to the South. Note that the studied region is also delimited by the domain of the regional ocean model used here, which was then subdivided into different ecoregions (Figure 3). We study the spawning process at a local scale, focusing on sampled sites, and then on a larger-spatial scale by analysing the previously defined ecoregions that contain substantial numbers of potential spawning areas.

2.2 Early-life history traits collection

The early life history traits data of *D. sargus* were used in this study. Juveniles on 11 sites were caught with a handnet in June 2008 (Di Franco *et al*, 2011) and June 2009 (Di Franco & Guidetti, 2011). Sampling sites are located all along the Italian coasts in the nursery sites of Genova (Liguria - Ligurian Sea), San Isidoro (Apulia – Ionian Sea), Maratea (Basilicata - Tyrrhenian Sea), Torre Guaceto (Apulia – Adriatic Sea) in 2008 (Di Franco *et al*, 2011) and Bari, Monopoli, Hotel La Darsena, Torre Guaceto Marine Protected Area (MPA), Punta Penne, Casalabate and San Andrea (Apulia – Adriatic Sea) in 2009 (Di Franco & Guidetti, 2011) which
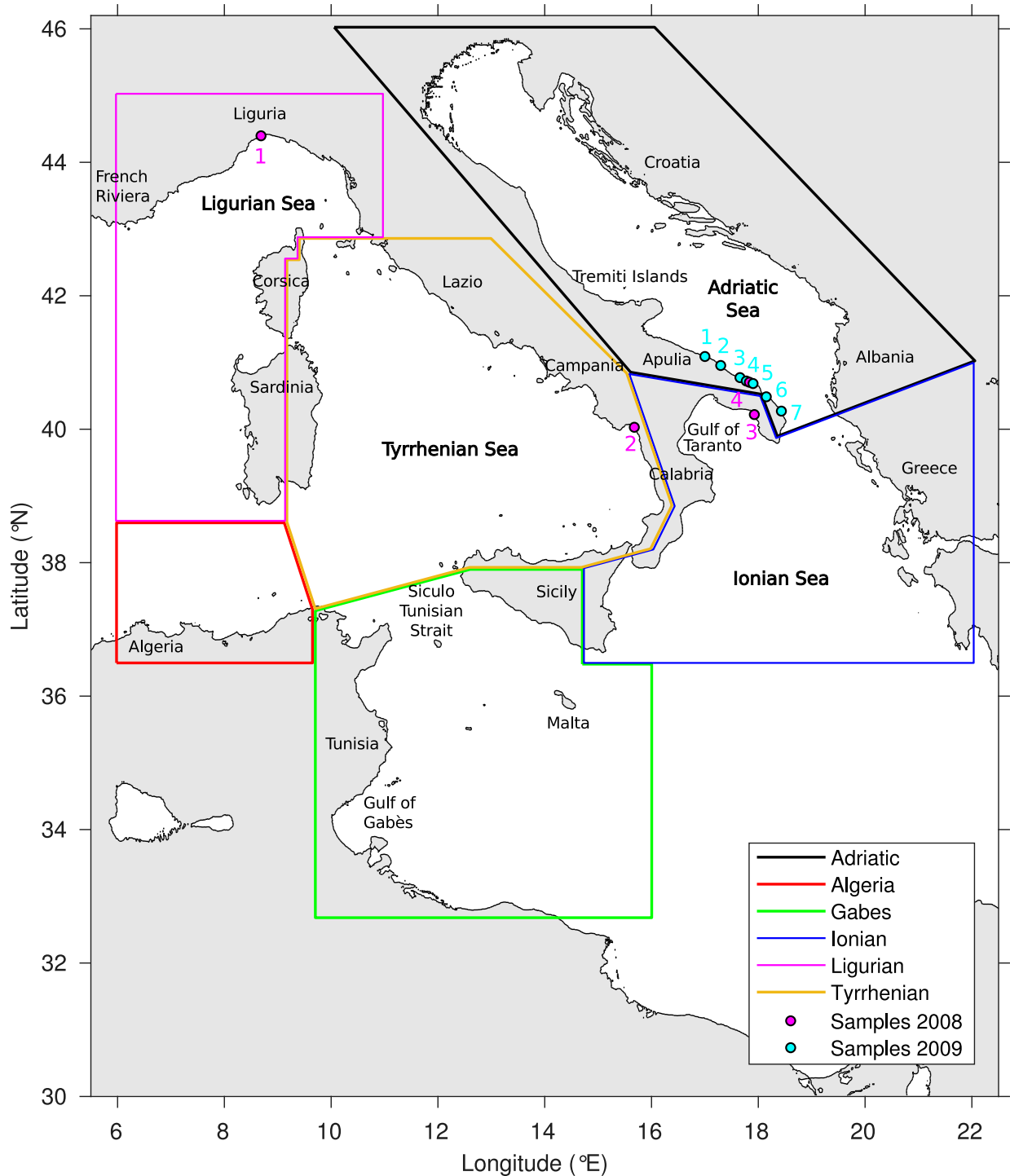
Figure 3: Subdivision of the AIFS domain into ecoregions (colors will be kept for further analyses). The major site names are in black. The sites of 2008 are in pink color: 1. Genova, 2. Maratea, 3. San Isidoro, 4. Torre Guaceto. The sites of 2009 are light blue: 1. Bari, 2. Monopoli, 3. Hotel La Darsena, 4. Torre Guaceto MPA, 5. Punta Penne, 6. Casalabate, 7. San Andrea.

can be observed on the Figure 3. Samples were analysed via sclerochronology technics - which is the study of hard tissues in marine organisms by observing the growth increments reflecting time steps in the organism

life - on otoliths which are calcified concretions located in the inner ears of the fish and used for stability. Otoliths' increments are deposited daily through fish life, from hatching to sampling (Tsuji & Aoyama, 1982). That's how early life traits can be determined for each fish from a given year and site. Otoliths have been extracted from the samples to read their daily increments with a microscope. The goal here is to determine the spawning phenology of the fish, represented by the spawning date and the Pelagic Larval Duration (PLD) which is the time spent by the larvae between hatching and settlement (Di Franco *et al*, 2011 ; Di Franco & Guidetti, 2011). Knowing the sampling date, i) the settlement date was back-calculated by counting the daily increments from the last ring of the otolith to the transitional ring representing the settlement - when larvae metamorphose into juveniles (Figure 1). Then, (ii) the spawning date was back-calculated by counting the daily increments from the settlement date to the otolith centre represented by the nucleus/primordium - forming during the embryonic development in the egg (Di Franco *et al*, 2011). Then, we must account the time between spawning and hatching, which is about 3 days for *D. sargus* (Ranzi, 1933; Divanach *et al*, 1982 ; Jug-Dujakovic & Glamuzina, 1988). The PLD is thus the number of days - so the number of increments - between the spawning date and the settlement date.

2.3 Lagrangian model used for dispersive larval phase modelling

The Lagrangian Flow Network (LFN) methodology combines network theory tools and a particle-tracking model to investigate transport and dispersal processes in oceanic flows. As most off-line particle-tracking model, it can be coupled to any gridded two- or three-dimensional velocity fields available, returning dispersal diagnostics as realistic as the input flow field. Full description can be found in Rossi *et al* (2014), Ser-Giacomi *et al* (2015), Dubois *et al* (2016) and Monroy *et al* (2017). Here, the LFN simulates the dispersal of passively drifting larvae as horizontal Lagrangian trajectories obtained through the integration of a high-resolution flow field generated by a regional hydrodynamical model.

We use the Lagrangian Flow Network model (LFN), which combines network theory tools and particle-tracking modelling, to simulate the dispersal of fish early-life stages (Monroy *et al*, 2017). As any other Lagrangian model, it must be coupled to any gridded two-dimensional velocity fields. (i) The LFN discretizes the domain of interest, given by the velocity field dimension, in a mesh of relatively square box called nodes. (ii) It computes a land ratio for each node according to the number of grid point for which the hydrodynamical model simulates realistic velocities (e.g. a node with a land ratio of 0/1 is considered fully covered by sea/land, respectively). (iii) It then seeds homogeneously particles in each node, proportionally to its land ratio. (iv) It calculates passive horizontal trajectories by integrating the velocity fields of the hydrodynamical model, simulating the dispersal of passively drifting larvae for a pre-determined starting time and duration. Finally, the LFN builds a connectivity matrix to encode all particles exchanged between any pairs of nodes and/or retained within them. Such connectivity matrix contains all the dispersal information: each element of the matrix is characterized by a row, the departure node, and a column, the arrival node, while the element itself is the number of particles exchanged between these nodes. The diagonal elements of the matrix represent the retention of particles in each node. The elements of the matrix can be readily transformed into probabilities by normalizing the numbers of particles, that is dividing each element by the sum over the rows to study forward-in-time dynamics, or by the sum over the columns approximating backward-in-time dynamics, as done here (Ser-giacomi *et al* 2015 ; Legrand *et al* 2019).

We select the most adequate hydrodynamical model to the sampling sites, the Adriatic-Ionian REGional configuration (AIREG, Ciliberti *et al*, 2015 ; Oddo *et al*, 2006), which is based on the NEMO kernel (Madec and others, 2015). The model gives us daily two-dimensional high-resolution velocity fields (1/45°) on 121 depths for years ranging 2005 to 2014. We further configure the LFN by fine-tuning both numeric and biologic parameters:

- we select the velocity fields depth to 10 meters because the evidences available suggest that Sparid larvae disperse around this depth (Olivar & Sabatés, 1997) ;
- we set the node size to an horizontal resolution of 1/16° which represents a node of around 6 km long and a surface of around 40 km²;

- we choose the initial number of particles per node to 100, prior to the land ratio, as prescribed in Monroy *et al* (2017) ;
- we set the Runge-Kutta time step for the Lagrangian trajectories integration to 30 min, fulfilling the Courant-Friedrichs-Lewy condition (De Moura & Kubrusly, 2013) ;
- we choose the starting date of the Lagrangian experiments according to the spawning dates of D. sargus determined through otoliths' reading (Table 2) or the literature.
- we set the particle tracking durations according to the PLD of *D. sargus* determined through the otoliths' reading of each site (see section "Data-constrained dispersive larval phase modelling to locate spawning areas and determine favorable temperature" ; Table 2 ; see Appendix 4) or by a single value (16 days) obtained by averaging observed PLDs and values found in the literature (see section "Modelling the spatial and temporal variability of spawning for *D. sargus*" ; see Appendix 4).

2.4 Data-constrained dispersive larval phase modelling to locate spawning areas and determine favorable temperature

Based on effective sequences of spawning/dispersal/ recruitment events, as determined by the otoliths' reading, the aim here is to determine the actual spawning areas and to test the abilities of our modelling approach to address the role of abiotic factors (currents and temperature) on spawning. We call this part of the study *"Data based approach"*. First of all, we locate and delimit the spawning areas associated with each sampled site thanks to (i) the fine-tuning of our model parameters (i.e. starting date and particle-tracking duration are in accord with observed *D. sargus*'s early-life traits, cf. spawning dates and PLD reported in Table 2 and Appendix 4) and (ii) back-tracking larvae backward-in-time, from the settlement places back to where they originated, which are ultimately the spawning areas. Then, we determine and compile all the modelled temperatures found within these restrained spawning areas.

For each site, we derive a range of spawning dates (minimum and maximum) obtained by keeping 95 percent of a normal probability distribution adjusted on the spawning dates obtained by schlerochronology (Table 2). We consider this range of spawning dates as the temporal limits of that given spawning event and we run a LFN experiment for each day of the period. The LFN runs as many experiments as the numbers of successive days in the period while the median PLD is the LFN tracking-time. Thus, each LFN experiment predicts the location of the spawning area associated to each location where juveniles were collected. It identifies and evaluates the probability of all the origin nodes which would have sent particles to the arrival nodes encompassing the sampled sites.

Table 2: Median PLD, minimum and maximum spawning date for each sampling site and year (Di Franco *et al*, 2011 ; Di Franco & Guidetti, 2011).

Year	Site	PLD	Minimum spawning date	Maximum spawning date
2008	Maratea	14	28/05	12/06
	Torre Guaceto	17	05/05	04/06
	San Isidoro	15	22/05	01/06
	Genova	13	22/04	18/05
2009	Bari	16	07/05	18/05
	Monopoli	16	08/05	14/05
	Hotel La Darsena	16	09/05	18/05
	Torre Guaceto	17	10/05	15/05
	Punta Penne	17	04/05	18/05
	Casalabate	17	04/05	26/05
	San Andrea	16	10/05	22/05
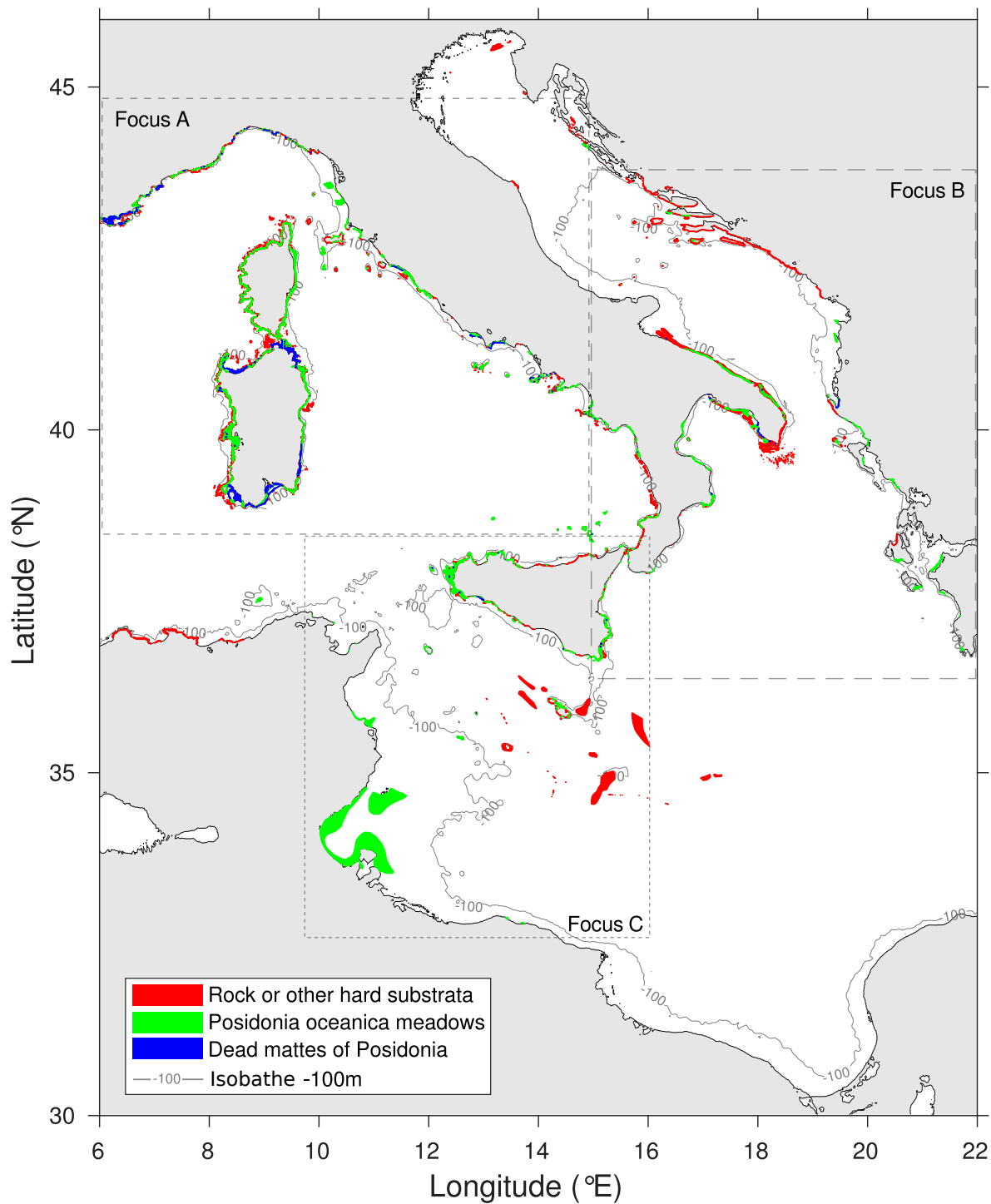
Figure 4: Substrats, from the EMODnet portal (European Marine Observation and Data Network, http://www.emodnet.eu/seabed-habitats), and isobath -100 meters used to determine the habitat of *D. sargus*, chosen in accord with the literature concerning *D. sargus* (Guidetti, 2000 ; Di Lorenzo *et al*, 2014 ; Aspillaga *et al*, 2016 ; Giacalone *et al*, 2018). The grey lines delimit three focus regions that will guide the results analysis (Figures 10, 11, 12 and 13).

While the full dispersal information is contained in the connectivity matrices, we must filter out some elements whose information is not adequate for our purpose, e.g. when origin and/or destination nodes cannot be candidates for spawning and/or nursery. The first filter on arrival nodes (i.e. columns of the connectivity matrices) to determine the sampling area is characterized as four sampling nodes selected for each site, which are chosen to encompass the sampling sites and to limit "beaching" artefacts (i.e. the mean land ratio of the four sampling nodes must be low and almost similar for each sampling site). The second filter on departure nodes (i.e. row of the connectivity matrices) is chosen accordingly to the biotope of our target species: *D. sargus* lives near the sea floor over the inner continental shelf on rocky substrate and *Posidonia oceanica* meadows (Guidetti, 2000). Since *D. sargus* have been observed at least until 80 meters depth during the spawning period (Aspillaga *et al*, 2016 ; Giacalone *et al*, 2018), a conservative representation of the spawning process was made within 100 meters depth. When considering the scale of our study and the precision of the ocean model, preliminary analyses revealed that changing this bathymetric limit to 50 or 80 m does not change largely the resulting habitat filter (not shown). Thus, the second filter was constructed by keeping departure nodes which encompass (*Posidonia oceanica* and rocks) substrates and are characterized by a bathymetry shallower than 100 meters depth (Figure 4). The habitat data was downloaded from the EMODnet portal (European Marine Observation and Data Network, http://www.emodnet.eu/seabed-habitats) and was also hand-corrected by experts (Legrand *et al*, 2019). The bathymetry data was taken from the ETOPO1 Global Relief Model, on the NOAA website. After the filtering process, filtered matrices are shaped in the same way: 1500 rows depict the spawning habitat, four columns depict the sampling area (i.e. the area made by the four sampling nodes) and each element represents the number of particles sent by the spawning habitat to the sampling node (Figure 5 ; see Appendix 5). The number of particles ranges from 0 to 100, where a non-zero value means that the spawning habitat is a spawning area which sends larvae to the sampling area.

After filtering, the matrices are normalized (i.e. to transform the number of particles exchange between spawning habitat and sampling nodes into a probability), weighted according to their significance in the spawning phenology, i.e. we approximate the spawning phenology as a Gaussian distribution fitted to the spawning date (Table 2 ; Appendix 1, 2 and 3) and combined to obtain the spawning potential of each spawning area (Figure 5). First, we divide each element of the filtered matrices (the number of particles sent by the spawning habitat to the sampling node) by the sum of the elements of its column (the total number of particles sent by the entire spawning habitat to the sampling node). Second, we sum the four columns (four sampling nodes) of the filtered matrices into one (i.e. considering the four sampling nodes into one sampling area) and normalize it (same procedure as above). Third, we weight each filtered and normalized matrices accordingly to its position in the Gaussian distribution fitted on the spawning dates (Figure 5). Thus, each filtered and normalized matrix is weighted differently depending on its position in the Gaussian approximation of the spawning phenology: more weight is given to connectivity matrices coinciding with the peak of spawning whereas less weight is given to matrices representing dispersal occurring at the extremity of the spawning range. Fourth, we combine all the weighted matrices into one following the weighted average described previously. Each element represents the probability of each spawning node to provide larvae into the sampling site during all the spawning period (Figure 5). Note that this procedure is done for each sampling site independently. When plotted, we map all the 11 spawning areas and characterize their larval contribution. This backtracking method consists in following the larvae backward-in-time from the sampling areas (nurseries) to the spawning areas (Legrand *et al* 2019).

Once the 11 spawning areas have been delineated in both space and time following the above-mentioned procedure, we study the range of modelled temperatures within them. If these temperatures more or less agree with those reported in the literature to trigger spawning, we have high confidence that our model is well adapted to study variability in spawning. We analysed all the sampling areas together (i.e. for all sampling sites in 2008 and 2009) for the whole duration of each spawning period (Table 2) to understand the patterns occurring in the studied areas at different scales. We compute the temperature values from the AIREG configuration (Ciliberti *et al*, 2015; Oddo *et al*, 2006), the same hydrodynamical model that we use for the velocity fields. The model gives us daily two-dimensional high-resolution temperature fields (1/45°) on 121 depths. We analysed the temperature inside each spawning area for depths ranging from 0 to 50 meters. Under these depths, the temperature was stable and showed no seasonal signal. We retained the temperature range which contains 95 percent among all the temperatures analysed by computing the

5 percent and the 95 percent quantiles (Figure 9). We then include our own model estimate in the list of temperature ranges gathered from the literature on *D. sargus*. We finally obtain averaged minimal and maximal temperatures triggering the spawning of *D. sargus* in the Mediterranean Sea. This range is then used in the next section "Modelling the spatial and temporal variability of spawning for *D.sargus*" as a threshold for modelling spawning.
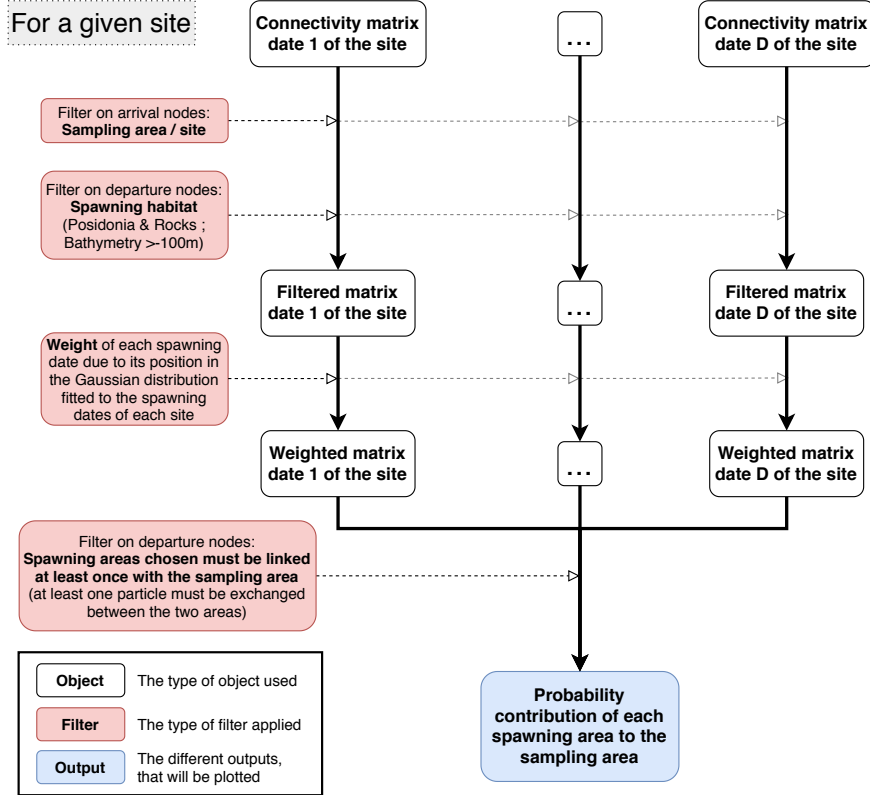

Figure 5: Representation of the method employed to process the connectivity matrices in the *data based approach*. Matrices (white boxes) are processed with the use of filters and weights (red boxes) to get the final output (blue box) as the probability of each spawning node contributing to each of the 11 sampled areas, seen in Figures 7 and 8. This method is done using all the daily connectivity matrices computed between the minimum and the maximum spawning dates for each site.

2.5 Modelling the spatial and temporal variability of spawning for *D. sargus*

Our aim here is to study simultaneously, and then separately, two abiotic sources of variability – namely currents and temperature – on the dispersal of early-life stages. In our modelling approach, ocean temperatures in favourable habitats determine the occurrence of spawning (e.g. starting point of dispersal) and ocean currents control the transport of propagules from the spawning areas to the nurseries. As such, we try to better understand how these abiotic factors influence the location and the phenology of spawning as well as the subsequent dispersal toward the nurseries. Thanks to this "*Modelling approach*", we can investigate the spatial and temporal variability of spawning over the entire model domain and for several years ranging from 2005 to 2014 (available data of the AIREG hydrodynamical model, Ciliberti *et al*, 2015 ; Oddo *et al*, 2006).

In this approach, we performed numerical experiments every five days since modelling this frequency of spawning has been shown to be equivalent to daily experiment for spawning season longer than three months,

according to Monroy *et al* (2017). Here we consider that the spawning season of *D. sargus*, as given by the literature (see also Table 3), spans the 1st of March to the 30th of June every year for the period 2005-2014. We choose a fixed tracking time of 17 days, equal to the median PLD given by all the otoliths analyses aggregated together (Table 2 ; Di Franco *et al*, 2011 ; Di Franco & Guidetti, 2011). Consequently, we built 25 connectivity matrices per year for ten years between 2005 and 2014.

Even though the *modelling approach* is not directly constrained by observations, it mirrors the filtering methods detailed in the *data based approach*. For each connectivity matrices, we filter out the departure nodes which are characterized by spawning habitat (Figure 6 ; see Appendix 5). However, instead of filtering the arrival nodes with the 11 sampling sites, we here consider all the possible nurseries of the domain, i.e. all the nodes characterized by a favourable settlement habitat. They must house favourable substrates (i.e. *Posidonia oceanica* and rocks) and be characterized by a bathymetry shallower than 100 meters depth (Figure 4). Note that this habitat filter is similar to the ones applied for spawning. After filtering, matrices have 1500 rows depicting the spawning habitat and 1500 columns depicting the settlement habitat.
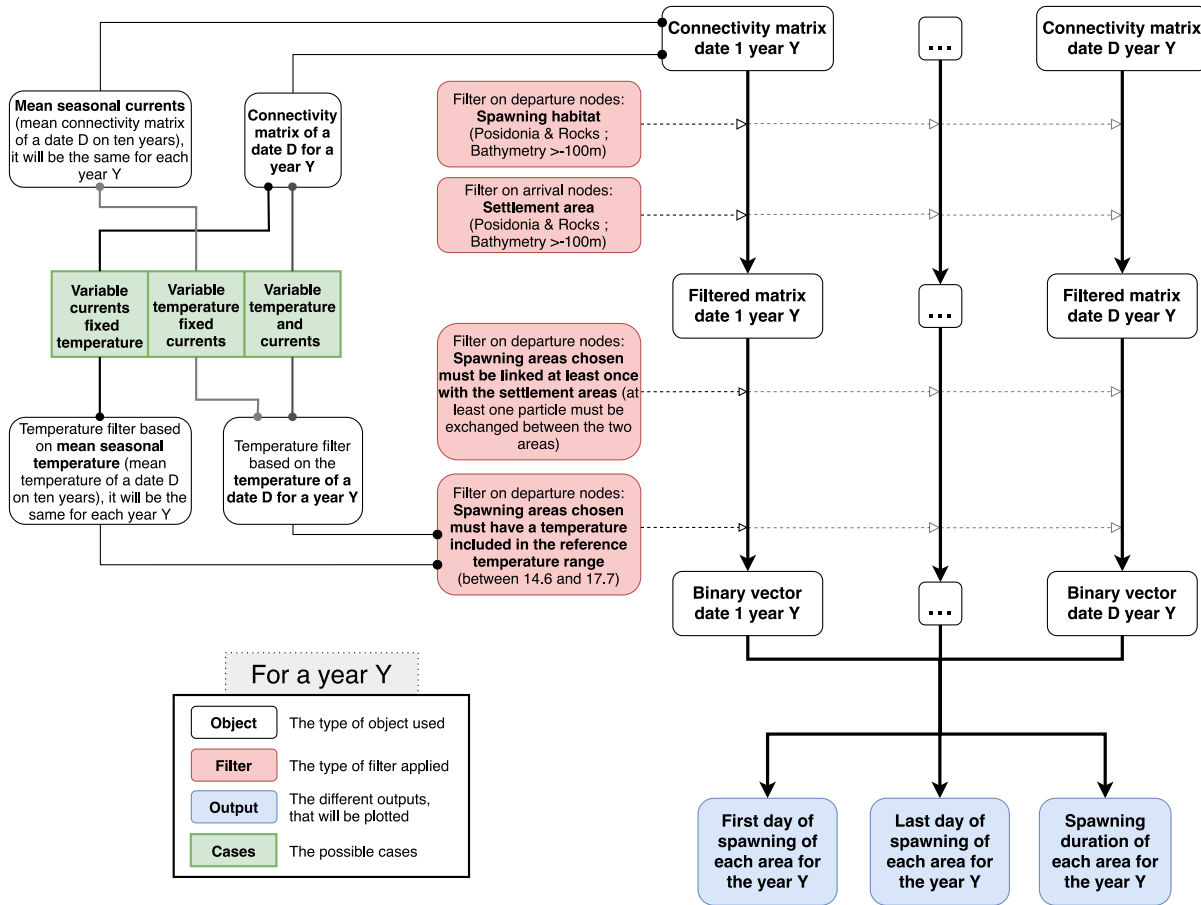
Figure 6: Representation of the method employed in the *modelling approach* described in section "Modelling the spatial and temporal variability of spawning for *D. sargus*". The objects (white boxes) represent matrices or vectors and are processed with the use of filters (red boxes) according to three different cases (green boxes) to get the final outputs (blue boxes). They are displayed in Figures 10, 11 (spawning duration), 12 (first date of spawning) and 13 (last date of spawning). The successive dates (1, ..., D) symbolize the onset of the successive spawning events of a given year Y (similar each year, chosen in the period from the 1st of March to the 30th of June, with a step of five days between two spawning dates).

To get meaningful probabilities, we then sum all the columns of the filtered matrices together (i.e. all the settlement habitats are then represented into one global settlement area): each element of the 1500x1 filtered matrices gives the number of particles send by a spawning area (i.e. a filtered departure node) to the global settlement (i.e. all filtered arrival nodes). If (i) an element displays a non-zero value, its corresponding spawning area is linked (with at least one particle exchanged) to the settlement area. If (ii) modelled temperatures inside a spawning area for depths ranging from 0 to 50 meters are included in the range of temperatures which triggers spawning of *D. sargus* in the Mediterranean Sea (14.6 -17.7 °C, see *data based approach*, Table 3), the fish are supposed to be able to spawn in this node. Then, we construct a binary vector, in which for each spawning area we attribute 1 if the two previous conditions are fulfil and 0 otherwise (Figure 6). For each year, we have 25 binary vectors representing the spawning phenology for *D. sargus* (i.e. each binary vector is related to a given spawning event occurring every 5 days between the 1st of March to the 30th of June). We then compute annual diagnostics of spawning for each node as follows: the first date when the spawning area is "activated" (i.e. the first date of the binary vector which displays 1 for that node), the last date when the spawning area is "activated" (i.e. the last date of the binary vector which display 1 for that node) and the spawning duration as the number of days when the spawning area is "activated" (i.e. the number of binary vectors between the first date and the last date which display 1 for that node ; this number is multiplied by five to take into account the five days periodicity of spawning events).

Three simulations are performed following this modelling approach (Figure 6, green part on the upper-right): the case "variable temperature and currents" consider together the full variability (e.g. using daily values, including seasonal and inter-annual changes) of temperature and currents for each spawning event over 10 years (Figure 6, case "variable temperature and currents"). By analysing the model outputs of case "variable temperature and currents", which assembles most of the natural variability of the spawning process in the ocean, we look for spatial patterns and we investigate the inter-annual variability. The two other cases allow each factor to be studied separately by letting one factor varying and by fixing the other one. The case "variable currents fixed temperature" is used to analyse the effect of the full variability of the oceanic circulation. In this case, the seasonal variability of temperature was kept as a mean seasonal cycle but its inter-annual variability has been removed. In other words, we compute a climatological mean of temperatures by averaging all temperatures modelled on a given date of the year over the 10 years considered. Climatological temperatures are applied each year similarly while ocean currents change every year (Figure 6, case "variable currents fixed temperature"). The case "variable temperature fixed currents", allows studying the effects of the full variability of temperature. In this case, the seasonal variability of the circulation was kept as a mean seasonal cycle but its inter-annual variability has been removed. To do so, we compute a climatological circulation by averaging connectivity matrices starting on a given date of the year over the 10 years considered. Climatological currents are then applied each year similarly while ocean temperature changes every year (Figure 6, case "variable temperature fixed currents"). The study of case "variable currents fixed temperature" and "variable temperature fixed currents", in comparison with the outputs of the case "variable temperature and currents", allow disentangling the source of variability of the spawning process and evaluating, among currents and temperature, which one is the preponderant factor responsible for the inter-annual changes of spawning.

We finally conduct a factorial analysis on the outputs of the case "variable temperature and currents" of the modelling approach (i.e. first day of spawning, last day of spawning and spawning duration) to determine the similarities and differences between years over the period 2005-2014 and between six ecoregions (previously defined in the Figure 3) using the R package FactoMineR (Lê *et al*, 2008). A Correspondence Analysis (CA) was applied on the number of days (Figure 15) as this diagnostic is quantitative. A Principal Component Analyses (PCA) were realized on the first date and the last date as these date can be considered as qualitative variables (Figures 16 and 17). The results of these statistical analyses allow determining temporal and spatial differences in spawning over the studied domain.

17

3 Results

3.1 Data-constrained dispersive larval phase modelling to locate spawning areas and determine favourable temperature
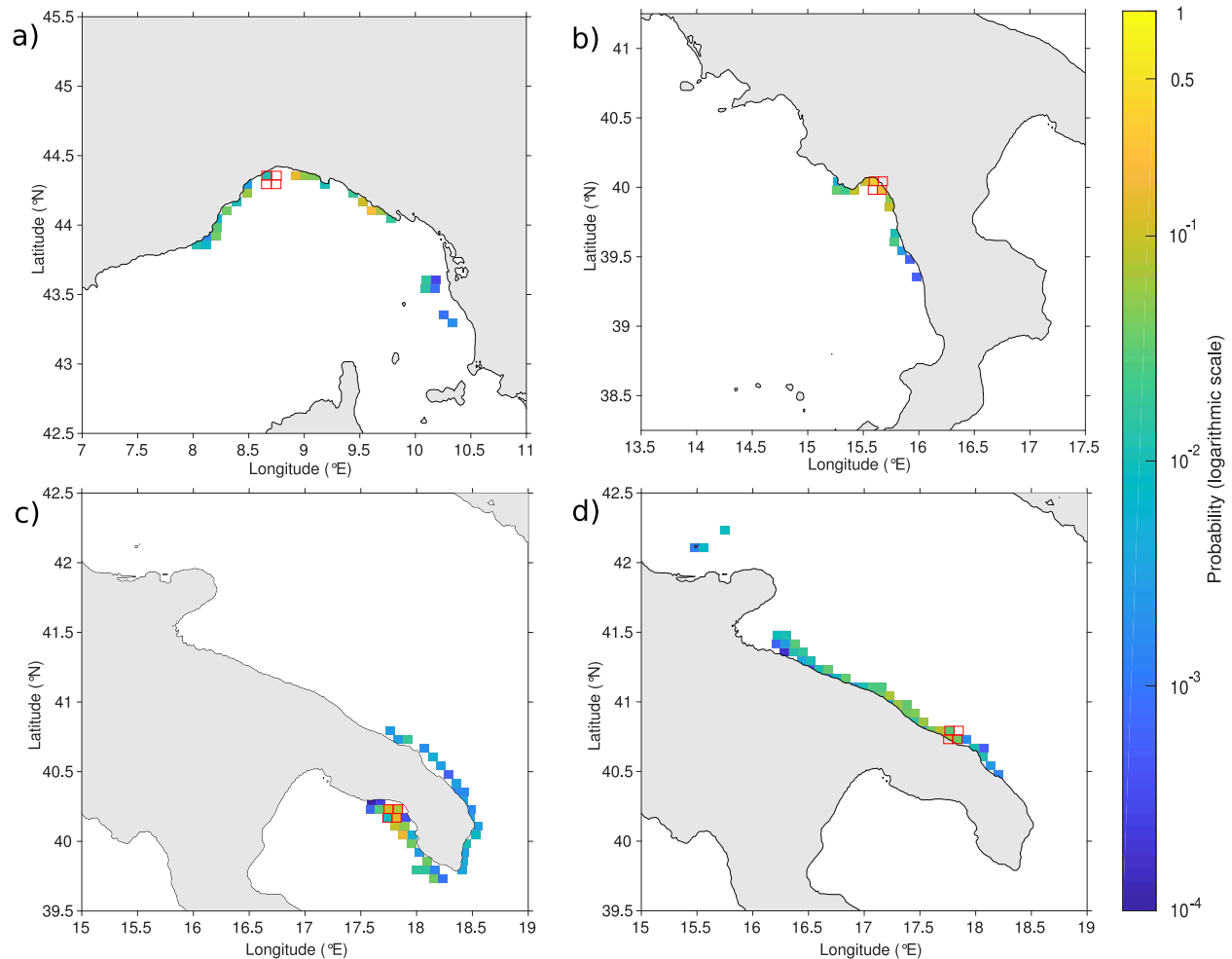

Figure 7: Locations of spawning areas and respective "larval" probability contribution based on 2008 sampling sites with a) Genova ; b) Maratea ; c) San Isidoro ; d) Torre Guaceto (see also Figure 3).

Discrete spawning areas have been found for each sampled site thanks to back-tracking experiment using the LFN model. They are displayed, along with the respective probability contribution of each node to the total larval pool, in Figure 7 for all sites sampled in 2008 and in Figure 8 for all sites sampled in 2009. In the Southern Adriatic Sea, our model suggests that most juveniles sampled in Apulia (Figures 8 and 3, light blue dots for sites 1 to 7) in 2009 originate from nearby spawning areas along the Apulian shores, especially in the Tremiti Islands (42.3°N, 15.6°E) and from the Gulf of Manfredonia to the South of Apulia (41.5°N, 16.3°E to 40.5°N, 18.3°E). In fact, for each site sampled in 2009, the spawning areas were found consistently northward of each sampled site. The same pattern occurred in 2008 for Torre Guaceto (site located in central Apulia, Figure 7d), with a few larvae coming from the Southern Apulian coastline (40.5°N, 18.3°E). In 2008 for the Ligurian Sea (Figure 7a), the juveniles sampled in Genova mainly come from spawning areas situated off Livorno and to the East of Genova (extending until La Spezia, 43.5°N, 10.3°E), while a relatively small proportion of eggs could have been released westward of Genova (until Imperia, 43.8°N, 8.2°E). Concerning the Tyrrhenian Sea (Figure 7b), the juveniles collected in Maratea would originate from larvae transported

18

from North Calabria (39.4°N, 16.0°E), Basilicata and South Campania (until Palinuro, 40°N, 15.4°E). Finally, the larvae contributing to the larval replenishment of San Isidoro (Figure 7c) in the Ionian Sea would have arrived from the Southern Gulf of Taranto and from the Southern Apulia coastline.

Concerning the contribution in larvae of each spawning area to the sampling site, it is highly variable and no specific pattern could be clearly identified. The minimum contribution is 10^{-4} and the maximum is around 0.5 for both years but the probabilities are not equally distributed within the "entire spawning area". For most sites a few nearby nodes constitute the main supplier (higher probabilities spanning 0.1 to 0.5, yellowish colors, Figures 7 and 8) while many more widespread nodes have significant but rather small contributions (probabilities inferior to 0.1). More generally, these dates - and locations - specific results suggest that (i) the exact locations of the main spawning areas (those with higher probabilities) vary among 2008 and 2009 for the single site that was repeatedly sampled (Torre Guaceto) and (ii) the spatial extent and distribution vary among ecoregions. Overall, it exemplify the spatial and temporal variability of the spawning process that will be studied in a systematic manner in the following.
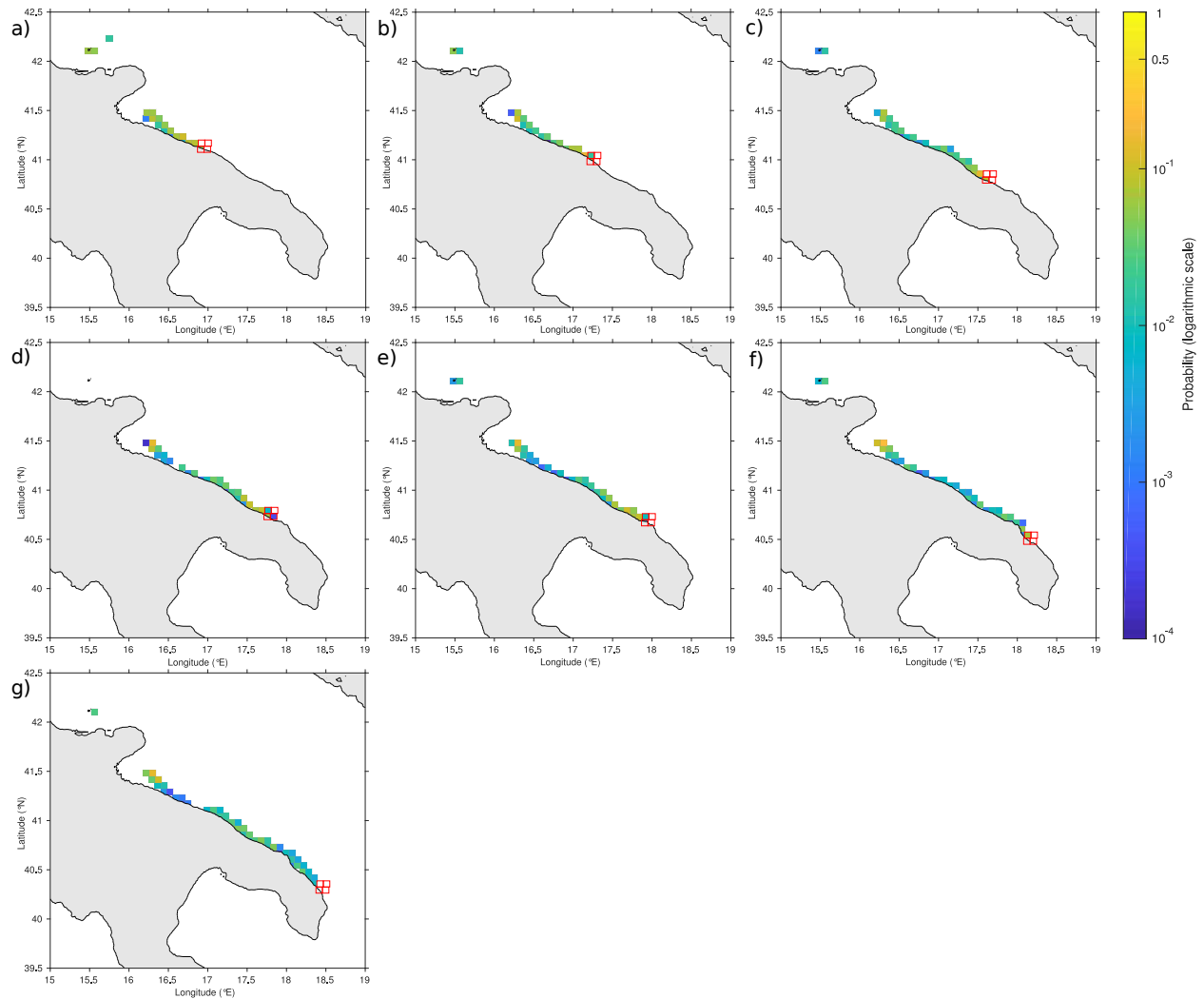
Figure 8: Location of spawning areas and respective "larval" probability contribution based on 2009 sampling sites with a) Bari ; b) Monopoli ; c) Hotel La Darsena ; d) Torre Guaceto ; e) Punta Penne ; f) Casalabate ; g) San Andrea.

When compiling all the modelled temperatures extracted from the exact dates and locations defined by these 11 backtracked spawning areas, we found a large range of temperature with a minimum around 13°C

and a maximum of 24°C (Figure 9). We found that 95 percent of all temperatures favourable for spawning range were between 14.8°C and 21.3°C (Figure 9), by taking 0.025 and 0.975 quantiles. After computing the average range combining our latter model estimate with the value compiled from the literature (Table 3), we obtain a final range between a minimum of 14.6°C and a maximum of 17.7°C that was then used as the triggering threshold of spawning in the following.
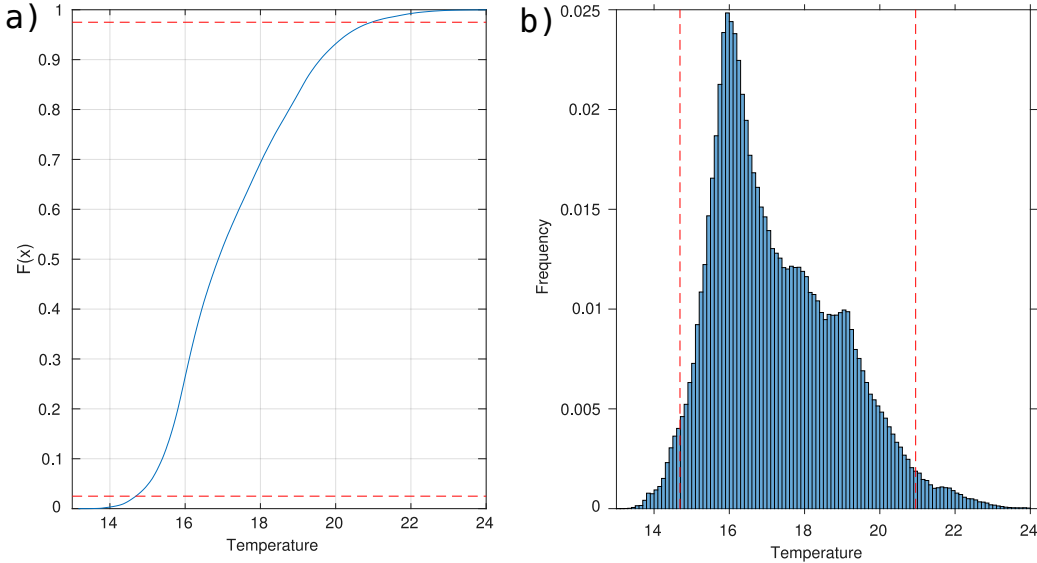

Figure 9: Model temperature favourable for spawning represented as a Cumulative Distribution Function (a) and as an histogram (b). The temperature of all sites are compiled for each grid point of the ocean model falling into a node favourable for spawning and for depths over 0 to 50 meters. The red lines represent the quantiles delimiting the domain containing 95 percent of all temperatures.

Table 3: Summary of the literature review about the minimum and maximum values of temperature triggering spawning (left column) and about spawning period (in month) documented for *Diplodus sargus* in the Mediterranean Sea. The penultimate line reports the values derived from the actual study; the last line presents the mean values.

Article	Minimum temperature	Maximum temperature	Minimum spawning date	Maximum spawning date
Aspillaga *et al* 2016	13	14.5	March	April
Di Lorenzo *et al* 2014	13	18	April	May
Mouine *et al* 2007	15	18	March	May
Mouine *et al* 2012	14.8	15.6	March	June
El Maghraby *et al* 1982	17	20	January	April
Benchalel & Kara 2010	15	18	February	April
Man-Wai 1985	14	16	April	May
Actual study	14.8	21.3	April	June
Mean	14.6	17.7	March	June

3.2 Modelling the spatial and temporal variability of spawning for *D. sargus*

The 10-year averages of our three diagnostics (i.e. first date, last date and spawning duration) for the case "variable temperature and currents" (Figure 10) are analysed to highlight spatial patterns. In comparison
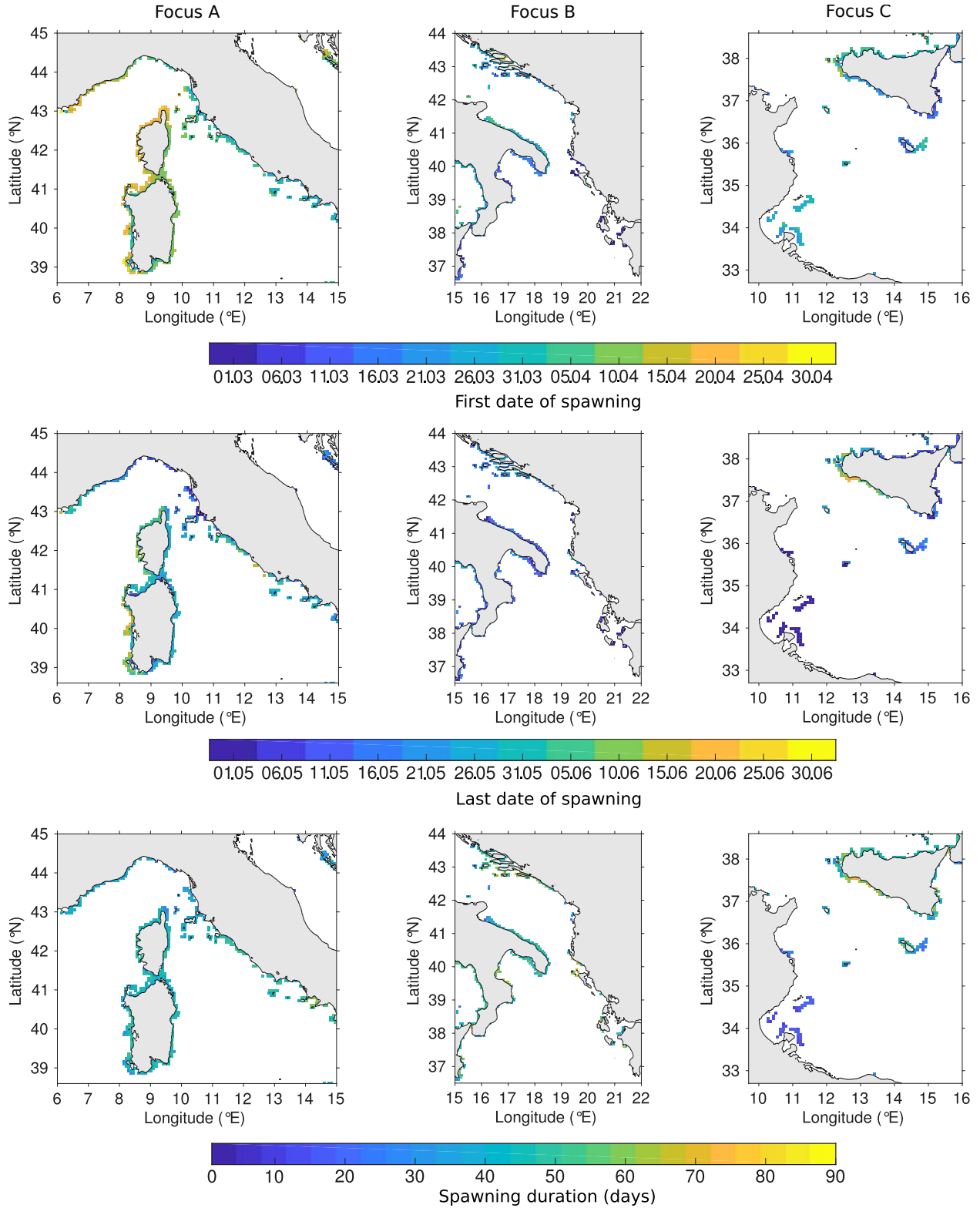
Figure 10: 10-year average for the case "variable temperature and currents" of the first date of spawning (onset, first row), the last date of spawning (termination, second row) and the spawning duration (in days, third row). The first column represents the regional focus A, the second column shows regional focus B and the third column displays the regional focus C.

with cases "variable currents fixed temperature" and "variable temperature fixed currents", note that the numerical experiments of case "variable temperature and currents" (Figure 6, green part on the right) were designed specially to mimic the environmental reality since it takes into account simultaneously the variability of both currents and temperature. As such, other scientists could also use these model results to compare against their observations or to guide future sampling efforts. The earliest averaged first dates (first row of Figure 10) range from the 1st of March to the 21st of March in the Ionian Sea (Greece, Albania, Gulf of Taranto, Eastern Sicily), the Croatian Islands (Figure 10, focus B), Malta and South-Western Sicily (Figure 10, focus C). The latest dates span April 10-30 in the French Riviera, the Corsica and Sardinia Islands (Figure 10, focus A) and the Western side of Sicily (Figure 10, focus C). For the other spawning areas, the averaged first spawning dates occurred between the 26th of March and the 10th of April. Concerning the last date of spawning (Figure 10, second row), it shows little spatial variations with spawning ending usually in May over most coastal regions. Exceptionally late spawning, until the middle or the end of June, take place in certain areas such as the Lazio, Western Corsica and Sardinia (Figure 10, focus A) and Western Sicily (Figure 10, focus C). Finally, the mean annual spawning duration (Figure 10, third row) does not exceed more than 90 days of spawning per year - that is equivalent to 74 percent of the maximum annual duration of 122 days for the retained period (from the 1st of March to the 30th of June). The areas with the lowest potential spawning duration - less than 20 percent of the total duration studied, that is around 25 days - are in the East of Malta and in the Gulf of Gabes (focus C). The highest ones, 65 days minimum, which is at least 50 percent of the spawning season, are located in the Campania (Figure 10, focus A), the Ionian Sea (South-Eastern Sicily, Eastern Calabria, Albania, Greece), the Croatian Islands (Figure 10, focus B) and the centre of Malta, the South-Western Sicily (Figure 10, focus C). The remaining areas exhibit between 20 and 50 percent of the maximum duration that is between 25 and 65 days. Concerning the case "variable temperature fixed currents" and the case "variable currents fixed temperature" (Figure 6, green parts on the right), the 10-year average outputs show very few differences among the variables studied of each case, so these two other cases will not be detailed here (Appendices 6 to 11).

We now analyse the maps of standard deviation (SD) computed over 10 years for three spawning diagnostics (Figures 11, 12 and 13) to assess their inter-annual variability and identify the regions where it is particularly strong. When studying the case "variable temperature and currents" alone, it provides the actual variability of spawning between years, as simulated by our approach. When comparing together maps of STD between the three cases, it allows evaluating which factor, among temperature and currents, is the most probable in driving the local variability.

The variability of spawning duration, for the case "variable temperature and currents" (Figure 11, first row), is visible over the entire domain at different levels. Minimum SD of 5 days are modelled around Corsica and Sardinia islands (Figure 11, focus A) and in the Gulf of Gabes (Figure 11, focus C). Maximum SD of about 20-25 days can be seen over Campania, Lazio and Northern Corsica (Figure 11, focus A). Other regions where the inter-annual variability is elevated are along the Apulian coastlines in the Adriatic (SD between 15 days and 20 days), in the Croatian islands (20 days ; 43.0°N, 17°E) (Figure 11, focus B) and in the Siculo-Tunisian Strait until Malta with a SD spanning 15 - 20 days (Figure 11, focus C).

Globally, the SD of the case "variable temperature and currents" is the same as the "variable temperature fixed currents" showing the major impact of temperature on spawning, with little influence of currents in Malta and in the Western point of Sicily. For the case "variable temperature fixed currents" (Figure 11, second row), highlighting the places where the variability is essentially due to the temperature, we overall observe that spatial patterns and levels of variability are quite similar to those of case "variable temperature and currents", with a minimum SD of 5 days. Looking more closely, we observe that this variability is particularly apparent in the Campania, Lazio and the Northern Corsica regions with a SD of around 25 days (Figure 11, focus A), but also in Adriatic with the Apulia (between 15 days and 20 days) and the Croatian islands (20 days) (Figure 11, focus B). It also affects the Siculo-Tunisian Strait until Malta with a SD of 15 days (Figure 11, focus C).

The variability driven by the currents (case "variable currents fixed temperature", third row of the Figure 11) seems to be of lower importance than the variability due to temperature since the SD are globally of lower amplitude. This is marked especially for the spawning duration (Figure 11) with a SD of less than 5
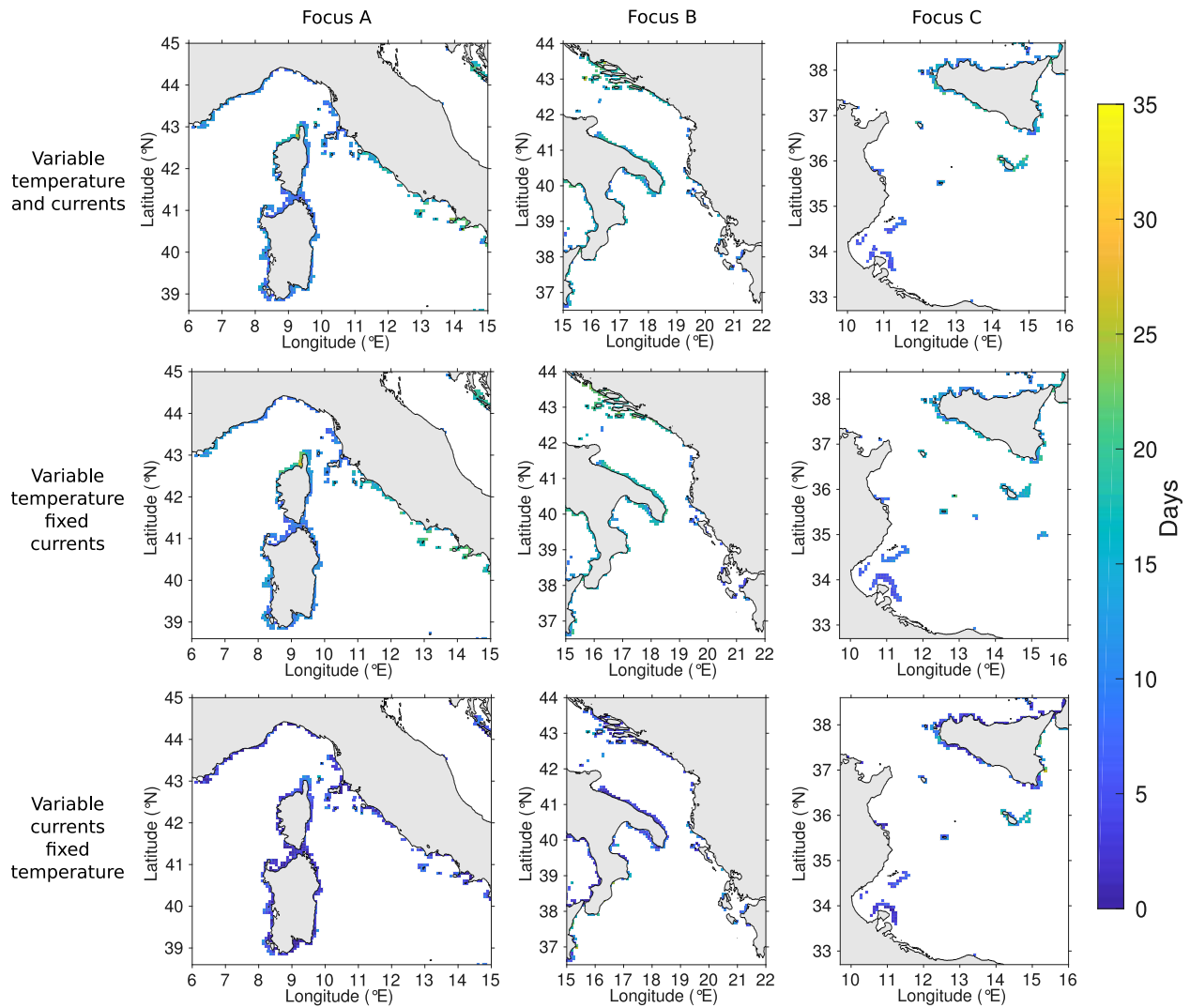
Figure 11: 10-year standard deviation of the spawning duration for the case "variable temperature and currents" (first row), the case "variable temperature fixed currents" (second row) and the case "variable currents fixed temperature" (third row). The first column represents the regional focus A, the second column shows the focus B and the third displays the focus C.

days for the entire map. Some exceptionally strong current-driven variability however around Eastern Sicily, Southern Calabria with a SD around 25 days (Figure 11, focus B) and also Western Sicily and Malta (37.9°N, 12.5°E) with a SD of 15 days (Figure 11, focus C).

For the case "variable temperature and currents" of the first date of spawning (Figure 12, first row), largest SD greater than 20 days is modelled in Campania, Northern Corsica and French Riviera. SD around Sardinia island is between 15 days and 20 days (Figure 12, focus A). It is about 20 days in the North of Apulia and south of the Gulf of Manfredonia. Around the Croatian Islands, inter-annual variability is more pronounced with SD ranging between 20 and 35 days, especially nearshore (Figure 12, focus B). The SD is high - between 20 days and 30 days - in the islands of the Siculo-Tunisian Strait until the East of Malta and, to a lower extent, in the Gulf of Gabes (15-20 days, Figure 12, focus C). Coastlines of Albania and Greece (Figure 12, focus B) exhibit a very low variability (less than 5 days). SD around 10 days or more is simulated for the remaining regions.

Concerning the variability of the first date of spawning for the case "variable temperature fixed currents" (Figure 12, second row), the SD is superior to 20 days in Campania, Northern Corsica and French Riviera, with also Sardinia between 15 days and 20 days (Figure 12, focus A). In the North of Apulia, under the Gulf of Manfredonia, it is about 20 days and for the Croatian Islands, it goes from 20 days to 35 days near the coasts (Figure 12, focus B). The SD is particularly strong in the Siculo-Tunisian Strait until Malta (between 20 days and 30 days) and, to a lower extent, in the Gulf of Gabes (between 15 days and 20 days, Figure 12, focus C). Albania and Greece (Figure 12, focus B) were represented by a very low variability (less than 5 days) but the rest of the map is above 10 days of SD minimum. Overall, the case "variable temperature fixed currents" (Figure 12, second row) seems quite close to the results obtained with the case "variable temperature and currents" (Figure 12, first row) for the first date of spawning. The case "variable temperature and currents" shows a little more variability along the Southern Apulian shores, in the Gulf of Taranto (between 20 days and 25 days) and in Eastern Sicily (15 days). There is also a far more variability in Southern Calabria (around 35 days, Figure 12, focus B), in Western Sicily (25 days) and along the Eastern shores of Malta (35 days) (Figure 12, focus C).

For the case "variable currents fixed temperature" (Figure 12, third row), the value of the SD for the first date is very low (less than 5 days) and similar over the entire domain. It suggests that currents are responsible for only a very little portion of the first date variability. Exceptions are observed in Eastern Sicily (20 days), the East coastlines of Malta (around 25 days) and the Western shores of Sicily (15 days, Figure 12, focus C).

For the spawning last date of the case "variable temperature and currents" (Figure 13, first row), the maximum value of SD found is around 25 to 30 days, indicating that spawning termination has less variability than spawning onset (Figure 12). SD of around 20 days can be found along the French Riviera, the Lazio (Figure 13, focus A), the Albanian shores, the South-Western coast of Sicily (Figure 13, focus B) and the Gulf of Gabes (Figure 13, focus C). The Gulf of Taranto and the Apulia have SD around 5 days and the Croatian Islands have higher variability with SD around 15 days (Figure 13, focus B). Finally, Eastern Malta exhibits the highest inter-annual variability with 25 to 30 days (Figure 13, focus C). The rest of the map is around 10 days.

For the case "variable temperature fixed currents" (Figure 13, second row), the French Riviera, the Lazio (Figure 13, focus A), the Albanian shores, the South-Western coast of Sicily (Figure 13, focus B) and the Gulf of Gabes (Figure 13, focus C) have all SD around 20 days. The Gulf of Taranto and the Apulian shores show little variability with SD of 5 days (Figure 13, focus B) while the SD of the rest of the map is around 10 days.

Concerning the SD of the last date of spawning for the case "variable currents fixed temperature" (Figure 13, third row), the entire map has a value of less than 5 days (even around 0 days), except on the East of Malta with a SD value between 15 days and 20 days (Figure 13, focus C), suggesting the very little influence of currents on the variability of the last date of spawning. As for the other diagnostics, there are important similarities with the case "variable temperature fixed currents" (Figure 13, second row) for the last date of

Figure 12: 10-year standard deviation of the first date of spawning for the case "variable temperature and currents" (first row), the case "variable temperature fixed currents" (second row) and the case "variable currents fixed temperature" (third row). The first column represents the regional focus A, the second column shows the focus B and the third displays the focus C.
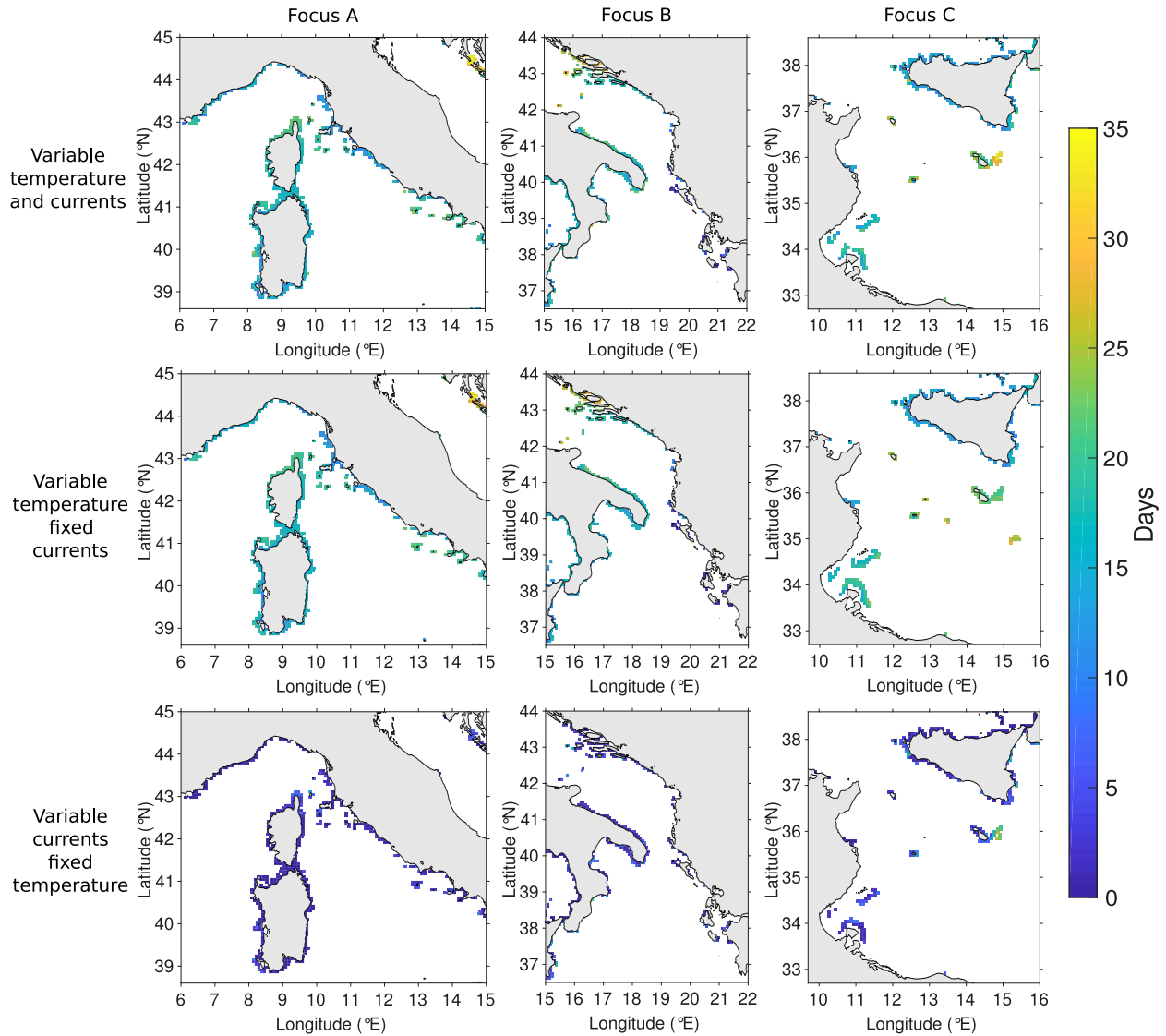
Figure 13: 10-year standard deviation of the last date of spawning for the case "variable temperature and currents" (first row), the case "variable temperature fixed currents" (second row) and the case "variable currents fixed temperature" (third row). The first column represents the regional focus A, the second column shows the focus B and the third displays the focus C.
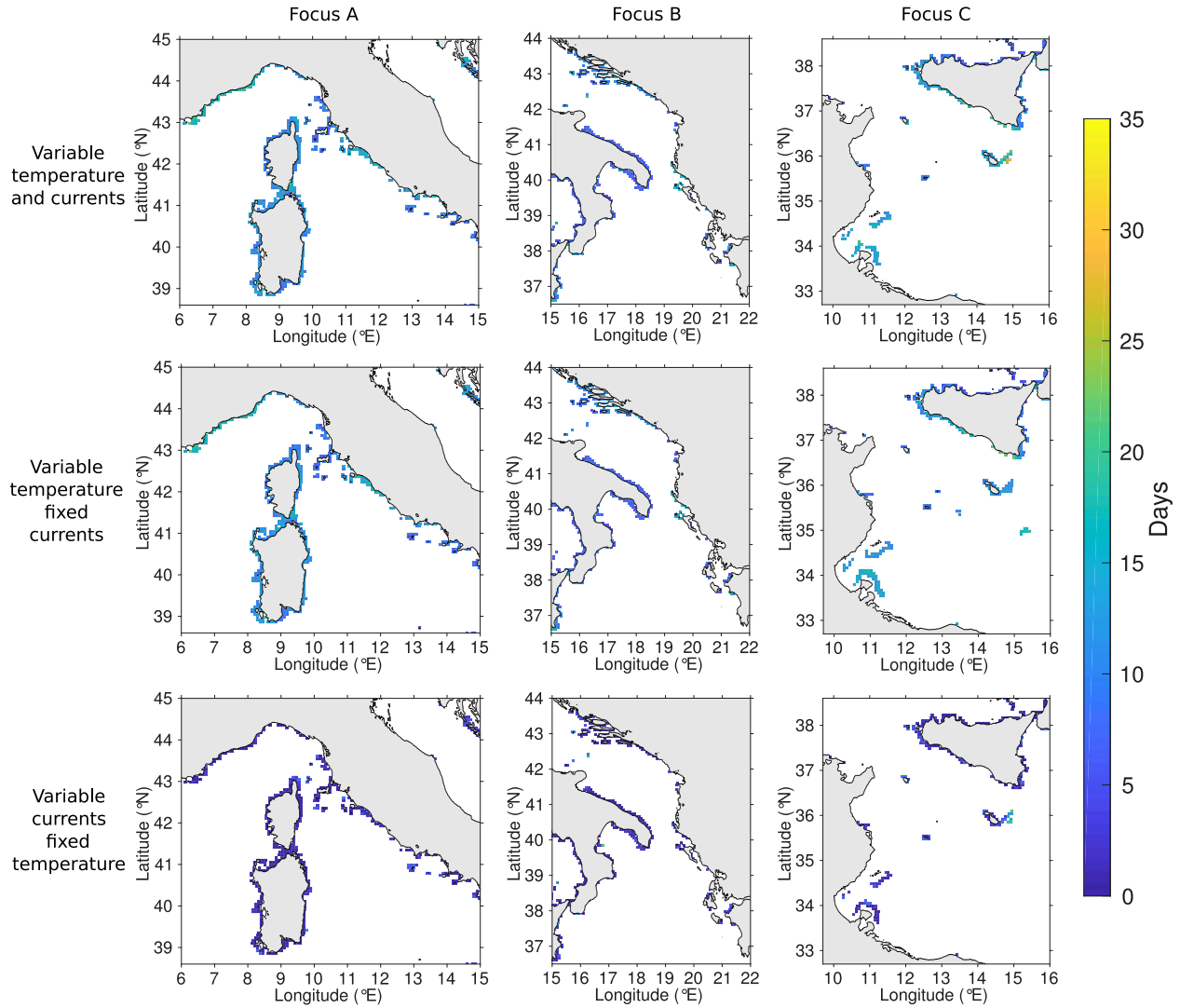
the case "variable temperature and currents" (Figure 13, first row), except on the East of Malta where the SD is higher (around 23 to 33 days, Figure 13, first row, focus C).
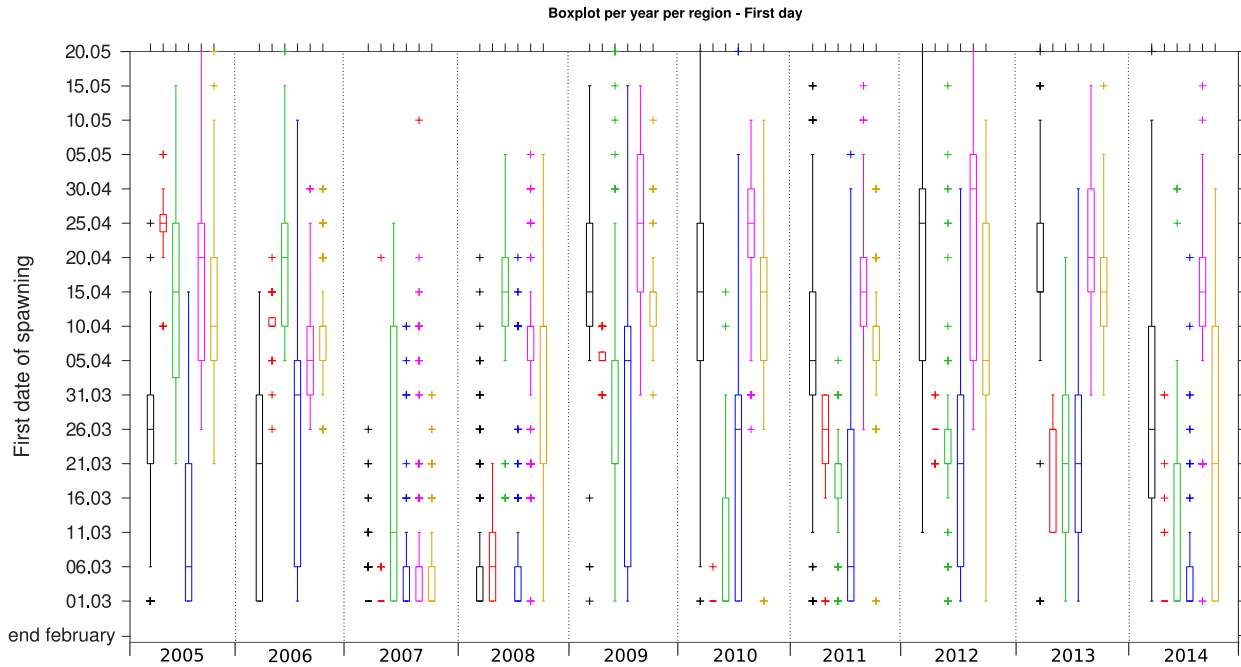

Figure 14: Boxplots representing the first dates of spawning for each ecoregion. The colors-code identifies the different ecoregions: Adriatic (black), Algeria (red), Gabes (green), Ionian (blue), Ligurian (pink) and Tyrrhenian (yellow). Central bars indicate the median ; colored crosses represent outliers.

The boxplots of the first date (Figure 14) of spawning allow analysing together inter-annual variability and geographical differences between ecoregions (Figure 3) about the onset of spawning. From 2009 to 2014, the Ionian (blue), Algeria (red) and Gabes (green) ecoregions are clearly separated from the Adriatic (black), the Ligurian (pink) and the Tyrrhenian (yellow) regions, highlighting a North-South difference with the spawning initiating earlier in the South - from the 1st of March to the 31st of March - than in the North - from the 31st of March to the 5th of May. Moreover, both 2007 and 2008 seem to be very particular years with early first date of spawning, from the 1st of March to the 11th of March for the entire domain. There are few differences between the ecoregions for the boxplots concerning the last date, that is generally between the middle of May and the middle of June - from the 10th of May to the 9th of June (Appendix 12). The boxplots on the spawning duration (Appendix 13) inform that generally the number of days of potential spawning of all years and ecoregions is between 30 and 50 days over the maximum duration of 122 days. Again, both 2007 and 2008 are exceptional years with the highest spawning duration of around 60 days (or more) of the decade studied here, which is more than 50 percent of the maximum duration.

The factorial analysis focus on the case "variable temperature and currents" since it simulates the full variability of spawning due to both currents and temperature. We run a Correspondence Analysis on the spawning duration to display spatial and temporal variability between years (Figure 15). Thus, this one highlights a spatial variability along the first dimension by the structuring existing among ecoregions. Indeed, this one is visible through a North-East (Adriatic, Ionian) / South-West (Algeria, Gabes) structuring represented by a variability of 29.47 percent over the first dimension. Concerning the spawning duration, there is also a temporal distinction over the first dimension between years 2005, 2006, 2007, 2008 on one hand (with negative values) and the rest of the years on the other hand (with positive values). The main reason behind this inter-annual structuring could be the distinction between long and short spawning season on the first dimension. In the analysis of the spawning duration, 2014 appears as a particular year and seems to represent, along with 2006 and 2013, a great part of the variability of the second dimension but this cannot be further explained.
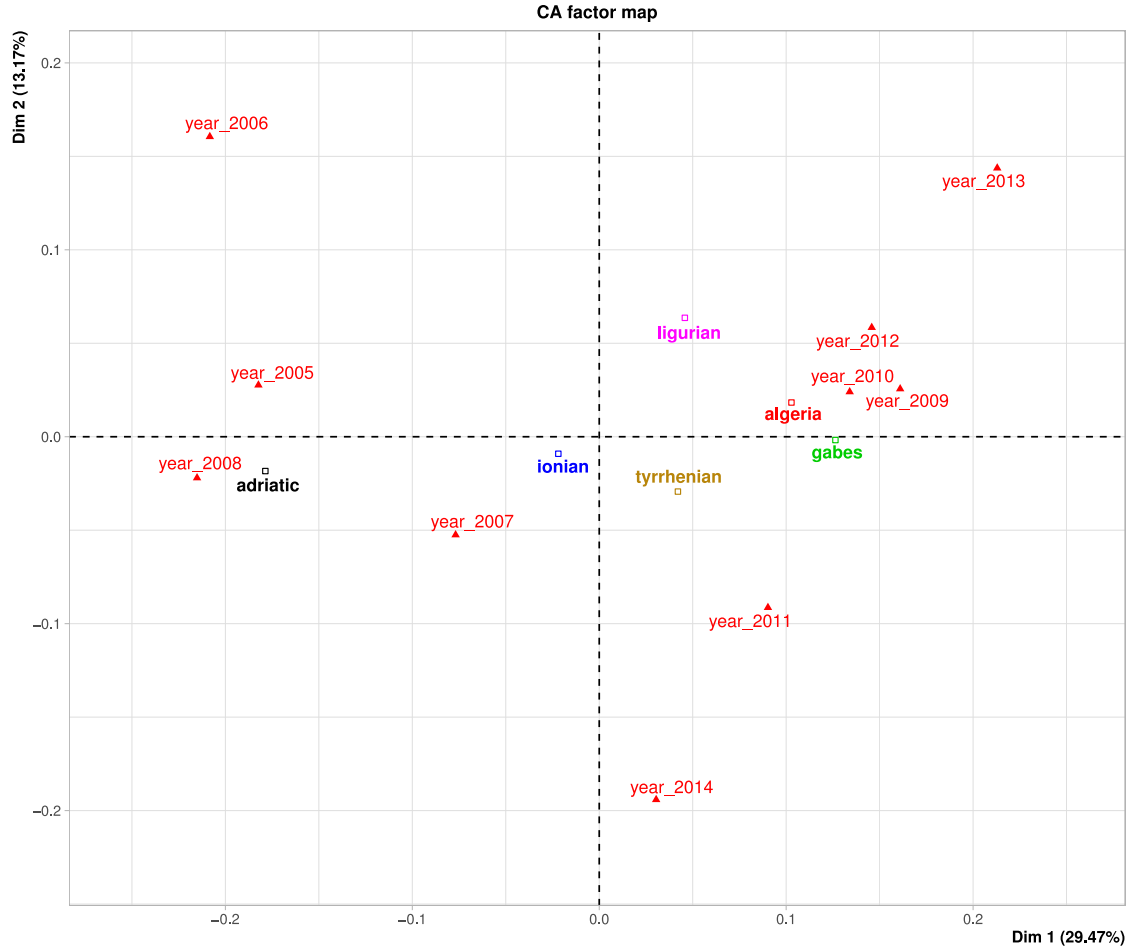
27

Figure 15: Correspondance Analysis on the spawning duration for the case "variable temperature and currents".

Concerning the first date of spawning (Figure 16), the Principal Component Analysis highlights a spatial structuring when looking at the ecoregions (Figure 16, graph of individuals): a North-West / South-East (Tyrrhenian and Ligurian with positive values against the Ionian with negative ones) structuring on the first dimension explaining 66.63 percent of the variability. A North-East / South-West (Gabes and Algeria with positive values against the Adriatic with negative ones) structure emerges along the second axis explaining 17.06 percent of the variability. Moreover, there is a clear separation between years 2005, 2006, 2007, 2008 and the rest of the years for the first date along the second dimension (Figure 16, graph of variables). The study of the boxplots (Figure 14) of all years and ecoregions on the first date of spawning highlighted the same North-South spatial and temporal separations. The main reason behind the difference between years could be an opposition between early and late onset of spawning (Figure 16, graph of variables).

Finally, for the last date of spawning (Figure 17, graph of individuals), the Principal Component Analysis displays a North-South opposition on the first dimension concerning the ecoregions with a variability explained for 94.27 percent. A separation between the years 2005, 2006, 2007, 2008 and the rest of the years can also be described on the second dimension but little variability is explained along this axis (2.1 percent, Figure 17, graph of variables). This difference between years is structured according to the early or late termination of the annual spawning season (Figure 17, graph of variables), but in a limited extent comparing with the first date of spawning. Otherwise, there is no other differences between years for the last date, as they are very similar and all described by the first dimension (Figure 17, graph of variables).
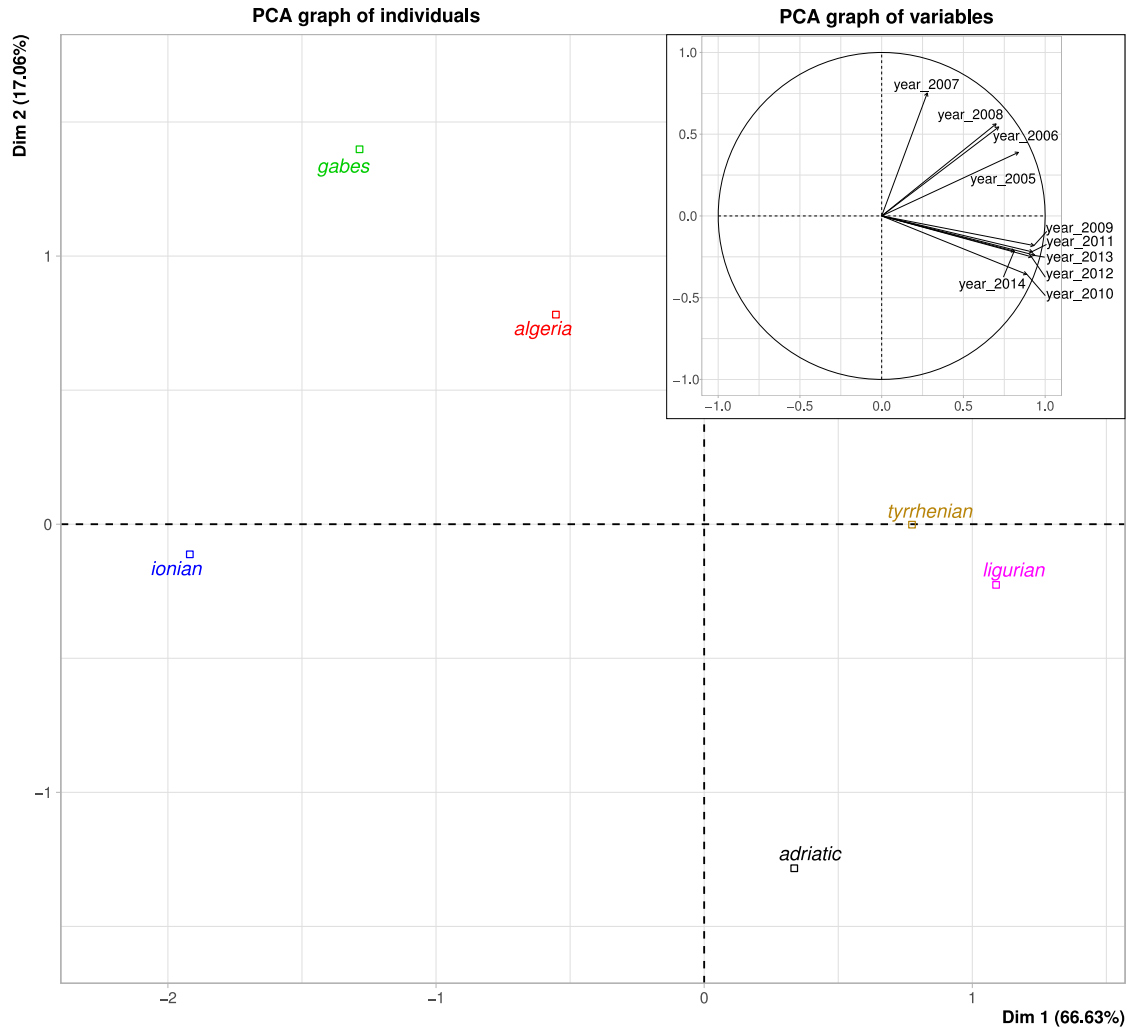
28

Figure 16: Principal Component Analysis on the first date of spawning for the case "variable temperature and currents".

By the way, the factorial analysis shows little variability explained when the currents were the only variable factor (Appendices 14, 15 and 16), with difficulties to separate years and regions along a dimension or another, contrary to the case with the variable temperature (Appendices 17, 18 and 19). It suggests that temperature variability is preponderant on the one of currents, because years are very similar in the case "variable currents fixed temperature", for the first date, the last date and the number of days, with no visible differences between ecoregions too, whereas there are same patterns between the case "variable temperature fixed currents" and the case "variable temperature and currents", with visible separation between years and same patterns concerning the ecoregions (Appendices 14 to 19).
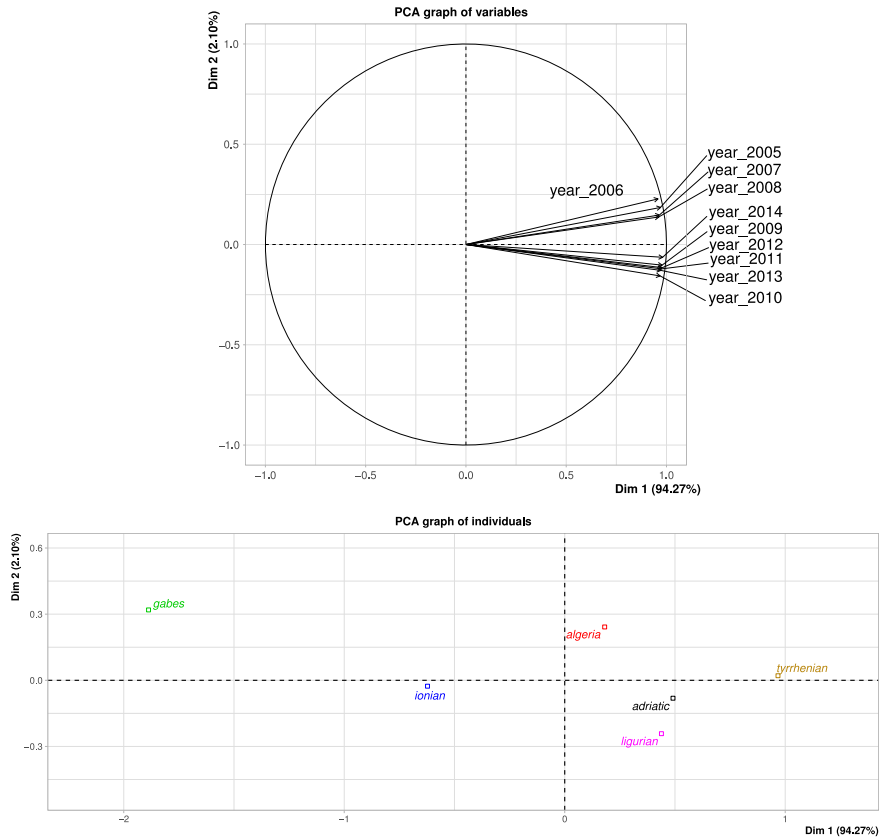
Figure 17: Principal Component Analysis on the last date of spawning for the case "variable temperature and currents".

4 Discussion

4.1 Analysing the environmental influences on spawning and its variability

4.1.1 Spatial variability of back-tracked spawning areas

Backtracking model experiments constrained by observations allowed us to identify and delineate several spawning areas that contributed to the larval replenishment of the 11 nurseries that were surveyed (Di Franco *et al*, 2011 ; Di Franco & Guidetti, 2011). Their spatial locations and relative contributions can be reasonably well explained by the local and regional hydrodynamics and topography. Our model identified the main spawning areas that delivered larvae to the Genova nursery (Figure 7a), off Livorno and eastward of Genova. This pattern follows the mean pathways of the Liguro-Provencal current, extended into the Northern Current (see Figure 2), entering the Ligurian Sea from the South (between Corsica and the Tuscan Archipelago) leaving the Gulf of Genova to the West (Millot & Taupier-Letage, 2005). Counter-intuitively, some weak spawning areas are located downstream, to the West of Genova. It could be due to the seasonal slowdown of the Liguro-Provencal current during short periods or to the presence of mesoscale eddies creating turbulent and anisotropic dispersal or of a coastal counter-current (Millot & Taupier-Letage, 2005 ; Poulain *et al*, 2013).

The spawning areas providing larvae to the Maratea nursery (Figure 7b) are located from Northern Calabria to the Basilicata region, following the northward coastal current of Sicily (the Algerian Current, see Figure 2) (Millot & Taupier-Letage, 2005). The counter-intuitive downstream larval sources modelled off

Southern Campania could be explained by the sharp changes of the coast orientation, potentially creating current instabilities and small-scale recirculation patterns (Poulain *et al*, 2013).

In the Ionian Sea, the spawning areas replenishing San Isidoro nursery (Figure 7c) are situated in the Gulf of Taranto and along the Apulian coastlines in Southern Adriatic. This pattern is following closely the main current from the Adriatic to the inner Gulf of Taranto, also pushed by a westward flow probably linked to the North Ionian Gyre (Gačić *et al*, 2010 ; Crisciani and Mosetti, 2016).

The Apulian site of Torre Guaceto in both 2008 and 2009 (Figures 7d and 8d), are mainly fed by upstream larval sources located north-westward, in agreement with the dominant south-westward alongshore transport associated with the Western South Adriatic (Poulain *et al*, 2013). Bray *et al* (2017) also showed that larvae of other species were following the Western Adriatic Currents and highlighted that Apulia coast acted as a sink of larvae, increasing the probable settlement in this region. Pujolar *et al* (2013) indicated the same patterns of connectivity in Apulia when modelled by a Lagrangian model for a PLD of 17 days, a dispersal depth of 10 meters and dates from the 9th to the 25th of May. They also pointed out that 12.75 percent of the larvae of Torre Guaceto MPA remained in the site. Note however that a small contribution originates from the Southern Apulian coastline in 2008 (but never in 2009), exemplifying the inter-annual variability of hydrodynamics. It could also be explained by the large range of spawning dates observed (about one month) in this site, that may be caused by intermittent current reversal perhaps due to the North Ionian Gyre (Gačić *et al*, 2010 ; Crisciani and Mosetti, 2016). For all Adriatic nurseries in 2009 (Figure 8), the spawning areas, and their respective contributions, were modelled along the Apulia shores and around the Tremiti Archipelago, in very good agreement Legrand *et al* (2019) using the same model with similar parameters.

Concerning the contributions of each spawning node, they follow the main current pattern, as a large part of the larvae are following the main currents occurring in a region. It also seems that "the closest to the settlement area, the highest the contribution" for some sites of 2008 (Figure 7b and 7c). It could be related to the relatively short PLDs of *D. sargus* and the sluggish circulation in these regions resulting in limited dispersal. For instance, Maratea and Genova sites have a less extended plume than the ones in Apulia, which can be explained by the shortest PLDs for these two sites (14 and 13 respectively, Table 2) so the larvae spend less time dispersing. For other nurseries, it depends on the coastline topography and the local circulation patterns. For instance, we model lower contributions from the bays and depressions situated just downstream of major promontories (e.g. see the 41.3°N, 16.7°E on Figures 8d, 8e, 8f and 8g). The coastal current is probably detaching from the coast and thus not entering these bays. It could also be linked with the precision of the Eulerian model (Ciliberti *et al*, 2015) or the node size chosen.

Spatially, a high variability of the first date - and of the duration - of spawning for the case "variable temperature fixed currents" and "variable temperature and currents" is visible in the Middle Adriatic, in Northern Apulia in the Gulf of Manfredonia and in the Croatian Islands (Figures 11 and 12). This pattern could be explained by a low bathymetry (above -100 meters depth) probably implying a quick rise of temperature in these areas and sluggish circulation around the Croatian islands. Furthermore, the Southern coast of Sicily presents an high mean spawning duration (around 75 days, Figure 11) which can be explained by the presence of sporadic upwelling in this area (prolonging the spawning season by slowing down the summer warming of the water column), coupled with the Maltese Channel Crest which is an anticyclonic gyre bringing back the currents to shore (37.0°N, 13.5°E), described by Piccioni *et al* (1988). Falcini *et al* (2015) investigated the impact of these hydrodynamic processes on the dispersal of anchovy eggs and larvae and shows that these ones can affect the recruitment of this pelagic species. A similar approach could be lead on eggs and larvae of coastal fishes to determine the impact of this kind of upwelling on the settlement, and to determine if this area could be worth protected.

4.1.2 Relative influences of temperature and currents

The variability analysis suggests that temperature variability seems to dominate over hydrodynamics. Globally, some places have little variability comparing to the others (Toscana and Northern Sicily) but overall, we

have shown that the preponderant factor in the inter-annual variability of spawning areas is the temperature. In contrast, the circulation variability have little impacts over most of our domain. Looking in more details, some regions have particularly high variability of temperature (Croatian Islands, Siculo-Tunisian Strait) or low (Albania, Greece), while a few specific areas have even bigger impacts of the circulation. This occurs in the Siculo-Tunisian Strait, especially around Malta. This region is known to have particularly high eddy kinetic energy due to the presence of the particurlay unstable Atlantic-Ionian stream (D'Ovidio *et al*, 2004), suggesting that spawning and dispersal would be highly variable in places where the circulation is highly turbulent (Cuttitta *et al*, 2016). In contrast, temperature affect every single spawning area of the entire studied domain but at different levels. Moreover, the factorial analysis shows little variability explained when the currents were the only variable factor contrary to the case with the variable temperature, which is very similar to the case "variable temperature and currents" (Figure 15, Appendices 14 to 19). It also suggests that temperature variability is preponderant on the one of currents. The shortest mean spawning duration of certain areas - East of Malta, Gulf of Gabes, some offshore areas - maybe due to an high variability of currents there, as seen in the case "variable currents fixed temperature" (Figure 10). For the longest spawning duration, it seems to be in places where the water is retained by the coast or with lower currents, such as shallow bays, and where the temperature can easily rise because of low bathymetry. Notice that the "binary" *modelling approach* used in this study is conservative because no weight is taken into account in the analyses: if there is one particle being exchanged between two nodes, the source node will be treated in the same way as a source node that exchanged lots of particles. Exploring a "probabilistic" approach by applying weights depending on the number of particles exchanged and on the percentage of temperature in the selected range of temperature could help refine our results.

4.1.3   Interannual variability of spawning

The factorial analysis shows that both spatial and temporal (inter-annual) variabilities are important when modelling spawning, as supported by the spatial structuring and differences between groups of years. While here we only investigate oceanic causes (e.g. changes of temperature and circulation), the next link to be investigated is with climate as the atmosphere is the main external forcing of the ocean. For instance, cold years with longer winter opposing warm years with mild winter, thus triggering the spawning at different periods depending on the year. Years 2006 to 2008 appeared quite specific in comparison with the other years (Figures 14, 15, 16 and 17) possibly because they were described by Gačić *et al* (2014) with an anticyclonic circulation of the North Ionian Gyre, the circulation being transitional between cyclonic and anticyclonic circulation in 2005. There also was a reversal of the seasonal basin-wide circulation in 2009 leading to a cyclonic circulation from 2010 to 2014 (Gačić *et al*, 2014). This could partly explain why those years where separated from the 2005 to 2008 years (Figures 15, 16 and 17). This regional-scale mechanism has been called BiOS (Adriatic-Ionian Bimodal Oscillating System). It corresponds to regime-shifts of the North Ionian Gyre on decadal time scale, modifying the nature of the currents entering the Adriatic Sea (Gačić *et al*, 2010 ; Crisciani and Mosetti, 2016). Those changes in circulation could explain the inter-annual variability described in the factorial analysis, the higher spawning duration and the earlier first date of spawning for the years from 2005 to 2008 comparatively to the rest of the years (Figures 15, 16 and 17). Note also that the Adriatic is a semi-closed sea so that local specific patterns of circulation may not affect other ecoregions. This may explain why, when looking at the boxplots (Figure14) all the ecoregions studied here tend to have their own modes of variability.

4.1.4   Implications for management

Information on the mean spawning duration, the mean onset of spawning and the mean termination of spawning can provide potential "stable" spawning areas all over the years where, for instance, it could be worth creating MPAs (Gaines *et al*, 2010). Coastal fishes, like Sparids, are mostly targeted by artisanal and recreational fishermen rather than industrial fleets. Since the stocks of *Diplodus sargus* are not assessed by the General Fisheries Commission for the Mediterranean (FAO, 2006), and MPAs or fishery regulations

represent very useful management tools to protect and rebuild populations of this species (Di Franco *et al*, 2012a ; Guidetti *et al*, 2014 ; Di Franco *et al*, 2018). The study of the mean spawning duration can be useful for management purposes by identifying these areas where spawning is more likely to be consistently long and stable each year. In fact, prohibiting fishing in these areas during the beginning of the spawning period for instance, or creating a MPAs network allowing the resilience of exploited areas thanks to the larval export, could thus help to the protection and the conservation of species with fisheries and patrimonial interest (Forgarty & Botsford, 2007 ; Jones *et al*, 2007). So this methodology could be used for other species with bipartite life cycle, with the same final goal of protection and by the determining of potential stable spawning areas. Our results could help taking into account the interannual variability of spawning in the management of resources, and more especially in the context of adaptive and dynamic management (Maxwell *et al*, 2015). Since our results suggest that inter-annual variability of spawning and dispersal is particularly high in some regions, they are ideal places to test implementing flexible protected area and adaptive measures of protection or regulation, such as the Siculo-Tunisian Strait. While our modelling approach could be well-adapted to guide these efforts, unfortunately ocean models currently perform quite well for multi-decadal hindcasts (historical runs) but not necessarily for long-term future simulations. In addition, the forecast lead-time of operational ocean models does not currently exceed a few day. On top of this natural variability, it is worth mentioning that fishes are more likely to move to higher latitudes due to the climate change, due to ocean warming, that is exacerbated near the coastline (Perry *et al*, 2005). Moreover, more effective recommendations could probably be achieved by considering an ecosystem-based approach that would study together multiple key species of an ecosystem to enhance their sustainability and reduce the impacts of human activities on these resources (Levin & Lubchenco, 2008 ; McLeod *et al*, 2012).

4.2 Temperature and other factors affecting spawning

The factor investigated in this study was the temperature as it appeared as the main factor affecting spawning onset and duration reported in literature (Table 1, "Temperature" row) but others could have been studied. The dispersive larval stage of bipartite life cycle organisms can be indeed controlled by multiple external or intrinsic factors (Figure 18 ; Table 1). For instance, one could not deny the potential influence of the lunar cycle to trigger fish spawning, especially through its effects on tides (e.g. largest tidal currents at spring tides could affect dispersal, thus putting larvae in the best condition to survive and reach settlement sites) (Appeldoorne *et al*, 1994 ; Colin, 2010 ; Kadota *et al*, 2010 ; Sheaves & Molony, 2013). Lunar cycle has also impact on ambient light levels (e.g. full moon nights are less dark than new moon nights), which help reducing the mortality rate of early-life stages due to predators (Garrett, 1993 ; Bradbury *et al*, 2004 ; Claydon, 2005 ; Sheaves & Molony, 2013 ; Figure 18, see "Moon cycle" box). The humphead wrasse *Cheilinus undulatus* in Palau (tropical environment) appeared to be susceptible to tidal currents because spawning occurred between high and low tides, two hours after the high tide (Colin, 2010). Kadota *et al* (2010) and Appeldoorne *et al* (1994) observed the same phenomenon in Japan with hawkfish *Paracirrhites forsteri* and in the Caribbean Islands with the bluehead wrasse *Thalassoma bifasciatum*. Spawning tends to occur around the high tides – especially during spring tides – probably in order to disperse eggs further away, but also more rapidly to avoid predators (Appeldoorne *et al*, 1994 ; Colin, 2010 ; Kadota *et al*, 2010). Yamahira (1997) showed a shift in the spawning time of the grass puffer *Takifugu niphobles* in Kyushu Island that could match with higher survival and hatching rate of the eggs. The mechanism was not fully explored but seemed to coincide with temperature and tidal cycles. Hereu *et al* (2006) studied the dusky grouper *Epinephelus marginatus* spawning in the North-West Mediterranean Sea and did not observe any lunar or tidal influences, probably due to the very limited tidal signals characterizing the Mediterranean Sea, so the influence of these two factors (lunar cycle and tides) on temperate Mediterranean Sparids could be limited. They observed however that spawning always occurred around sunset, probably limiting the predation of other species on their eggs and larvae. Bradbury *et al* (2004) observed a night-time spawning behaviour of *Osmerus mordax* in the Canadian rivers and also experienced higher hatching overnight. These behaviours are strongly linked to predation risk which is lowest in the dark. The effect of lunar periodicity and tides has been investigated on tropical Sparids too (Figure 18). Indeed, Garret (1993) studied *Acanthopagrus berda*, an estuary-dependant Sparid species, in the Kosi estuary located on the east coast of South Africa. Spawning occurred only at night on outgoing tides, starting right after the shift of the tide, but was low or absent
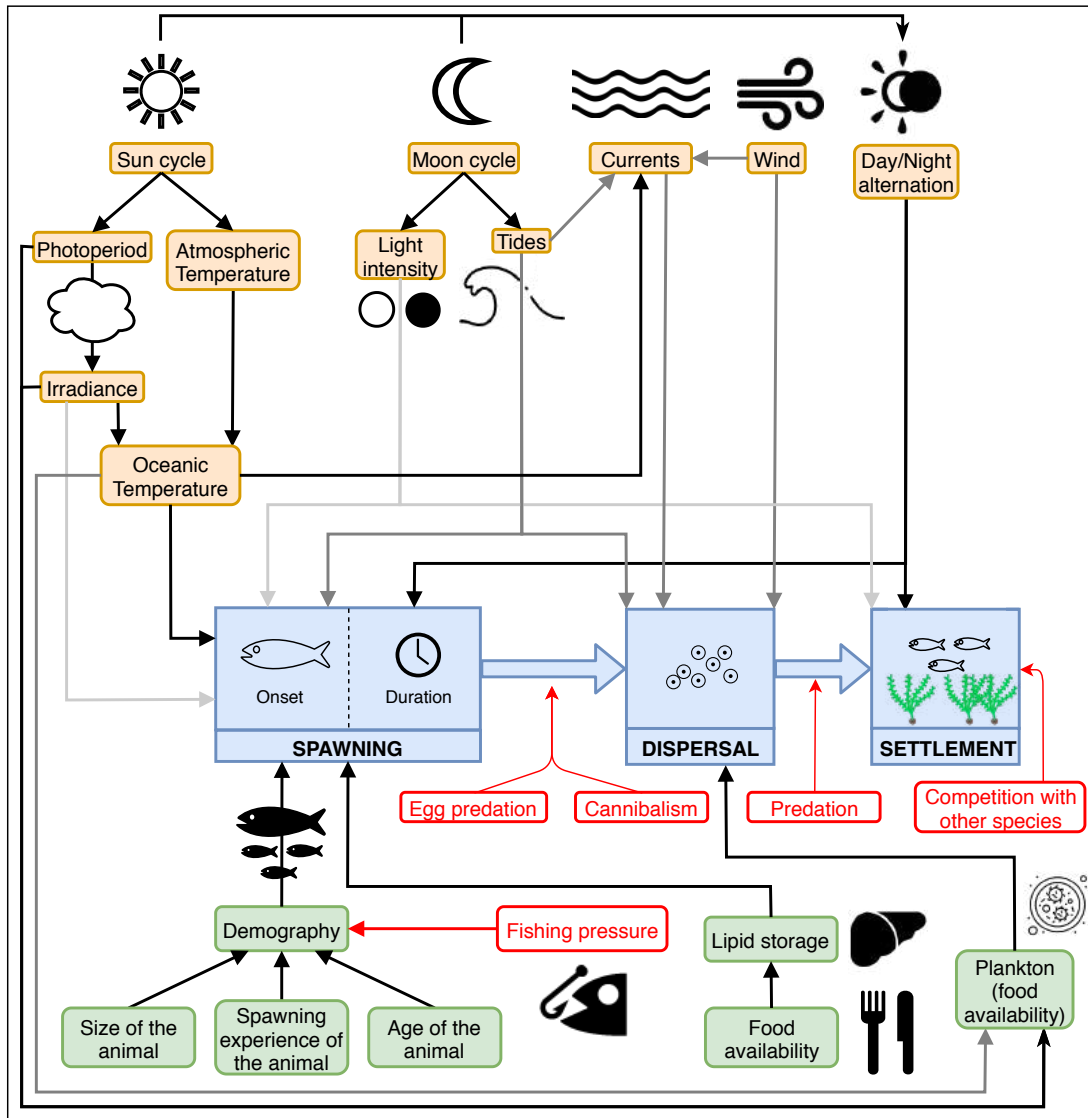
Figure 18: Schematic summarizing the most relevant influences of different factors on the early-life stages of a bipartite life cycle organism. External factors are represented in orange and internal ones are displayed in green. The life cycle is represented in blue and the biotic and human pressures are red. The black and grey arrows represent the interactions among factors or the influences of a factor on a specific life-stage of the life cycle.

when the outgoing tides approached dawn. That mechanism could be an adaptive response to predation on the eggs which are more visible under sunlight during day-time. Sheaves and Molony (2013) observed that the ovarian development of *Acanthopagrus pacificus* in north-eastern Australia was closely related to lunar periodicity and that the spawning peak appeared to be during night-time, in the full moon period, when ebb tidal movement was the greatest, thus probably maximizing the quick advection and efficient dispersal of eggs away from the spawning area where egg predators are known to be abundant (Claydon, 2005).

Similarly to environmental factors, intrinsic ones can directly modify the onset and the duration of spawning although they are themselves driven by external factors (Figure 18). Wright & Trippel (2009) demonstrated that demography – age, size or spawning experience (the number of time a fish spawned in its life) of individuals – could lead to variation in the spawning period, especially when demography is largely affected by fisheries. Indeed, bigger and older female spawn earlier and larger batch of eggs (exponentially

related with the body length), and by reducing the average lifetime of fish, fishing pressure could increase the variability on the onset on spawning and so the reproductive success (Wright & Trippel, 2009 ; Hunter *et al*, 2015). Lipid storage has also been investigated, in the mosquitofish, for which only a portion of fat was used during the winter and the reserves remaining were rapidly used at the beginning of the spawning season (Reznick & Braun, 1987). Larger batch of eggs were laid early in the spring when lipids were high after winter, whereas later spawners tend to comparatively lay little batch of eggs at the end of the summer. According to Reznick and Braun (1987), this mechanism seems to not only be triggered by food availability but also intrinsic factors as a reproductive adaptation. It has finally been observed that the spawning period tends to differ slightly among closely-related species as a mechanism to avoid competition. For instance, *D. sargus*'s spawning period does not overlap the one of *D. vulgaris* and it could be to minimize competition for food availability and for settlement between the two species. Indeed, both *Diplodus* species share habitat requirements for settling – shallow sandy and rocky bays (Harmelin-Vivien *et al*, 1995) – and there may also be a link with the zooplankton availability at the time of settlement, especially for *D. sargus* – so linked to the productivity cycle (Planes *et al*, 1999).

Notice that some publications (Garrett, 1993 ; Appeldoorne *et al*, 1994 ; Yamahira, 1997 ; Bradbury *et al*, 2004 ; Claydon, 2005 ; Hereu *et al*, 2006 ; Colin, 2010 ; Kadota *et al*, 2010 ; Molony, 2013 ; Table 1) studied primarily one or more external environmental factors and their effects on spawning, while discussing the type of internal process (e.g. physiological or nutritional status) which would explain how environmental forcing indirectly control fish spawning behaviour. Instead, other publications (Reznick & Braun, 1987 ; Harmelin-Vivien *et al*, 1995 ; Planes *et al*, 1999 ; Wright & Trippel, 2009 ; Table 1, see "Lipid storage", "Demography" and "Settlement" rows) studied especially one or more intrinsic factors and their effects on spawning, while discussing what kind of external forcing would directly affect the intrinsic process that is being investigated and that finally manifest itself by a change of spawning onset or duration. Here we retain temperature as it is a factor related to numerous other environmental factors, thus modifying them or itself being modified by others. So it is worth noting that there is an interdependence between the different factors (see Figure 18) and that their separation is somehow operational. At least it is a way to better understand the complexity of the interactions between marine life and its physical environment. Moreover, it is important to notice that numerous studies have been made on temperature comparatively with other factors (Table 1), which could skewed the representation of this factor in the literature. This drawback is however easily ruled out since many studies reported major influences of seawater temperature on other factors and marine life in general. For instance, global patterns of marine biodiversity are essentially explained by latitudinal gradients of temperature (Tittensor *et al*, 2010 ; Burrows *et al*, 2019).

Considering our results, the range of model temperatures favourable for spawning derived from the *data based approach* (14.8°C for the minimum and 21.3°C for the maximum) is thus consistent with the threshold compiled from the literature (Table 3). While the minima agree well, our estimate of the maximum is a bit larger than previous estimates. Notice that the last date of spawning, determined here by this maximum temperature and supposedly representing the termination of the spawning season, may have a different explanation in nature. It could be rather related to biological and internal factors, such as the fact that most of the fish would have already spawned after a certain duration of active spawning. It suggests that for the spawning termination, external factors may not play a major role. However, determining the first date of spawning based on a temperature threshold triggering spawning is in accord with the literature which has been mainly focused so far on explaining the peak of spawning (Di Franco & Guidetti, 2011 ; Table 1). Looking at the standard deviation, there is also more variability on the first date of spawning than on the last one for all cases (Figures 12 and 13), confirming again the higher significance of considering temperature as the onset of spawning as compared to its completion.

4.3   Methodological considerations

Certain methodological choices have been made and are discussed in the following. The choice of the inputs of the LFN model has been led by the observations - the sampling locations forced the choice of the velocity fields and the domain, the PLD and the spawning dates were directly derived from the sampled juveniles -

but also by processing concerns. Different values of lateral spacing - equivalent to the number of particles per node - and of Runge-Kutta step between particles positions have been tested. A node size of 1/16°was kept because it was relevant in relation to the domain coverage, the intricate coastlines and the typical size of islands, after different tests and literature reading (Legrand *et al*, 2019). Indeed, the parameters could be refined but were also limited by the available computing power.

Some limits of the LFN model can also be highlighted. Biological processes affect connectivity patterns and the model does not take into account all the biological processes such as the eggs and larvae survival rate during the dispersive larval stage (which is generally around 1/1000) (Dahlberg, 1979). It is a time in early life when mortality is unusually high, and it is at this stage that the longer-term survival rates of the cohort is determined - this is the "critical period" hypothesis (Hjort, 1914). Moreover, a part of the larvae, which experience favourable feeding conditions and therefore grow quickly, will achieve metamorphosis at earlier ages and experience lower cumulative mortality due to predation during the larval stage, when mortality rates are supposedly high. This is known as the "stage duration" hypothesis: the longer the PLD, the higher the mortality rates because of predation (Anderson, 1988) and this aspect is not included in the model too. Another point is that the larvae acquire the capability to swim during the competence period, at the end of the dispersive larval phase just before settlement (Clark *et al*, 2005), and orientate to the more suitable settlement site (Staaterman *et al*, 2012 ; Failletaz *et al*, 2018). They can reach a distance of 1 or 2 km maximum and choose the settlement site that suits the best (Staaterman *et al*, 2012 ; Failletaz *et al*, 2018). Each node of the model is about 6 km long (a node surface of around 40 km^2) so this behaviour isn't taken into account in the model and larvae are represented as passive drifters - it can be considered as included into the model because the movement isn't perceptible in nodes of 6 km long. The same issue occurs with adults' movements during spawning, with individuals performing movements outside their home range of about 1 or 2 km maximum, knowing that these ones are already very territorial - usually about 1 km^2 of home range (Di Lorenzo *et al*, 2014). The habitat filter used for settlement in the *modelling approach* is the same as the spawning one whereas, in nature, the literature specifies that juveniles live between 0 and 2 meters deep between sandy bays and rocky shores (Harmelin-Vivien *et al*, 1995 ; Lenfant & Planes, 1996). The node size chosen for the model is however too wide to distinguish settlement sites at this scale, so the same filter was kept. Even if the LFN could accommodate smaller nodes, the current resolution of ocean model is the limiting factor. Moreover, changing in the buoyancy or ontogeny - development of the organism - of the larvae could modify the depth position and so the current applying on the larvae, thus it can modify their trajectories (Pineda *et al*, 2007). However, to our knowledge, no study have documented this effect in our target species yet.

Finally, if we could benefit from more sampling effort, it would allow increasing the numbers of surveyed sites and of juveniles sampled. Also, a good spread over space and time of these new sampling efforts could have been achieve. It would thus return more statistics to compare years and provide higher confidence on the temperature threshold we found. Despite the limited sampling, the observed data are considered representative of each site and year, the sampling being realised during the supposed settlement peak for each site. Note that some larvae possibly arrived in groups at a same period and thus can saturate a site, making the access impossible for other larvae to settle, explaining a probable variability between sites and similarities within concerning the PLD and the spawning date observed (Di Franco *et al*, 2013). So a higher number of sampled could have highlighted a local adaptation. Furthermore, in Figure 9, the statistical distribution of all model temperatures favourable for D. sargus's spawning resemble a Poisson distribution with a main peak at 16 °C (note two smaller peaks at about 17.75°C and 19.25°C which may suggest a multi-modal Gaussian distribution). A first analysis on the 2008 and 2009 years (not shown here) pointed out a peak for each year, with a statistical distribution similar to a Gaussian distribution. Knowing that the sites of 2009 are all located in Apulia and that the others are more dispersed, this pattern could be analysed further according to space, to see if these peaks are due to regional patterns. Furthermore, the otoliths have been read multiple times by different operators, thus limiting the estimation bias, and in case of difference between results the PLD or the spawning date were considered as the mean of the readings - by the way, the uncertainty is about 1 or 2 days maximum (Di Franco *et al*, 2011). The idea of the *modelling approach* was thus to compile this data to try to give the more reliable results on spawning location across the years. Also, a weighted dispersal could have been taken into account depending on the location, especially for places like

MPAs where fish are supposed to be larger in size due to less fisheries activities, thus spawning a higher number of eggs - knowing that the number of eggs produced and released is proportional to the size of the individual, following an exponential relationship (Lester *et al*, 2009 ; Marshall *et al*, 2019). Di Franco *et al* (2012b) analyses suggest that high densities of *D. sargus* spawners in Torre Guaceto MPA were contributing to the replenishment of unprotected areas around by larval dispersal. Legrand *et al* (2019) took the degree of protection of MPAs into account to determine the real degree of contribution of an area, thus highlighting the benefits of MPAs in the replenishment of surrounding populations.

The choice of the studied factors of the *modelling approach* was led by literature (Table 1). In fact, the temperature was recognized as a trigger of spawning for Sparid fishes and especially for *Diplodus sargus* (Table 1, blue parts). Concerning the choice of studying currents, it was led by the use of the LFN model and by the articles of Dubois *et al* (2016) and Rossi *et al* (2014) showing that circulation had an effective impact on spawning and settlement, using the same Lagrangian model. When talking about ocean dispersal, it also seems logical to take a look to currents. Moreover, the currents data comes from the AIFS model (Oddo *et al*, 2006 ; Ciliberti *et al*, 2015) and is used in the LFN model, such as the temperature data, coming from the AIFS model too. Thus, the same uncertainty occurs between the back-tracking model and the temperature analyses, comparatively to a set of temperatures that could have come from *in situ* observations or Sea Surface Temperature from remote-sensing, whereas there are multiple layers and their interactions taken into account in this model. Furthermore, there seems to be no apparent edge effect in the model as the edges of the map have no specific behaviour, but in some areas where the islands are close and numerous comparatively with the size of a node and the model precision (Ciliberti *et al*, 2015), the currents can be more difficult to simulate and to represent reality, so the results must be interpreted cautiously.

4.4 Conclusion

The goal of this report was to determine how abiotic factors could influence the interannual variability of spawning in Sparids in order to localise spawning areas and periods for management of fishery resources. Temperature came out as the preponderant factor triggering spawning onset and location for *Diplodus sargus*. This study also helped to model as reliably as possible the connectivity patterns involved and define stable areas, at a temporal and a spatial scale, that could thus be used in management to protect coastal fishes with a bipartite life-cycle. In the other hand, the variability of spawning pointed out the necessity of the creation of dynamic and adaptive tools, thus taking environmental variability into account concerning their impacts on marine populations.

Bibliography

Anderson, J.T. (1988). A review of size dependent survival during pre-recruit stages of fishes in relation to recruitment. Journal of Northwest Atlantic Fishery Science 8, 55–66.

Appeldoorn, R. S., Hensley, D. A., Shapiro, D. Y., Kioroglou, S., & Sanderson, B. G. (1994). Egg Dispersal in a Caribbean Coral Reef Fish, *Thalassoma bifasciatum*. II. Dispersal off the Reef Platform. Bulletin of Marine Science, 54(1), 271–280.

Aspillaga, E., Bartumeus, F., Linares, C., Starr, R. M., López-Sanz, À., Díaz, D., Zabala, M., & Hereu, B. (2016). Ordinary and Extraordinary Movement Behaviour of Small Resident Fish within a Mediterranean Marine Protected Area. PLOS ONE, 11(7), e0159813.
https://doi.org/10.1371/journal.pone.0159813

Auth, T. D., Daly, E. A., Brodeur, R. D., & Fisher, J. L. (2017). Phenological and distributional shifts in ichthyoplankton associated with recent warming in the northeast Pacific Ocean. Global Change Biology, 24(1), 259–272.
https://doi.org/10.1111/gcb.13872

Ayata, S.-D., Irisson, J.-O., Aubert, A., Berline, L., Dutay, J.-C., Mayot, N., Nieblas, A.-E., D'Ortenzio, F., Palmiéri, J., Reygondeau, G., Rossi, V., & Guieu, C. (2018). Regionalisation of the Mediterranean basin, a MERMEX synthesis. Progress in Oceanography, 163, 7-20.
https://doi.org/10.1016/j.pocean.2017.09.016

Benchalel, W., & Kara, M. H. (2010). Age, croissance et reproduction du sar commun *Diplodus sargus sargus* (Sparidae) des côtes de l'est Algerien. Rapp Comm int Mer Medit, 39:451.

Bianchi, C.N., & Morri, C. (2000). Marine Biodiversity of the Mediterranean Sea: Situation, Problems and Prospects for Future Research. Marine Pollution Bulletin, 40(5), 367-376, ISSN 0025-326X.
https://doi.org/10.1016/S0025-326X(00)00027-8.

Bradbury, I. R., Campana, S. E., Bentzen, P., & Snelgrove, P. V. R. (2004). Synchronized hatch and its ecological significance in rainbow smelt *Osmerus mordax* in St. Mary's Bay, Newfoundland. Limnology and Oceanography, 49(6), 2310–2315.
https://doi.org/10.4319/lo.2004.49.6.2310

Bray, L., Kassis, D., & Hall-Spencer, J. M. (2017). Assessing larval connectivity for marine spatial planning in the Adriatic. Marine Environmental Research, 125, 73-81, ISSN 0141-1136.
https://doi.org/10.1016/j.marenvres.2017.01.006.

Burgess, S.C., Baskett, M.L., Grosberg, R.K., Morgan, S.G., & Strathmann, R.R. (2016). When is dispersal for dispersal? Unifying marine and terrestrial perspectives. Biol Rev, 91, 867-882. doi:10.1111/brv.12198

Burgess, S.C., Nickols, K.J., Griesemer, C.D., Barnett, L.A.K., Dedrick, A.G., Satterthwaite, E.V., Yamane, L., Morgan, S.G., White, J.W., & Botsford, L.W. (2014). Beyond connectivity: how empirical methods can quantify population persistence to improve marine protected-area design. Ecological Applications, 24, 257-270. doi:10.1890/13-0710.1

Burrows, M.T., Bates, A.E., Costello, M.J. *et al* (2019). Ocean community warming responses explained by thermal affinities and temperature gradients. Nat. Clim. Chang., 9, 959-963.
https://doi.org/10.1038/s41558-019-0631-5

Ciliberti, S.A., Pinardi, N., Coppini, G., Oddo, P., Vukicevic, T., Lecci, R., Verri, G., Kumkar, Y., & Creti, S. (2015). A high resolution Adriatic-Ionian Sea circulation model for operational forecasting. In: EGU General Assembly Conference Abstracts.

Clark, D.L., Leis, J.M., Hay, A.C., & Trnski, T. (2005). Swimming ontogeny of larvae of four temperate marine fishes. Mar. Ecol. Prog. Ser. 292, 287–300.

Claudet, J., & Fraschetti, S. (2010). Human-driven impacts on marine habitats: A regional meta-analysis in the Mediterranean Sea. Biological Conservation, 143(9), 2195-2206, ISSN 0006-3207. https://doi.org/10.1016/j.biocon.2010.06.004.

Claydon, J. (2005). Spawning aggregations of coral reef fishes: characteristics, hypotheses, threats and management. Oceanography and Marine Biology: An Annual Review, 42, 265–301.

Colin, P. L. (2010). Aggregation and spawning of the humphead wrasse *Cheilinus undulatus* (Pisces: Labridae): general aspects of spawning behaviour. Journal of Fish Biology, 76(4), 987–1007. https://doi.org/10.1111/j.1095-8649.2010.02553.x

Coll, M., Piroddi, C., Steenbeek, J., Kaschner, K., Ben Rais Lasram, F., *et al.* (2010). The Biodiversity of the Mediterranean Sea: Estimates, Patterns, and Threats. PLOS ONE, 5(8): e11842. https://doi.org/10.1371/journal.pone.0011842

Coulson, P. G., Norriss, J. V., Jackson, G., & Fairclough, D. V. (2019). Reproductive characteristics of the fishery important temperate demersal berycid *Centroberyx gerrardi* indicate greater reproductive output in regions of upwelling. Fisheries Management and Ecology, 26(3), 236–248. https://doi.org/10.1111/fme.12343

Cowen, R. K., Paris, C. B., & Srinivasan, A. (2006). Scaling of connectivity in marine populations. Science, 311, 522-527.

Cowen, R. K., & Sponaugle, S. (2009). Larval Dispersal and Marine Population Connectivity. Annual Review of Marine Science, 1(1), 443-466. https://doi.org/10.1146/annurev.marine.010908.163757

Cresciani, F., & Mosetti, R. (2016). Is the Bimodal Oscillating Adriatic-Ionian Circulation a Stochastic Resonance? Bollettino Di Geofisica Teorica et Applicata, 57(3), 275-85. https://doi.org/10.4430/bgta0176.

Cuadros, A., Basterretxea, G., Cardona, L., Cheminée, A., Hidalgo, M., & Moranta, J. (2018). Settlement and post-settlement survival rates of the white seabream (*Diplodus sargus*) in the western Mediterranean Sea. PLoS ONE 13(1): e0190278. https://doi.org/10.1371/journal.pone.0190278

Cushing, D.H. (1990). Plankton Production and Year-class Strength in Fish Populations: an Update of the Match/Mismatch Hypothesis. Advances in Marine Biology, Academic Press, 26, 249-293, ISSN 0065-2881, ISBN 9780120261260. https://doi.org/10.1016/S0065-2881(08)60202-3.

Cuttitta *et al* (2016). Different key roles of mesoscale oceanographic structures and ocean bathymetry in shaping larval fish distribution pattern: A case study in Sicilian waters in summer 2009. Journal of Sea Research, 115, 6-17. https://doi.org/10.1016/j.seares.2016.04.005.

D'Aloia, C. C., Bogdanowicz, S. M., Francis, R. K., Majoris, J. E., Harrison, R. G., & Buston, P. M. (2015). Patterns, causes, and consequences of marine larval dispersal. Proceedings of the National Academy of Sciences, 112(45), 13940-13945. https://doi.org/10.1073/pnas.1513754112

D'Ovidio, F., Fernandez, V., Hernandez-Garcia, E. & Lopez, C. (2004). Mixing structures in the Mediterranean Sea from finite-size Lyapunov exponents. Geophys. Res. Lett., 31, L17203. doi:10.1029/2004GL020328.

Dahlberg, M. D. (1979). A Review of Survival Rates of Fish Eggs and Larvae in Relation to Impact Assessments. Marine Fisheries Review, 12.

De Moura, C. A., & Kubrusly, C. S. (2013). The Courant–Friedrichs–Lewy (CFL) Condition. Birkhäuser. https://doi.org/10.1007/978-0-8176-8394-8

De Vlaming, V. L. (1972). Environmental control of teleost reproductive cycles: A brief review. Journal of Fish Biology, 4(1), 131–140.
https://doi.org/10.1111/j.1095-8649.1972.tb05661.x

Di Franco, A., Benedetto, G., Rinaldis, G., Raventos, N., & Sahyoun, R. (2011). Large scale-variability in otolith microstructure and microchemistry: The case study of *Diplodus sargus sargus* (Pisces: Sparidae) in the Mediterranean Sea. Italian Journal of Zoology. 78. 182-192. DOI: 10.1080/11250003.2011.566227.

Di Franco, A., & Guidetti, P. (2011). Patterns of variability in early-life traits of fishes depend on spatial scale of analysis. Biology Letters, 7(3), 454-456.
https://doi.org/10.1098/rsbl.2010.1149

Di Franco, A., Coppini, G., Pujolar, J. M., De Leo, G. A., Gatto, M., *et al* (2012a). Assessing Dispersal Patterns of Fish Propagules from an Effective Mediterranean Marine Protected Area. PLOS ONE, 7(12), e52108.
https://doi.org/10.1371/journal.pone.0052108

Di Franco, A., Gillanders, B. M., De Benedetto, G., Pennetta, A., De Leo, G. A., & Guidetti, P. (2012b). Dispersal Patterns of Coastal Fish: Implications for Designing Networks of Marine Protected Areas. PLoS ONE, 7(2), e31681.
https://doi.org/10.1371/journal.pone.0031681

Di Franco, A., Qian, K., Calò, A., Di Lorenzo, M., Planes, S., & Guidetti, P. (2013). Patterns of variability in early life traits of a Mediterranean coastal fish. Marine Ecology Progress Series, 476, 227-235.
https://doi.org/10.3354/meps10117

Di Franco, A., Plass-Johnson, J. G., Di Lorenzo, M., Meola, B., Claudet, J., Gaines, S. D., García-Charton, J. A., Giakoumi, S., Grorud-Colvert, K., Werner Hackradt, C., Micheli, F., & Guidetti, P. (2018). Linking home ranges to protected area size: The case study of the Mediterranean Sea. Biological Conservation, 221, 175-181, ISSN 0006-3207.
https://doi.org/10.1016/j.biocon.2018.03.012.

Di Lorenzo, M., D'Anna, G., Badalamenti, F., Giacalone, V., Starr, R., & Guidetti, P. (2014). Fitting the size of no-take zones to species movement patterns: A case study on a Mediterranean seabream. Marine Ecology Progress Series, 502, 245–255.
https://doi.org/10.3354/meps10723

Divanach, P., Kentouri, M., & Paris, J. (1982). Etapes du developpement embryonnaire et larvaire du sar, *Diplodus sargus* L., en elevage. Aquaculture, 27(4), 339–353.
doi:10.1016/0044-8486(82)90122-3

Druon, J.-N., Fiorentino, F., Murenu, M., Knittweis, L., Colloca, F., Osio, C., Mérigot, B., Garofalo, G., Mannini, A., Jadaud, A., Sbrana, M., Scarcella, G., Tserpes, G., Peristeraki, P., Carlucci, R., & Heikkonen, J. (2015). Modelling of European hake nurseries in the Mediterranean Sea: An ecological niche approach. Progress in Oceanography, 130, 188-204.
https://doi.org/10.1016/j.pocean.2014.11.005

Dubois, M., Rossi, V., Ser-Giacomi, E., Arnaud-Haond, S., López, C., & Hernández-García, E. (2016). Linking basin-scale connectivity, oceanography and population dynamics for the conservation and management of marine ecosystems: Large-scale connectivity and management of marine ecosystems. Global Ecology

and Biogeography, 25(5), 503-515.
https://doi.org/10.1111/geb.12431

El Maghraby, A. M., Botros, G. A., Hashem, M. T., Wassef, E. A. (1982). Maturation, spawning and fecundity of two sparid fish *Diplodus sargus*, L. and *Diplodus vulgaris*, Geoff. in the Egyptian Mediterranean waters. Bulletin Bull Inst Oceanogr Fish ARE 8:51–67.

Faillettaz, R., Durand, E., Paris, C.B., Koubbi, P., Irisson, J.O., 2018. Swimming speeds of Mediterranean settlement-stage fish larvae nuance Hjort's aberrant drift hypothesis. Limnol. Oceanogr. 63, 509–523.

Falcini, F., Palatella, L., Cuttitta, A., Buongiorno Nardelli, B., Lacorata, G., Lanotte, A. S., Patti, B., & Santoleri, R. (2015). The Role of Hydrodynamic Processes on Anchovy Eggs and Larvae Distribution in the Sicily Channel (Mediterranean Sea): A Case Study for the 2004 Data Set. PLOS ONE, 10(4), e0123213. https://doi.org/10.1371/journal.pone.0123213

FAO, (2006). General Fisheries Commission for the Mediterranean/Commission générale des pêches pour la Méditerranée. Report of the ninth session of the Scientific Advisory Committee. Rome, 24–27 October 2006/Rapport de la neuvième session du Comité scientifique consultatif. Rome, 24-27 octobre 2006. FAO Fisheries Report/FAO Rapport sur les pêches. No. 814. Rome, FAO. 106p.

FAO, (2018). The State of Mediterranean and Black Sea Fisheries. General Fisheries Commission for the Mediterranean. Rome. 172 pp. Licence: CC BY-NC-SA 3.0 IGO.

Fincham, J. I., Rijnsdorp, A. D., & Engelhard, G. H. (2013). Shifts in the timing of spawning in sole linked to warming sea temperatures. Journal of Sea Research, 75, 69–76.
https://doi.org/10.1016/j.seares.2012.07.004

Fogarty, M., & Botsford, L. (2007). Population Connectivity and Spatial Management of Marine Fisheries. Oceanography, 20(3), 112-123.
https://doi.org/10.5670/oceanog.2007.34

Gačić, M., Borzelli, G. L. E., Civitarese, G., Cardin, V., & Yari, S. (2010). Can internal processes sustain reversals of the ocean upper circulation? The Ionian Sea example. Geophys. Res. Lett., 37, L09608. doi:10.1029/2010GL043216.

Gačić, M., G. Civitarese, V. Kovačević, L. Ursella, M. Bensi, M. Menna, V. Cardin, *et al.* (2014). Extreme Winter 2012 in the Adriatic: An Example of Climatic Effect on the BiOS Rhythm. Ocean Science, 10(3), 513-22.
https://doi.org/10.5194/os-10-513-2014.

Gaines, S. D., Gaylord, B., Gerber, L.R., Hastings, A.,& Kinlan, B. (2007). Connecting Places: The Ecological Consequences of Dispersal in the Sea. Oceanography, 20(3), 90-99.
https://doi.org/10.5670/oceanog.2007.32

Gaines, S. D., White, C., Carr, M. H., & Palumbi, S. R. (2010). Designing marine reserve networks for both conservation and fisheries management. Proceedings of the National Academy of Sciences, 107(43), 18286-18293.
https://doi.org/10.1073/pnas.0906473107

Garratt, P. A. (1993). Spawning of riverbream, *Acanthopagrus berda* , in Kosi estuary. South African Journal of Zoology, 28(1), 26–31.
https://doi.org/10.1080/02541858.1993.11448284

Giacalone, V., Pipitone, C., Badalamenti, F., Sacco, F., Zenone, A., Ferreri, R., Micale, V., Basilone, G., & D'Anna, G. (2018). Home range, movements and daily activity of the white seabream Diplodus sargus sargus (L., 1758) during the spawning season. Cahiers de Biologie Marine.

Gill, H. S., Wise, B. S., Potter, I. C., & Chaplin, J. A. (1996). Biannual spawning periods and resultant divergent patterns of growth in the estuarine goby *Pseudogobius olorum*: Temperature-induced? Marine Biology, 125, 453–466.

Gonçalves, J. M. D. S. (2000). Fisheries Biology and Population Dynamics of *Diplodus vulgaris* (Geoffr.) and *Spondyliosoma cantharus* (L.) (Pisces, Sparidae) from the southwest coast of Portugal. Universidade do Algarve.

Guidetti, P. (2000). Differences among fish assemblages associated with nearshore *Posidonia oceanica* seagrass beds, rocky–algal reefs and unvegetated sand habitats in the Adriatic Sea. Estuar. Coast Shelf Sci. 50, 515–529.

Guidetti, P., Baiata, P., Ballesteros, E., Di Franco, A., Hereu, B., *et al* (2014). Large-Scale Assessment of Mediterranean Marine Protected Areas Effects on Fish Assemblages. PLOS ONE, 9(4), e91841. https://doi.org/10.1371/journal.pone.0091841

Harmelin-Vivien, M. L., Harmelin, J. G., & Leboulleux, V. (1995). Microhabitat requirements for settlement of juvenile sparid fishes on Mediterranean rocky shores. Hydrobiologia, 300/301, 309–320.

Hereu, B., Zabala, M., Linares, C., & Sala, E. (2005). The effects of predator abundance and habitat structural complexity on survival of juvenile sea urchins. Marine Biology, 146(2), 293-299. https://doi.org/10.1007/s00227-004-1439-y

Hereu, B., Diaz, D., Pasqual, J., Zabala, M., & Sala, E. (2006). Temporal patterns of spawning of the dusky grouper *Epinephelus marginatus* in relation to environmental factors. Marine Ecology Progress Series, 325, 187–194. https://doi.org/10.3354/meps325187

Hjort, J. (1914). Fluctuations in the great fisheries of northern Europe viewed in the light of biological research. Rapports Et Proces-Verbaux De La Commission Internationale Pour L'exploration Scientifique De La Mer, 20(1), 228.

Hunter, A., Speirs, D. C., & Heath, M. R. (2015). Fishery-induced changes to age and length dependent maturation schedules of three demersal fish species in the Firth of Clyde. Fisheries Research, 170, 14-23, ISSN 0165-7836. https://doi.org/10.1016/j.fishres.2015.05.004.

Jones, G., Srinivasan, M., & Almany, G. (2007). Population Connectivity and Conservation of Marine Biodiversity. Oceanography, 20(3), 100-111. https://doi.org/10.5670/oceanog.2007.33

Jug-Dujakovic, J., & Glamuzina, B. (1988). Preliminary studies of reproduction and early life history of *Diplodus vulgaris* (E. Geoffroy Saint-Hilaire 1817) in captivity. Aquaculture 69: 367-377.

Kadota, T., Sakai, Y., Hashimoto, H., & Gushima, K. (2010). Diel and lunar spawning periodicity of the hawkfish *Paracirrhites forsteri* (Cirrhitidae) on the reefs of Kuchierabu-jima Island, southern Japan. Ichthyological Research, 57(1), 102–106. https://doi.org/10.1007/s10228-009-0124-z

King, A. J., Gwinn, D. C., Tonkin, Z., Mahoney, J., Raymond, S., & Beesley, L. (2016). Using abiotic drivers of fish spawning to inform environmental flow management. Journal of Applied Ecology, 53(1), 34–43. https://doi.org/10.1111/1365-2664.12542

Lê, S., Josse, J. & Husson, F. (2008). FactoMineR: An R Package for Multivariate Analysis. Journal of Statistical Software, 25(1), 1-18.

Lenfant, P., Planes, S. (1996). Genetic differentiation of white sea bream within the Lion's gulf and the Ligurian sea (Mediterranean Sea). J. Fish Biol. 49, 613–621.

Lester, S.E., Halpern, B.S., Grorud-Colvert, K., Lubchenco, J., Ruttenberg, B.I., Gaines, S.D., Airamé, S., & Warner, R.R. (2009). Biological effects within no-take marine reserves: a global synthesis. Mar. Ecol. Prog. Ser. 384, 33–46.

Levin, S. A., & Lubchenco, J. (2008) .Resilience, Robustness, and Marine Ecosystem-based Management, BioScience, Volume 58, Issue 1, Pages 27–32, https://doi.org/10.1641/B580107

Madec, G., Bourdallé-Badie, R., Bouttier, P. A., Bricaud, C., Bruciaferri, D., Calvert, D., *et al.* (2017). NEMO ocean engine. Notes Du Pôle De Modélisation De L'institut Pierre-simon Laplace (IPSL). Zenodo. http://doi.org/10.5281/zenodo.3248739

Lluch-Belda, D., Lluch-Cota, D. B., Hernandez-Vazquez, S., Salinas-Zavala, C. A., & Schwartzlose, R. A. (1991). Sardine and Anchovy Spawning as related to Temperature and Upwelling in the California Current System. 32, 8.

Man-Wai, R. (1985). Les sars du golfe du Lion, *Diplodus sargus*, *D.vulgaris*, *D. annularis* (Pisces, Sparidae). Ecobiologie, Pêche. Dissertation, University of Montpellier.

Marshall, D.J., Gaines, S., Warner, R., Barneche, D.R., & Bode, M. (2019). Underestimating the benefits of marine protected areas for the replenishment of fished populations. Front. Ecol. Environ. https://doi.org/10.1002/fee.2075.

Maxwell, S. M., Hazen, E. L., Lewison, R. L., Dunn, D. C., Bailey, H., Bograd, S. J., Briscoe, D. K., Fossette, S., Hobday, A. J., Bennett, M. , Benson, S., Caldwell, M. R., Costa, D. P., Dewar, H., Eguchi, T., Hazen, L., Kohin, S., Sippel, T., & Crowder, L. B. (2015). Dynamic ocean management: Defining and conceptualizing real-time management of the ocean, Marine Policy, 58, 42-50, ISSN 0308-597X. https://doi.org/10.1016/j.marpol.2015.03.014.

McLeod, K., Leslie, H., Aburto, M., Alessa, L., De Los Angeles Carvajal, M., Barr, B., Barbier, E.B., Boesch, D.F., Boyd, J., Crowder, L.B. & others (2012). Ecosystem-Based Management for the Oceans. Island Press, 392p. ISBN: 9781610911313.

McQueen, K., & Marshall, C. T. (2017). Shifts in spawning phenology of cod linked to rising sea temperatures. ICES Journal of Marine Science, 74(6), 1561–1573. https://doi.org/10.1093/icesjms/fsx025

Millot, C., & Taupier-Letage, I. (2005). Circulation in the Mediterranean Sea. In A. Saliot (Éd.), The Mediterranean Sea (Vol. 5K, p. 29-66). Springer Berlin Heidelberg. https://doi.org/10.1007/b107143

Mischke, C. C., & Morris, J. E. (1997). Out-of-Season Spawning of Sunfish *Lepomis spp.* In the Laboratory. The Progressive-Fish Culturist, 59(4), 297–302. https://doi.org/10.1577/1548-8640(1997)059<0297:OOSSOS>2.3.CO;2

Monroy, P., Rossi, V., Ser-Giacomi, E., López, C., & Hernández-García, E. (2017). Sensitivity and robustness of larval connectivity diagnostics obtained from Lagrangian Flow Networks. ICES Journal of Marine Science, 74(6), 1763-1779. https://doi.org/10.1093/icesjms/fsw235

Morato, T., Afonso, P., Lourinho, P., Nash, R. D. M., & Santos, R. S. (2003). Reproductive biology and recruitment of the white sea bream in the Azores. Journal of Fish Biology, 63(1), 59–72. https://doi.org/10.1046/j.1095-8649.2003.00129.x

Mouine, N., Francour, P., Ktari, M.-H., & Chakroun-Marzouk, N. (2007). The reproductive biology of *Diplodus sargus sargus* in the Gulf of Tunis (central Mediterranean). Scientia Marina, 71(3), 461–469. https://doi.org/10.3989/scimar.2007.71n3461

Mouine, N. (2009). Reproduction, âge et croissance des espèces du genre *Diplodus* et du genre *Spondyliosoma* du golfe de Tunis. PhD thesis. Faculté des Sciences de Tunis, Tunisia.

Mouine, N., Francour, P., Ktari, M. H., & Chakroun-Marzouk, N. (2012). Reproductive biology of four Diplodus species *Diplodus vulgaris*, *D. annularis*, *D. sargus sargus* and *D. puntazzo* (Sparidae) in the Gulf of Tunis (central Mediterranean). Journal of the Marine Biological Association of the United Kingdom, 92(3), 623–631.
https://doi.org/10.1017/S0025315411000798

Nathan, R., Perry, G., Cronin, J.T., Strand, A.E., & Cain, M.L. (2003). Methods for estimating long-distance dispersal. Oikos, 103, 261–273.

Oddo, P., Pinardi, N., Zavatarelli, M., & Coluccelli, A. (2006). The Adriatic system. Acta Adriat.: Int. J. Mar. Sci. 47, 169–184.

Olivar, M., & Sabatés, A. (1997). Vertical distribution of fish larvae in the north-west Mediterranean Sea in spring. Mar. Biol. 129, 289–300.

Pajuelo, J. G., Lorenzo, J. M., Bilbao, A., Ayza, O., & Ramos, A. G. (2006). Reproductive characteristics of the benthic coastal fish *Diplodus vulgaris* (Teleostei: Sparidae) in the Canarian archipelago, northwest Africa. Journal of Applied Ichthyology, 22(5), 414–418.
https://doi.org/10.1111/j.1439-0426.2006.00766.x

Pajuelo, J. G., Lorenzo, J. M., & Domínguez-Seoane, R. (2007). Gonadal development and spawning cycle in the digynic hermaphrodite sharpsnout seabream *Diplodus puntazzo* (Sparidae) off the Canary Islands, northwest of Africa. Journal of Applied Ichthyology.
https://doi.org/10.1111/j.1439-0426.2007.01010.x

Pajuelo, J. G., Lorenzo, J. M., Domınguez, R., Ramos, A., & Gregoire, M. (n.d.). On the population ecology of the zebra seabream *Diplodus cervinus cervinus* (Lowe 1838) from the coasts of the Canarian archipelago, North West Africa. 10.

Pelc, R. A., Warner, R. R., Gaines, S. D., & Paris, C. B. (2010). Detecting larval export from marine reserves. Proceedings of the National Academy of Sciences, 107(43), 18266-18271.

Perry, A. L., Low, P. J., Ellis, J. R. & Reynolds, J. D. (2005). Climate Change and Distribution Shifts in Marine Fishes. Science, 308 (5730), 1912-1915. DOI: 10.1126/science.1111322

Piccioni, A., Gabriele, M., Salusti, E., & Zambianchi, E. (1988). Wind-Induced Upwellings off the Southern Coast of Sicily. Oceanologica Acta, 11(4), 309-314.

Pinardi, N., & Masetti, E. (2000). Variability of the large scale general circulation of the Mediterranean Sea from observations and modelling: a review. Palaeogeography, Palaeoclimatology, Palaeoecology, 158, 153–173.

Pineda, J., Hare, J. A., & Sponaugle, S. (2007). Larval Transport and Dispersal in the Coastal Ocean and Consequences for Population Connectivity. Oceanography, 20(3), 22-39.

Planes, S., Macpherson, E., Biagi, F., Garcia-Rubies, A., Harmelin, J., Harmelin-Vivien, M., Jouvenel, J.-Y., Tunesi, L., Vigliola, L., & Galzin, R. (1999). Spatio-temporal variability in growth of juvenile sparid fishes from the Mediterranean littoral zone. Journal of the Marine Biological Association of the United Kingdom, 79(1), 137–143.

https://doi.org/10.1017/S0025315498000150

Potts, W. M., Booth, A. J., Richardson, T. J., & Sauer, W. H. H. (2014). Ocean warming affects the distribution and abundance of resident fishes by changing their reproductive scope. Reviews in Fish Biology and Fisheries, 24(2), 493–504.
https://doi.org/10.1007/s11160-013-9329-3

Poulain, P.M., Menna, M. & Mauri, E. (2012). Surface geostrophic circulation of the Mediterranean Sea derived from drifter and satellite altimeter data. Journal of Physical Oceanography, 42, 973–990.

Poulain, P.-M., Bussani, A., Gerin, R., Jungwirth, R., Mauri, E., Menna, M., & Notarstefano, G. (2013). Mediterranean Surface Currents Measured with Drifters: From Basin to Subinertial Scales. Oceanography, 26(1), 38-47.
https://doi.org/10.5670/oceanog.2013.03

Ranzi, S. (1933). Sparidae, Lobotidae in Uova, larve e stadi giovanili di Teleostei. Fauna Flora Golfo Napoli 38, 374 –376.

Reglero, P., Ciannelli, L., Alvarez-Berastegui, D., Balbín, R., López-Jurado, J., & Alemany, F. (2012). Geographically and environmentally driven spawning distributions of tuna species in the western Mediterranean Sea. Marine Ecology Progress Series, 463, 273-284.
https://doi.org/10.3354/meps09800

Reznick, D. N., & Braun, B. (1987). Fat cycling in the mosquitofish (*Gambusia affinis*): Fat storage as a reproductive adaptation. Oecologia, 73(3), 401–413.
https://doi.org/10.1007/BF00385257

Rossi, V., Ser-Giacomi, E., López, C., & Hernández-García, E. (2014). Hydrodynamic provinces and oceanic connectivity from a transport network help designing marine reserves. Geophysical Research Letters, 41(8), 2883-2891.
https://doi.org/10.1002/2014GL059540

Sala, E., Boudouresque, C. F., & Harmelin-Vivien, M. (1998). Fishing, Trophic Cascades, and the Structure of Algal Assemblages: Evaluation of an Old but Untested Paradigm. Oikos, 82(3), 425. doi:10.2307/3546364

Ser-Giacomi, E., Rossi, V., López, C., & Hernández-García, E. (2015). Flow networks: A characterization of geophysical fluid transport, Chaos, 25(3), 036404. doi:10.1063/1.4908231

Ser-Giacomi, E., Rodríguez-Méndez, V., López, C., & Hernández-García, E. (2017). Lagrangian Flow Network approach to an open flow model. Eur. Phys. J. Spec. Top. 226, 2057–2068.
https://doi.org/10.1140/epjst/e2017-70044-2.

Sheaves, M. (2006). Is the timing of spawning in sparid fishes a response to sea temperature regimes? Coral Reefs, 25(4), 655–669.
https://doi.org/10.1007/s00338-006-0150-5

Sheaves, M., & Molony, B. (2013). Reproductive periodicity of the sparid, *Acanthopagrus pacificus*, on a hierarchy of temporal scales. Journal of Fish Biology, 82(2), 538–554.
https://doi.org/10.1111/jfb.12010

Staaterman, E., Paris, C. B., & Helgers, J. (2012). Orientation behavior in fish larvae: A missing piece to Hjort's critical period hypothesis. Journal of Theoretical Biology, 304, 188-196.
https://doi.org/10.1016/j.jtbi.2012.03.016

Tittensor, D., Mora, C., Jetz, W. *et al* (2010). Global patterns and predictors of marine biodiversity across taxa. Nature 466, 1098-1101.

https://doi.org/10.1038/nature09329

Tsikliras, A. C., Dinouli, A., Tsiros, V.-Z., & Tsalkou, E. (2015). The Mediterranean and Black Sea Fisheries at Risk from Overexploitation. PLOS ONE, 10(3), e0121188. https://doi.org/10.1371/journal.pone.0121188

Tsuji, S., & Aoyama, T. (1982). Daily growth increments observed in otoliths of the larvae of Japanese red sea bream *Pagrus major* (Temminch et Schlegel). Bull Jpn Soc Sci Fish 48: 1559-1562.

Thresher, R.E., Colin, P.L., Bell, L.J., 1989. Planktonic duration, distribution and population structure of western and central pacific damselfishes (pomacentridae). Copeia 1989 420–434. https://doi.org/10.2307/1445439.

Van Gennip, S.J., Popova, E.E., Yool, A., Pecl, G.T., Hobday, A.J., & Sorte, C.J.B. (2017). Going with the flow: the role of ocean circulation in global marine ecosystems under a changing climate. Global Change Biology, 23, 2602-2617. doi:10.1111/gcb.13586

Vinagre, C., Ferreira, T., Matos, L., Costa, M. J., & Cabral, H. N. (2009). Latitudinal gradients in growth and spawning of sea bass, *Dicentrarchus labrax*, and their relationship with temperature and photoperiod. Estuarine, Coastal and Shelf Science, 81(3), 375–380. https://doi.org/10.1016/j.ecss.2008.11.015

Winters, G. H., & Wheeler, J. P. (1996). Environmental and phenotypic factors affecting the reproductive cycle of Atlantic herring. ICES Journal of Marine Science, 53(1), 73–88. https://doi.org/10.1006/jmsc.1996.0007

Wright, P. J., & Trippel, E. A. (2009). Fishery-induced demographic changes in the timing of spawning: Consequences for reproductive success. Fish and Fisheries, 10(3), 283–304. https://doi.org/10.1111/j.1467-2979.2008.00322.x

Yamahira, K. (1997). Hatching success affects the timing of spawning by the intertidally spawning puffer *Takifugu niphobles*. Marine Ecology Progress Series, 155, 239–248. https://doi.org/10.3354/meps155239
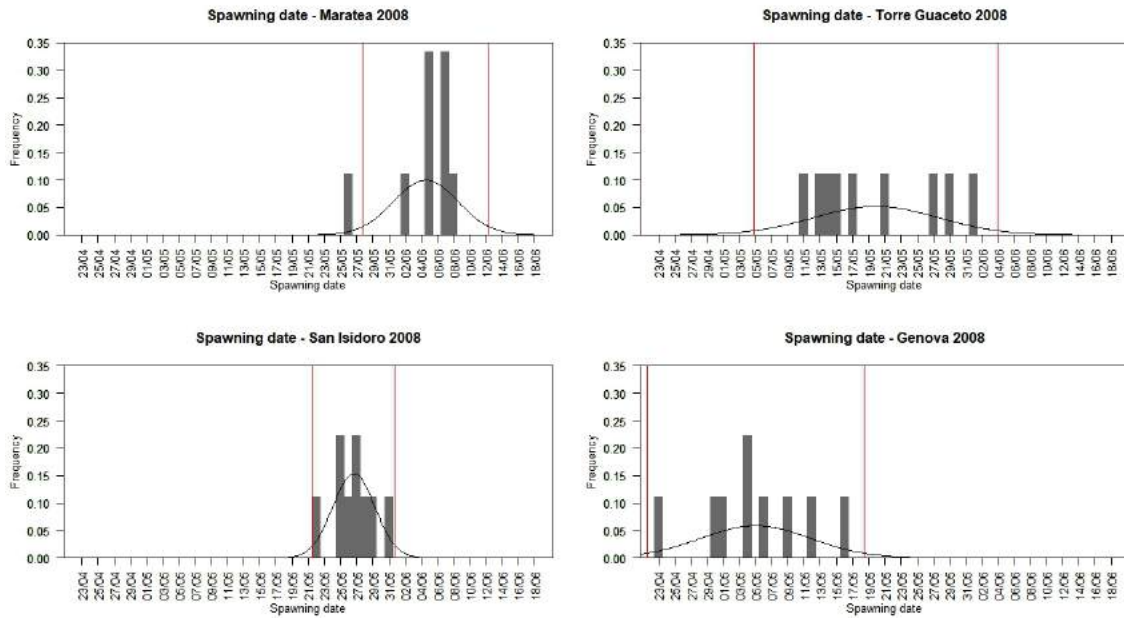
Appendix

Appendix 1: Gaussian distribution over the spawning dates for all the sites sampled in 2008: Maratea (upper left), Torre Guaceto (upper right), San Isidoro (bottom left) and Genova (bottom right). The red lines delimit the domain containing the 95 percent of the spawning dates.
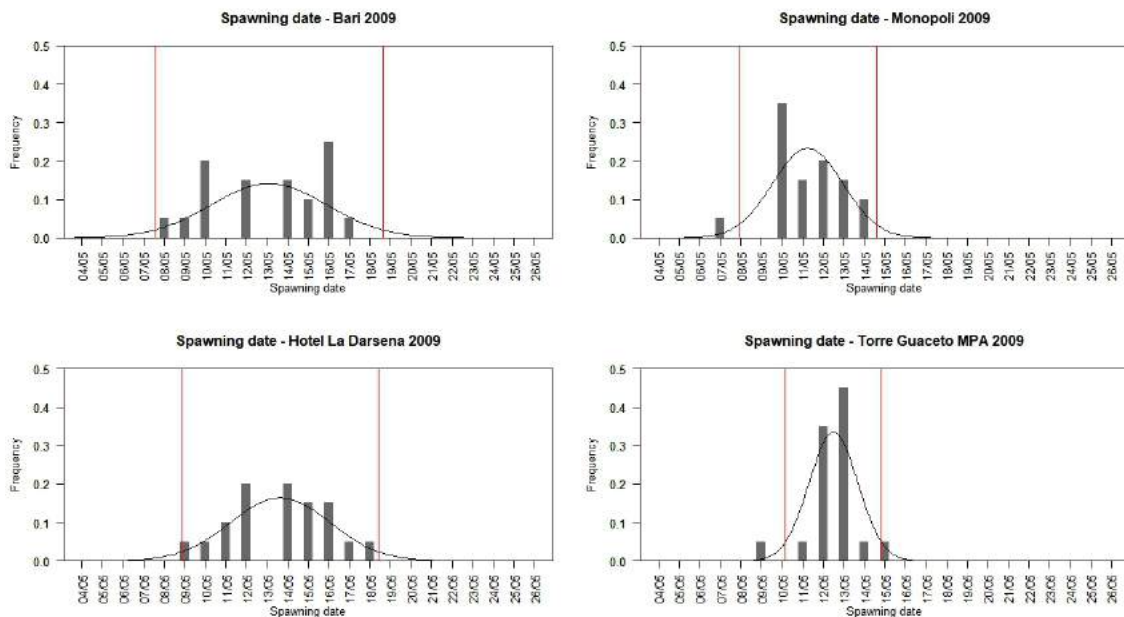

Appendix 2: Gaussian distribution over the spawning dates for the sites sampled in for some sites sampled in 2009: Bari (upper left), Monopoli (upper right), Hotel La Darsena (bottom left) and Torre Guaceto MPA (bottom right). The red lines delimit the domain containing the 95 percent of the spawning dates.
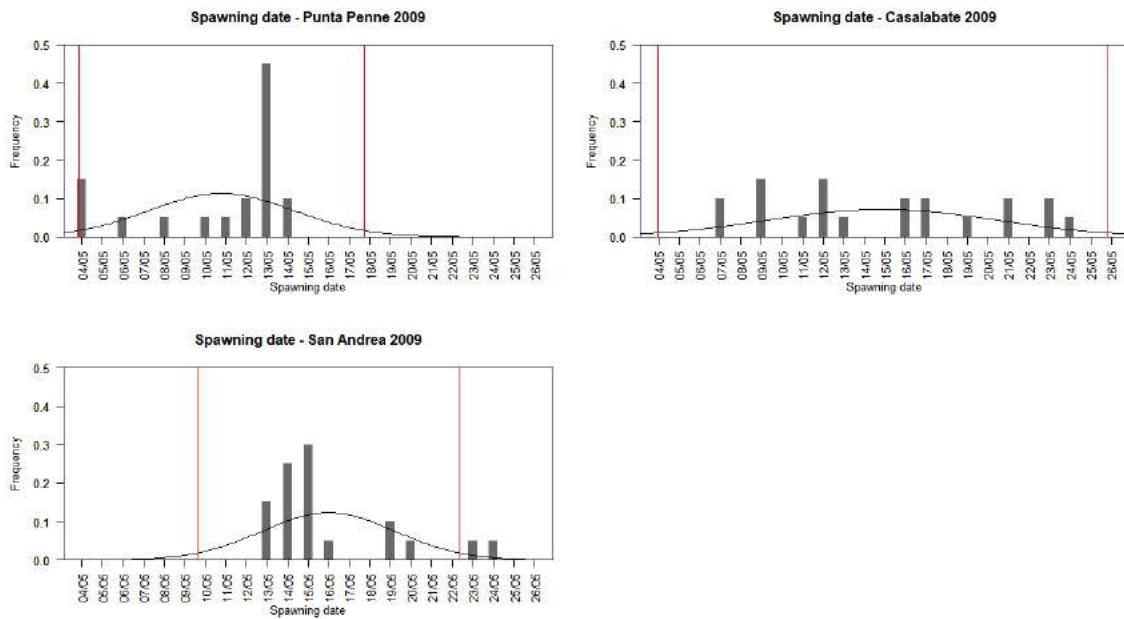
Appendix 3: Gaussian distribution over the spawning dates for some sites sampled in 2009: Punta Penne (upper left), Casalabate (upper right) and San Andrea (bottom left). The red lines delimit the domain containing the 95 percent of the spawning dates.

Run 2008	Minimum spawning date	Maximum spawning date	PLD	Number of connectivity matrices
1	28/05	12/06	14	16
2	05/05	04/06	17	31
3	22/05	01/06	15	11
4	22/04	18/05	13	27
Run 2009	Minimum spawning date	Maximum spawning date	PLD	Number of connectivity matrices
1	07/05	22/05	16	16
2	04/05	26/05	17	23
Run years 2005-2014	Minimum spawning date	Maximum spawning date	PLD	Number of connectivity matrices
1	01/03	30/06 (step = 5 days)	16	25/year = 250

Appendix 4: Parameters of the experiments run by the LFN model for the *data based approach* and the *modelling approach*.
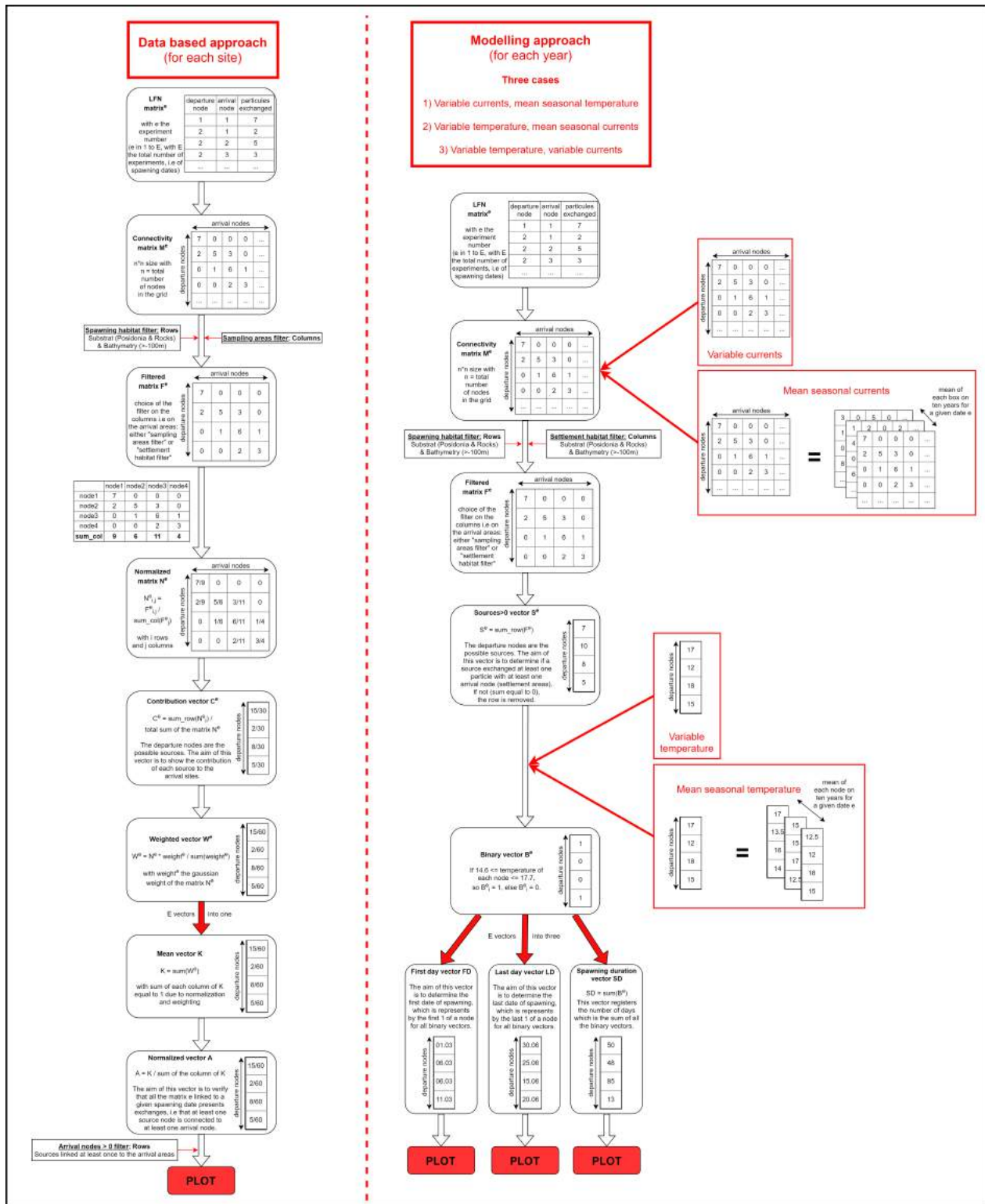
Appendix 5: Schematic representation of the connectivity matrix process for the *data based approach* and the *modelling approach*.
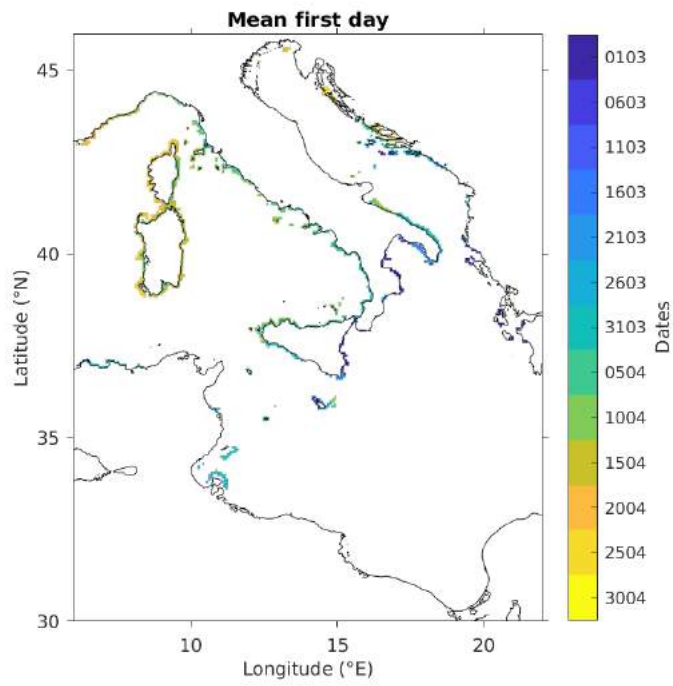
Appendix 6: 10-year average for the case "variable currents fixed temperature" of the first date of spawning.
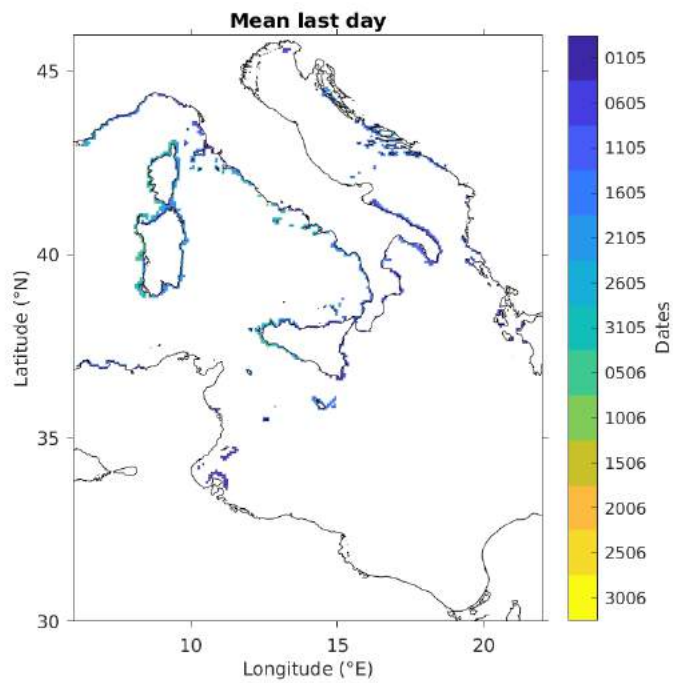
Appendix 7: 10-year average for the case "variable currents fixed temperature" of the last date of spawning.
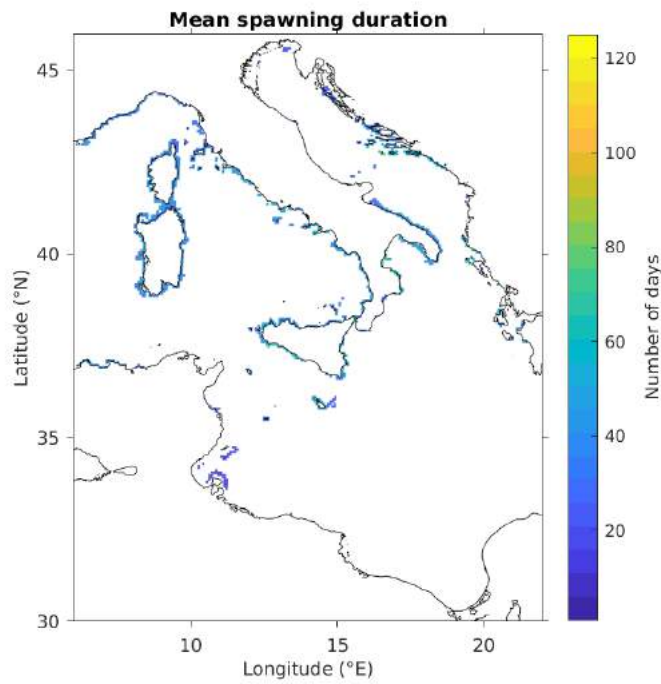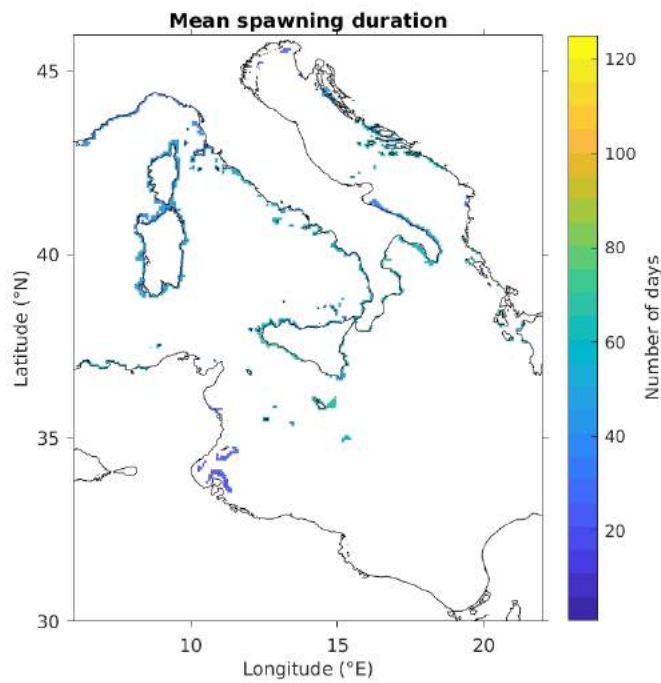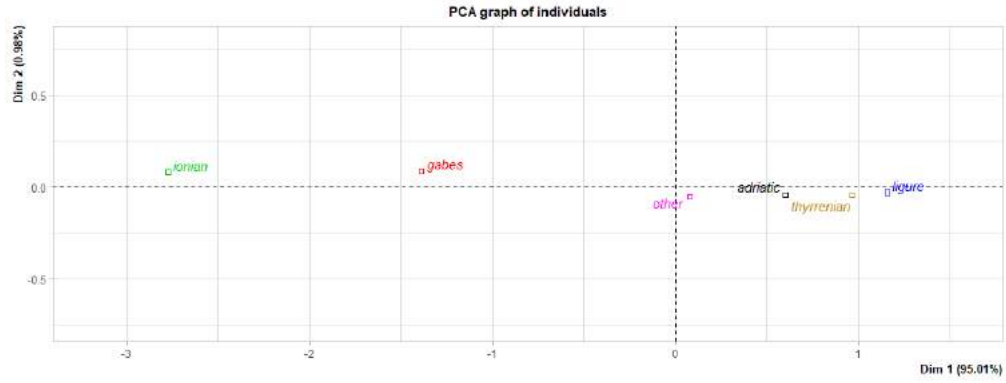
Appendix 8: 10-year average for the case "variable currents fixed temperature" of the spawning duration.
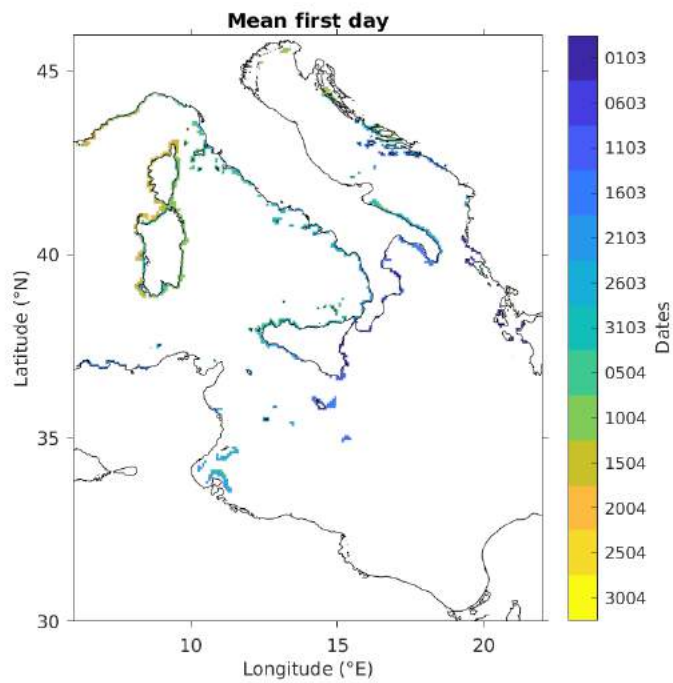
Appendix 9: 10-year average for the case "variable temperature fixed currents" of the first date of spawning.
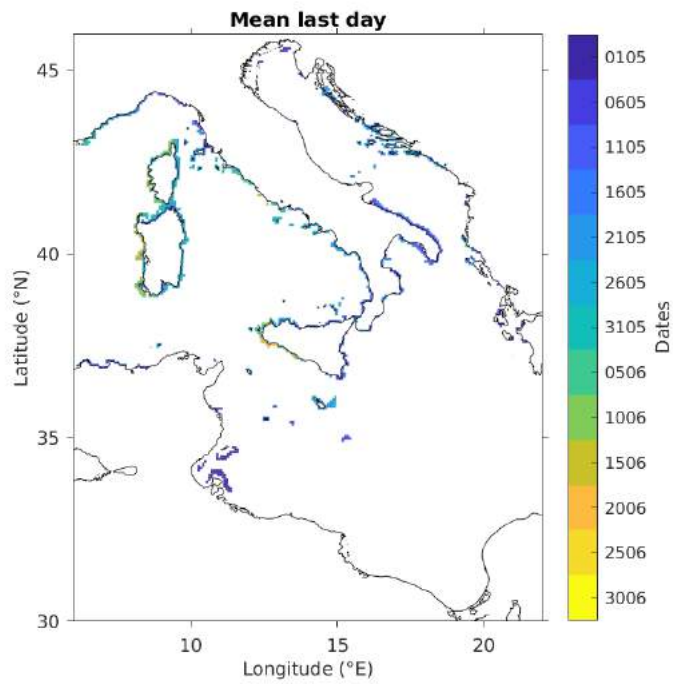
Appendix 10: 10-year average for the case "variable temperature fixed currents" of the last date of spawning.

Appendix 11: 10-year average for the case "variable temperature fixed currents" of the spawning duration.
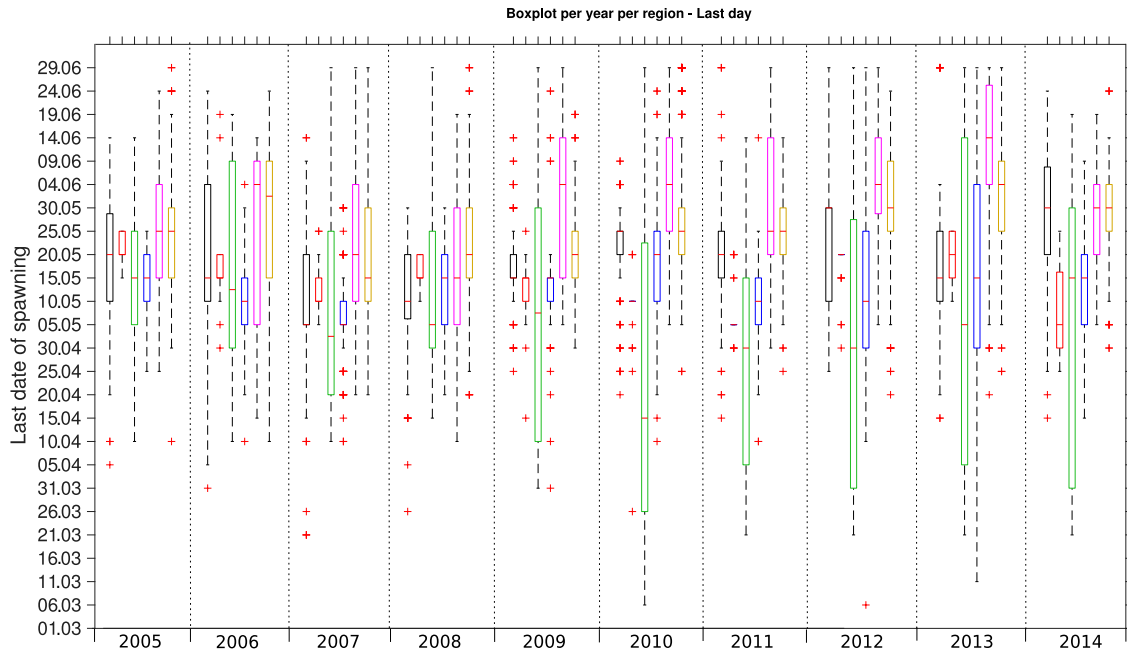
Appendix 12: Boxplots representing the last dates of spawning for each ecoregion. The colors-code identifies the different ecoregions: Adriatic (black), Algeria (red), Gabes (green), Ionian (blue), Ligurian (pink) and Tyrrhenian (yellow).Central bars indicate the median ; colored crosses represent outliers.
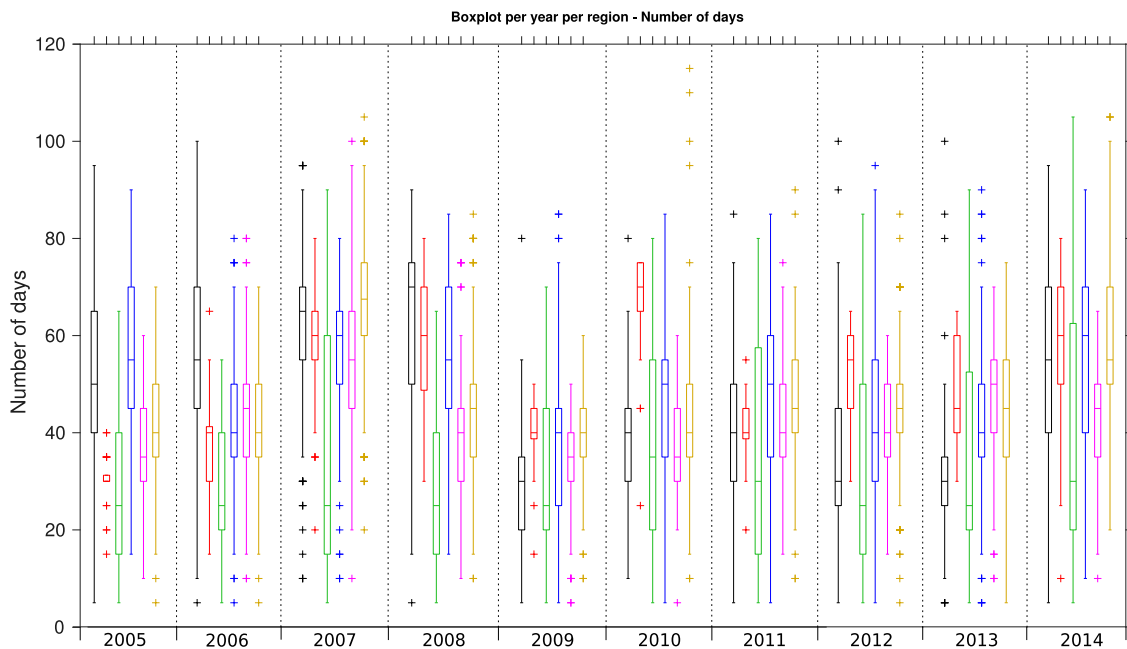

Appendix 13: Boxplots representing the spawning duration for each ecoregion. The colors-code identifies the different ecoregions: Adriatic (black), Algeria (red), Gabes (green), Ionian (blue), Ligurian (pink) and Tyrrhenian (yellow).Central bars indicate the median ; colored crosses represent outliers.

Appendix 14: Principal Component Analysis on the first date of spawning for the case "variable currents fixed temperature".
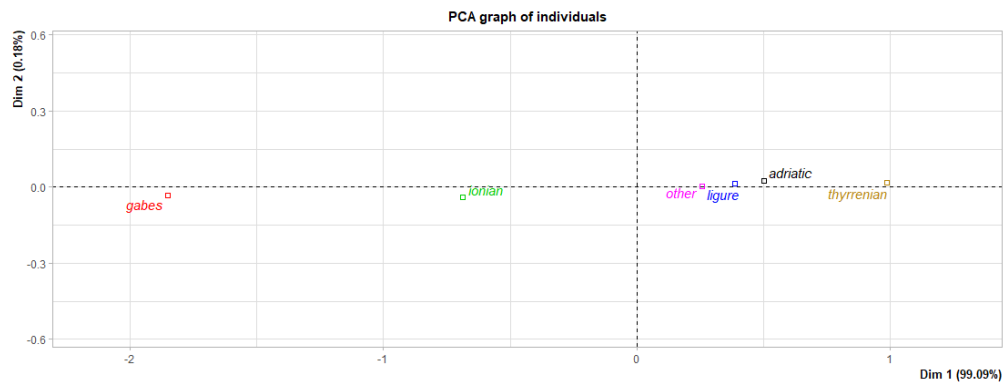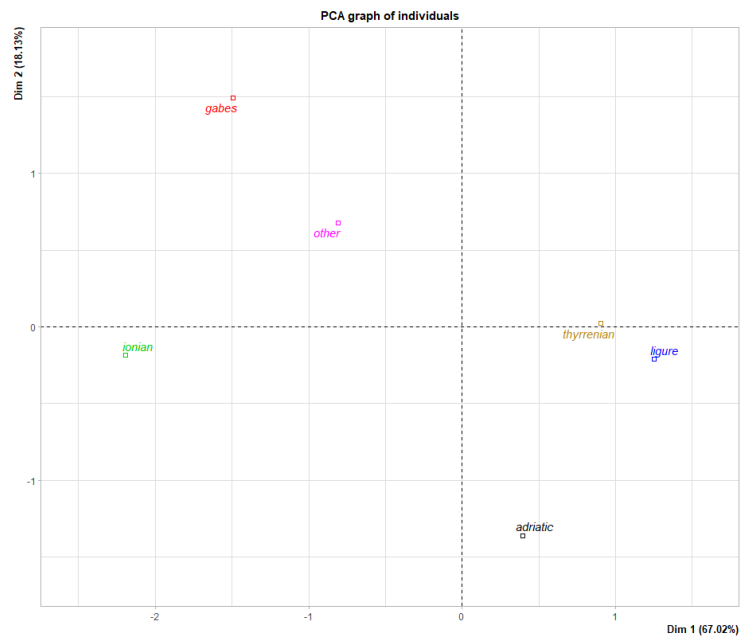

Appendix 15: Principal Component Analysis on the last date of spawning for the case "variable currents fixed temperature".
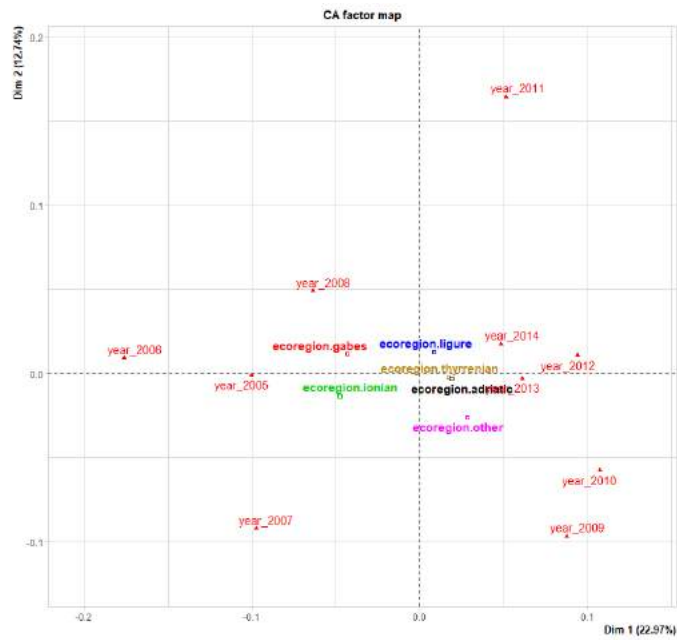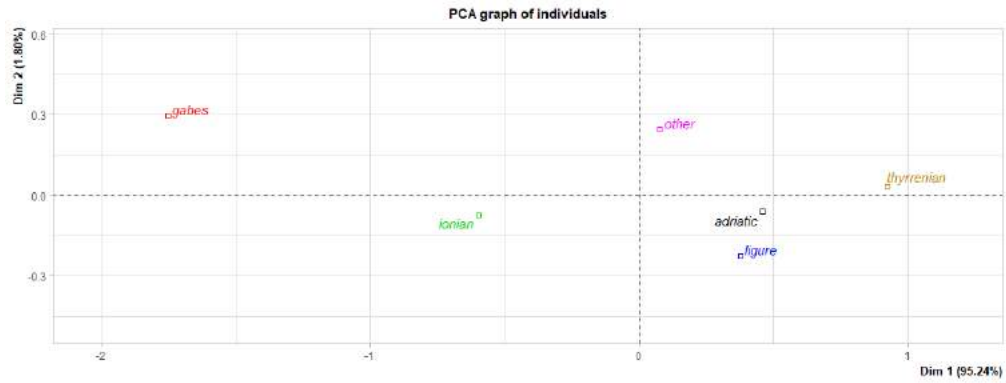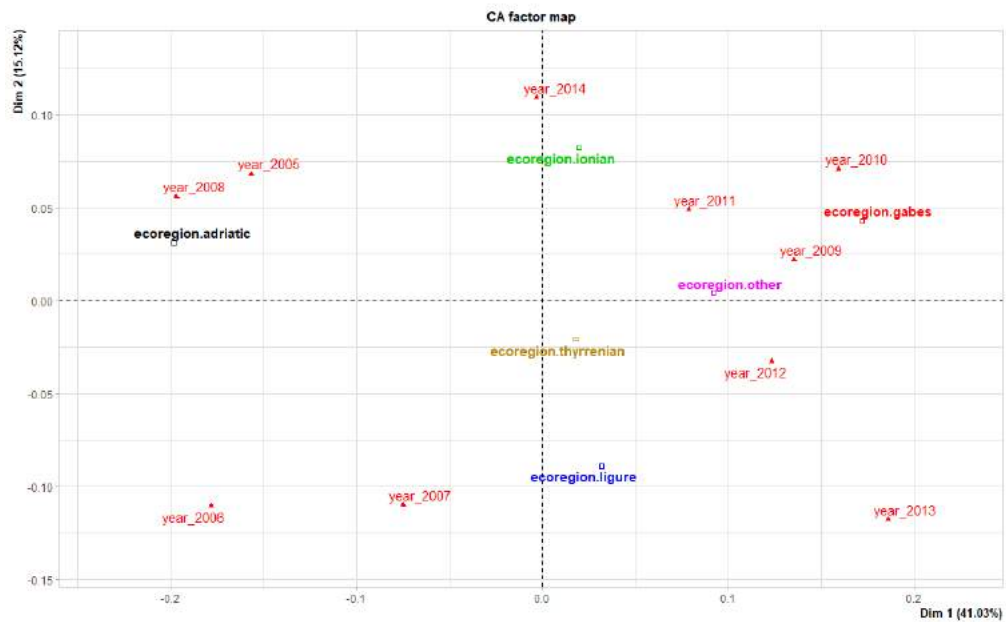
Appendix 16: Correspondance Analysis on the spawning duration for the case "variable currents fixed temperature".

Appendix 17: Principal Component Analysis on the first date of spawning for the case "variable temperature fixed currents".

55

Appendix 18: Principal Component Analysis on the last date of spawning for the case "variable temperature fixed currents".

Appendix 19: Correspondance Analysis on the spawning duration for the case "variable temperature fixed currents".

l'institut Agro	Diplôme : Ingénieur agronome (diplôme délivré par l'ENSAIA)
agriculture · alimentation · environnement	Spécialité : Sciences halieutiques et aquacoles
	Spécialisation / option : Ressources et écosystèmes aquatiques
	Enseignant référent : Etienne RIVOT

Auteur(s) : Marine DI STEFANO	Organisme d'accueil :
	Aix Marseille Université
Date de naissance* : 18/02/1996	Adresse :
Nb pages : 57p (34p sans bibliographie et autres)	MIO Institut Méditerranéen d'Océanologie, 163 Avenue de Luminy 13288 Marseille CEDEX 9
Annexe(s) : 19 annexes (10 pages)	Maître de stage : Vincent ROSSI
Année de soutenance : 2020	

Titre français :

Variabilité spatio-temporelle de la ponte chez des poissons côtiers en Méditerranée

Titre anglais :

Spatial and temporal variability of spawning in Mediterranean coastal fishes

Résumé (1600 caractères maximum) : La ponte est cruciale dans la dynamique spatio-temporelle et le repeuplement des populations marines. Pour les espèces à cycle de vie bipartite, elle débute la phase dispersive via l'émission de propagules qui sont ensuite disséminées par les courants. Malgré l'importance de la ponte et de la dispersion larvaire dans la gestion des ressources, ces processus sont mal connus. En étudiant le sar commun *Diplodus sargus* en Méditerranée, on se demande quels facteurs abiotiques contrôlent la ponte et comment ils affectent sa variabilité. Par une étude bibliographique, on déduit que la température est un facteur prépondérant du déclenchement de la ponte, en particulier chez les Sparidés. En combinant des données d'otolithométrie et un modèle hydrodynamique, on a localisé 11 zones de ponte nous permettant de déterminer une plage de températures modélisées déclenchant la ponte. Nous modélisons les zones de ponte en fonction de la température, basé sur la relation précédente, et des courants pendant 10 ans afin d'étudier comment la variabilité abiotique se répercute sur celle de la ponte de manière spatiale et temporelle. Des variations interannuelles et par écorégions de la ponte sont mises en évidence, avec la température comme principal facteur gouvernant où et quand la ponte est simulée. Bien que nos résultats délimitent certaines zones de ponte relativement stables, ils soulignent aussi l'importance de leur variabilité. Ainsi, les outils de protection et de gestion pourraient être dynamiques, adaptés aux variations environnementales et à leurs impacts sur les populations marines.

Abstract (1600 caractères maximum) : Spawning is crucial for the spatio-temporal dynamics, including the annual recruitment, of marine populations. For bipartite life-cycle species, it initiates the dispersive stage via the release of propagules that are then widespread by currents across the seascape. Despite the importance of spawning and subsequent dispersal in the management of resources, both processes remain poorly understood. By focusing on the white seabream *Diplodus sargus* in the Mediterranean Sea, we wonder what are the abiotic factors that trigger spawning and how they affect its variability. Thanks to a literature review, we found that temperature is a preponderant factor in the triggering of spawning, especially for Sparids. Combining otolithometry data with hydrodynamic modelling, we identified and located 11 spawning areas allowing us to determine a range of modelled temperature triggering spawning. Based on this relationship, we model the spatio-temporal variability of spawning areas as a function of temperature and currents, in order to study how abiotic variability can influence spawning. We found marked variability at inter-annual time-scale and among eco-regions, with temperature as a main driver of where and when the onset of spawning is simulated. Although our results delineated relatively stable spawning areas, they also highlighted the significance of their variability. Thus, tools used in management and protection could be adaptive and dynamic, following environmental variations and to their impacts on marine populations.

Mots-clés : connectivité marine, modèle Lagrangien, *Diplodus sargus*, variabilité de la ponte, facteurs abiotiques

Key Words: marine connectivity, Lagrangian model, *Diplodus sargus*, spawning variability, abiotic factors

* *Elément qui permet d'enregistrer les notices auteurs dans le catalogue des bibliothèques universitaires*

Document à intégrer au mémoire